



**EFFECTS OF MICROCRACKS AND IMPERFECT INTERFACE  
ON THE THERMOELASTIC RESPONSE AND  
FAILURE OF COMPOSITES**

Technical Final Report  
MSC TFR 3702/DA08  
February, 1997

**DTIC QUALITY INSPECTED**

Contract No. F49620-93-C-0073

**Distribution Statement A: Approved for Public Release; Distribution  
is Unlimited**

Prepared For:

Air Force Office of Scientific Research  
Bolling Air Force Base, DC 20332

Suite 250, 500 Office Center Drive  
Fort Washington, PA 19034  
Tel: 215-542-8400 Fax: 215-542-8401

**25** Advanced  
Years Composites  
Technology

19970623 323

REPORT DOCUMENTATION PAGE			Form Approved OMB No. 0704-0188	
<small>Public reporting burden for this collection of information is estimated to average 1 hour per response, including the time for reviewing instructions, searching existing data sources, gathering and maintaining the data needed, and completing and reviewing the collection of information. Send comments regarding this burden estimate or any other aspect of this collection of information, including suggestions for reducing the burden, to Washington Headquarters Services, Directorate for Information Operations and Reports, 1215 Jefferson Davis Highway, Suite 1204, Arlington, VA 22202-4302, and to the Office of Management and Budget Paperwork Reduction Project (0704-0188), Washington, DC 20503.</small>				
1. AGENCY USE ONLY (Leave blank)	2. REPORT DATE February 1997	3. REPORT TYPE AND DATES COVERED Final Report - 9/93 - 1/97		
4. TITLE AND SUBTITLE  Effects of Microcracks and Imperfect Interface on the Thermoelastic Response and Failure of Composites		5. FUNDING NUMBERS  F49620-93-C-0073		
6. AUTHORS(S)  Z. Hashin				
7. PERFORMING ORGANIZATION NAME(S) AND ADDRESS(ES) Materials Sciences Corporation 500 Office Center Drive, Suite 250 Fort Washington, PA 19034		8. PERFORMING ORGANIZATION REPORT NUMBER  MSC TFR 3702/DA08		
9. SPONSORING/MONITORING AGENCY NAME(S) AND ADDRESS(ES)  AFOSR/PKA Air Force Office of Scientific Research 110 Duncan Avenue, Suite B115 Bolling Air Force Base, DC 20332		10. SPONSORING/MONITORING AGENCY REPORT NUMBER		
11. SUPPLEMENTARY NOTES				
12a. DISTRIBUTION/AVAILABILITY STATEMENT Distribution Statement A: Approved for Public Release; Distribution is Unlimited			12B. DISTRIBUTION CODE	
13. ABSTRACT (Maximum 200 words)  The thermoelastic behavior of composites containing many dispersed microcracks has been studied. A variational analysis of thermoelastic properties and internal stresses of cracked laminates with imperfect interlaminar interface has been developed. Effective elastic moduli and thermal expansion coefficient of particulate and fiber composites containing many microcracks have been evaluated on the basis of the differential scheme. Macro-residual strains produced by cyclic loading of brittle composites have been expressed in terms of the effective thermal expansion coefficients. A finite fracture criterion for the spontaneous development of new crack surface has been established and has been applied for prediction of crack initiation in laminates. A criterion for debonding of the entire interface in a composite has been established in terms of applied average stresses and temperature.				
14. SUBJECT TERMS  Thermoelasticity, microcracks, composites, imperfect interfaces, fracture criterion, debonding			15. NUMBER OF PAGES 126	
			16. PRICE CODE	
17. SECURITY CLASSIFICATION OF REPORT UNCLASSIFIED	18. SECURITY CLASSIFICATION OF THIS PAGE UNCLASSIFIED	19. SECURITY CLASSIFICATION OF ABSTRACT UNCLASSIFIED	20. LIMITATION OF ABSTRACT	

## TABLE OF CONTENTS

1. Executive Summary
2. Cracked Laminates with Imperfect Interlaminar Interface
3. Differential Scheme for Effective Thermoelastic Properties of Cracked Composite Materials.
4. Macro-Residual Strains due to Cyclic Loading of Composites
5. Finite Thermoelastic Fracture Criterion with Application to Laminate Cracking Analysis
6. Interface Debond Analysis
7. Conclusion

## 1. EXECUTIVE SUMMARY

The research investigations contained in this report are concerned with thermoelastic behavior of cracked composite materials and with analysis of damage formation in the forms of cracks and debonding of the interface between the constituents. In the first case the damage is geometrically defined, for example in the form of crack distributions or degraded interface, and the goal is to evaluate the effect of such damage on the stiffness and the thermal expansion coefficients (TEC) of the composite material. In the second case the goal is to predict the crack density which is produced within a certain composite by specified load and temperature inputs and to evaluate load/temperature inputs which produce complete debonding of the constituents.

There are five parts as listed in the table of contents. The first three are concerned with evaluation of thermoelastic properties and the last two are concerned with the evaluation of damage. These investigations will now be discussed sequentially.

### **Cracked Laminates with Imperfect Interlaminar Interface**

This work deals with analysis of laminates with imperfect interlaminar interface. Such an imperfect interface models the case when there is a thin layer in-between the plies of the laminate, a situation encountered when there are oxidation protection layers, or when the interface has suffered damage for whatever reasons. The mathematical description of such imperfection is a discontinuity of displacement which is related to the interface traction. In our case the relation between interface displacement discontinuity and traction is linear. Such a relation is called an **imperfect interface condition**.

It should be noted that in the common case of a symmetric laminate subjected to membrane loads in its plane the imperfect interface has no effect, neither on internal stresses nor on the laminate thermoplastic properties. But the present analysis shows that the situation is entirely different for a laminate which has intralaminar cracks. The method of analysis is an extension of a previous one which dealt with analysis of cracked laminates with perfect interface [1]. This analysis was based on an application of the classical variational principle of minimum complementary energy. This minimum principle has been extended to the case of imperfect interface in [2] and this extended principle has been applied for the present situation.

The analysis shows that for ceramic composite cross-ply laminates interface imperfection has only a small effect on the in-plane Young's modulus and TEC of the composite but has a significant effect on the laminate shear modulus and the interlaminar shear and normal stresses.

### **Differential Scheme for Effective Thermoelastic Properties of Cracked Composite Materials.**

The most common damage in composite materials is in the form of microcracks. The research described in paragraph 1 above was concerned with microcracks through laminate ply thickness. Another very important problem is the effect of matrix microcracks in a unidirectional fiber composite or in a particulate composite. The size of such micro

cracks is of the order of fiber or particle diameters. Essentially, such a cracked composite is a three phase material consisting of matrix, reinforcement (fibers or particles) and cracks. the goal of the research is to evaluate the effect of such microcracks on thermoelastic properties, that is stiffness and TEC. There exists a very extensive literature on evaluation of thermoelastic properties of reinforced materials and of cracked materials. The difficulty of the problem is demonstrated by the fact that there exists almost no literature on evaluation of properties of cracked composites of the kind described.

The problem can be solved exactly only in the case when the composite is described by a matrix containing a small amount of non interacting fibers/particles and cracks. But such a problem is only of academic interest. It is therefore necessary to resort to approximate methods. Two well known methods of approximation are the self consistent scheme (SCS) and the differential scheme (DS). The SCS has actually been applied to the problem under consideration ,however , it is well known that the SCS results for cracked homogeneous materials gives unreliable results in that it seriously underestimates the stiffness. It can therefore not be expected to yield reliable results for cracked composites. On the other hand the DS results for cracked homogeneous materials are much more acceptable and also agree with experiments performed. It appeared therefore reasonable to apply this method for the present problem.

The basic premise of the DS is that when a small number of inhomogeneities (fibers,particles,cracks) are added within a composite then their incremental effect is given by dilute concentration theory with respect to the current properties of the composite. The DS becomes a quite accurate method when the added inhomogeneities are by an order of magnitude larger than the ones previously added.

The present investigation has resulted in evaluation of effective elastic moduli and TEC of a composite containing particles or fibers and matrix cracks. To the best of our knowledge this the first time that the TEC of this kind of composite has been analyzed.

### **Macro-Residual Strains due to Cyclic Loading of Composites**

It is well known that when ceramic composites are subjected to load cycles, at room temperature, macro-residual strains remain. Such residual strains are commonly observed in metals which have been loaded into a plastic state and then unloaded. However, ceramic composites are elastic-brittle and thus the phenomenon requires explanation . It is shown that such residual strains are formed because of the residual stress state in the composite which is due to the fact that the composite is stress free at it's high formation temperature and thus develops residual stress due to cooldown. If the loading part of the load cycle produces internal cracks then the residual stress state changes. The stresses due to the load disappear on unloading but the composite is now in a state of **different** residual stress and strain and therefore the average or macro-strain has changed after unloading. The difference between the average strain before loading and after unloading is the measured macro-residual strain.

The fundamental novel result found in this investigation is that the macro-residual strain can be expressed in terms of the difference between the effective TEC after and before the loading cycle. Furthermore, this explains the physical phenomenon observed that after many load cycles the residual strain will achieve a limit value which cannot be

increased by additional load cycles.. The reason for this is that crack density cannot grow indefinitely and at some time crack saturation will take place, which implies that no additional cracks can be introduced into the material. Now the effective TEC are functions of the crack geometry and thus at crack saturation the effective TEC assumes a limit value. Therefore, the macro-residual strain also assumes a limit value since it is uniquely determined by the effective TEC.

### **Finite Thermoelastic Fracture Criterion with Application to Laminate Cracking Analysis**

The origin of classical fracture mechanics is with a differential energy balance. The question posed is : what is the load which permits differential extension of a crack without load increase ? The answer is given by an energy balance in which the change in external work due to crack extension is equated to the internal energy change plus the energy needed to open up the crack. The concern is with **single** cracks or perhaps with a number of cracks at well known locations within a **homogeneous** material.

In composite materials in general, and in fiber composite laminates in particular, the formation of damage consists of the accumulation of a multitude of interacting cracks. It is impossible to follow the differential extensions of such cracks which appear suddenly and at unspecified locations. Instead we have what may be called **fracture events** which may be assumed to occur spontaneously. Therefore a different approach has been developed which defines a critical load as one which permits two simultaneous different crack geometry's which differ by **finite** fracture surface. Therefore the approach may be termed **finite fracture mechanics**.

Another consideration which is peculiar to composites is that there are residual stresses which are a result of cooldown after manufacturing at high temperature and constituent TEC mismatch. Thus load produces stresses which must be added to the residual stresses.

We have constructed a criterion for evaluation of the critical load which permits the spontaneous appearance of finite new fracture surface. This criterion is expressed solely in terms of the stress fields before and after the appearance of the new fracture surface. Moreover, it has been shown that the critical energy release which is needed to produce the new fracture surface can be bounded from above by use of admissible stress fields instead of the actual stress fields.

This theory has been applied to prediction of intralaminar crack densities in laminates which are cooled down from a stress-free temperature and are subsequently subjected to mechanical load. For this purpose a novel variational method for analysis of thermoplastic stresses in laminates has been constructed. The loads which initiate intralaminar cracking have been evaluate for various cross-ply laminates .Good agreement with experimental results has been obtained.

### **Interface Debond Analysis**

A possible failure mechnism in composite materials is debonding of the interface between the constituents. If this happens the reinforcing fibers or inclusions are essentially

replaced by voids and the composite material is replaced by a porous material. A porous material is weaker than the matrix and cannot serve as a structural material.

The debonding process consists of the growth of interface cracks which separate the constituents. Analysis of such a process is an impossible task for even the partial debonding of a single inclusion isolated in an infinite matrix is a very formidable problem. Here we consider a different problem : what is the load/ temperature combination which produces debonding of the **entire** interface ? This problem can be treated in relatively simple fashion by considering it in terms of the finite fracture criterion theory discussed in par. 4, above. It is assumed that the debonding of the interface is a spontaneous fracture event. Then the two comparison stress states are the stress in the composite for perfect bond and the stress for complete debonding, i.e. a porous material. These stress fields can be evaluated for suitable models of a composite. In the present study we have chosen the model known by the name Generalized Self Consistent Scheme.

The analysis produces a temperature dependent debond failure surface which is expressed in terms of applied average stress and temperature. The validity of the failure surface is limited by the need to assure that after debonding particles do not penetrate the matrix. The theory has been applied to evaluation of debond failure surfaces of a unidirectional fiber composite which is loaded transversely with temperature change.

#### References

1. Z. Hashin, "Analysis of cracked laminates : a variational approach", *Mechanics of Materials*, 4, 121-136, (1985)
2. Z. Hashin, "Extremum principles for elastic heterogeneous media with imperfect interface and their application to bounding of effective moduli", *J.Mech.Physics Solids*, 40, 767-781, (1992)

The work described and documented in this report has been performed by

Dr. Z. Hashin

Dr. B.W. Rosen

Mr. V. Vinogradov, graduate student

### Papers Published

1. Z. Hashin, "Cracked laminates with imperfect interlaminar interface", Proc. IUTAM Symposium on Microstructure-Property Interactions in Composite Materials, R. Pyrz, Ed., Kluwer Academic Publishers, 113-128, (1995)
2. Z. Hashin, "Finite thermoelastic fracture criterion with application to laminate cracking", J. Mech. Physics Solids, **44**, 1129-1145, (1996)
3. Z. Hashin and B.W. Rosen, "Macro-residual strains due to cyclic loading of composites", (submitted)



CRACKED LAMINATES WITH IMPERFECT  
INTERLAMINAR INTERFACE

Z. Hashin

# **Cracked Laminates with Imperfect Interlaminar Interface**

## **1. Introduction**

The present work is concerned with the effect of intralaminar crack (IC) accumulation on the thermomechanical properties of fiber composite laminates and the resulting internal stress distributions. Such cracks develop in the matrix along fibers due to load or temperature change. They are thus parallel crack distributions within the layers which propagate very rapidly until the laminate edges. Therefore, the formation of a typical IC is not viewed as a crack propagation phenomenon but as a fracture event which occurs instantaneously. Thus, the concern is with a laminate which contains IC distributions which are quantitatively described by crack density, the number of IC per unit length. The problems are then to determine deterioration of thermoelastic properties in terms of crack density, laminate internal geometry and ply properties, internal stresses resulting from crack accumulation and their relation to failure mechanisms, and more ambitiously - to predict crack density due to load or temperature.

The problems outlined have been the subject of a large number of research papers over the last 15 years. There are two major approaches : the first may be termed the micromechanics approach and the second, the continuum damage approach. In the first approach it is attempted to carry out analysis recognizing the cracks as defects on which the tractions must vanish. The advantage of this approach is physical realism and information about internal (micro) stresses, which is important for failure considerations. The disadvantage is analytical difficulty and for this reason the micromechanics approach has to date been confined to cross-ply.

In the second approach effect of IC on a layer is modeled by an abstract damage function whose form is not unique and which invariably contains unknown coefficients. The disadvantage is that such coefficients must be backed out from experiment on the laminate and it is not clear whether such coefficients qualify as ply material parameters or are fitting parameters which change from laminate to laminate. The advantage of the approach is that it can be applied to practical laminates, more complicated than cross-ply.

The present work is concerned with the micromechanics approach for cross-ply laminates. Review of the voluminous literature is not within the present scope. It is recalled that initial analytical efforts were based on the shear-lag approximation e.g. Reifsnider and Jamison (1982), Laws and Dvorak (1988). This method requires the determination of a so-called shear lag parameter on the basis of the fracture toughness of the ply materials. Analysis in terms of a displacement formulation represented, arbitrarily, by hyperbolic functions was given by Tsai *et al.* (1990). Work of similar nature with the choice of different form displacement functions has been done by Lee *et al.* (1990). A variational method based on the principle of minimum complementary energy has been developed by Hashin (1985) with application to stiffness reduction and stress analysis of cross-ply laminates with one layer cracked. This has been extended to the case of all layers cracked in Hashin (1987) and to evaluation of thermal expansion coefficients in Hashin (1988). The only assumption made in the variational analysis is that in plane stresses in the ply are constant over the thickness. Analysis based on similar assumptions has been given by McCartney (1992). Analysis for more general in-plane stresses has been given by Varna and Berglund (1994). Nairn *et al.* (1993) have successfully used the variational analysis for prediction of crack density resulting from in plane loading of cross-ply laminates.

The purpose of the work presented here is to extend the variational analysis to the evaluation of thermoelastic properties and internal stresses of cross-ply laminates when there is imperfect interlaminar bond between the layers.

## 2. Thermoelastic Extremum Principle for Imperfect Interface

Perfect interface between two solid constituents implies continuity of traction and displacement vectors at the interface. When the interface displacement vector is discontinuous, while the traction vector remains continuous for reasons of equilibrium, the interface is called imperfect. Let the displacement jump at interface  $S_{12}$  be denoted

$$[u] = u^2 - u^1. \quad (1)$$

Then the simplest imperfect interface condition is

$$\begin{aligned} T_n &= D_n [u_n] \\ T_s &= D_s [u_s] \\ T_t &= D_t [u_t], \end{aligned} \quad (2)$$

where  $n, s, t$  are normal and tangential components of the interface normal  $\mathbf{n}$ , assumed here as pointing into phase 2, and  $D_n, D_s, D_t$  are spring constant type interface parameters. With respect to a fixed cartesian coordinate system, (2) assumes the forms

$$\mathbf{T} = \mathbf{D} \cdot [\mathbf{u}] \quad [\mathbf{u}] = \mathbf{R} \cdot \mathbf{T} \quad \mathbf{R} = \mathbf{D}^{-1}, \quad (3)$$

where the Cartesian components of  $\mathbf{D}$  and its inverse  $\mathbf{R}$  now vary along the interface. It has been shown in Hashin (1990) that the effect of a thin and very compliant interphase between constituents can actually be expressed in the form (2) and that the interface parameters can be expressed in terms of interphase thickness and stiffness.

In the variational analysis to be employed here the generalization of the extremum principle of minimum complementary energy for imperfect interface conditions will be needed, Hashin (1992). This will here be further generalized to the thermoelastic case and will be stated for the case when tractions are prescribed over the entire external surface  $S$ . Let  $\sigma$  be the actual stress field and  $\tilde{\sigma}$  an admissible stress field for a body with surface load  $\mathbf{T}(S)$  and imperfect interface  $S_{12}$ . Define

$$\begin{aligned} W &= \frac{1}{2} \sigma : S : \sigma \\ \tilde{W} &= \frac{1}{2} \tilde{\sigma} : S : \tilde{\sigma}, \end{aligned} \quad (4)$$

where  $S$  is the compliance tensor. Here  $W$  is the stress energy density while  $\tilde{W}$  has no physical meaning. Next define the functionals

$$\begin{aligned} U &= \int_V [W + \alpha \cdot \sigma \cdot \theta - c_p (\theta^2 / 2\theta_0)] dV + \frac{1}{2} \int_{S_{12}} \mathbf{T} : \mathbf{R} : \mathbf{T} dS \\ \tilde{U} &= \int_V [\tilde{W} + \alpha \cdot \tilde{\sigma} \cdot \theta - c_p (\theta^2 / 2\theta_0)] dV + \frac{1}{2} \int_{S_{12}} \tilde{\mathbf{T}} : \mathbf{R} : \tilde{\mathbf{T}} dS \end{aligned} \quad (5)$$

Here  $\alpha$  is the thermal expansion tensor,  $c_p$  the specific heat at constant pressure and  $\theta$  is the (known) temperature relative to a reference temperature  $\theta_0$ . Then the thermoelastic principle of minimum complementary energy is expressed by the inequality

$$\tilde{U} \geq U, \quad (6)$$

equality occurring if, and only if,  $\tilde{\sigma} = \sigma$ .

For composite materials applications it is of importance to consider the case of constant temperature and so-called homogeneous traction boundary conditions which are defined as

$$T(S) = \sigma^o \cdot n(S) \quad (7)$$

Where  $\sigma^o$  is a constant stress tensor. Then  $\sigma^o$  is the average stress tensor and it can be shown that the first of (5) is, rigorously

$$U = \frac{1}{2} \left[ \sigma^o : S^* : \sigma^o + \alpha^* \cdot \sigma^o - c_p^* (\theta^2 / 2\theta_0) \right] V \quad (8)$$

where  $S^*$ ,  $\alpha^*$  and  $c_p^*$  are the effective elastic compliance tensor, thermal expansion tensor and specific heat, respectively.

In the following the variational principle will be exploited to analyze approximately thermo-elastic properties and internal stresses in cracked laminates.

### 3. Cross-Ply Laminates with One Ply Family Cracked

The case to be considered here is a  $[0_m^0, 90_n^0]_s$  laminate in which either the  $0^0$  or the  $90^0$  plies are cracked, fig. 1a. The variational method will be employed to obtain strict lower bounds for the effective Young's modulus  $E_x^*$  and the effective shear modulus  $G_{xy}^*$  and approximations for the effective thermal expansion coefficient  $\alpha_x^*$  and internal stresses, for the case of imperfect interlaminar interface as defined by a damaged interphase between plies.

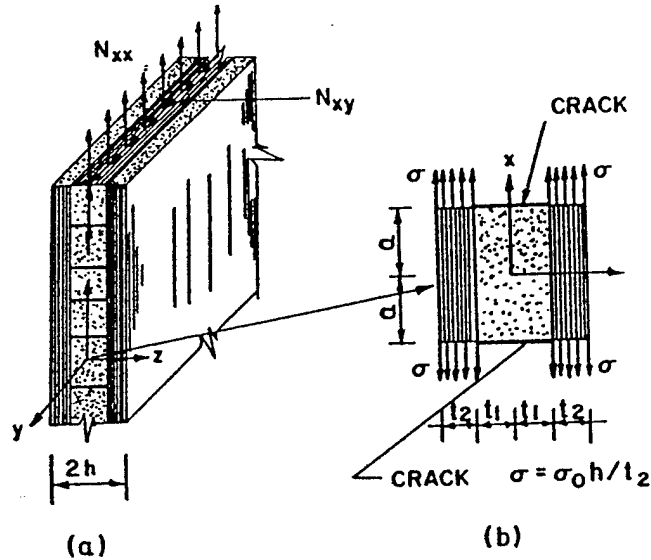


Figure 1. Cracked laminate

### 3.1. EFFECTIVE YOUNG'S MODULUS

Let it be assumed that the laminate is subjected to a constant tensile membrane force  $N_{xx}$  and let the  $\sigma_{xx}$  stresses in the layers of the uncracked laminate be denoted  $\sigma_1$  and  $\sigma_2$ , respectively, where from now on the label 1 refers to the  $90^\circ$  ply and 2 refers to the  $0^\circ$  ply. As is well known, these stresses are constant throughout the layers. The actual stress state in the cracked laminate is described by generalized plane strain in reference to the  $y$  axis, and therefore all stresses are functions of  $x, z$  only. It is at present assumed that only the  $90^\circ$  ply is cracked. The admissible stress state in the cracked laminate will be constructed on the basis of the simplification that the  $\sigma_{xx}$  stresses are functions of  $x$  and not of  $z$ . Thus these stresses may be written in the form

$$\sigma_{xx}^{(1)} = \sigma_1 [1 - \phi_1(x)] \quad (9)$$

$$\sigma_{xx}^{(2)} = \sigma_2 [1 - \phi_2(x)]$$

where  $\phi_1$  and  $\phi_2$  are unknown functions. These functions are, however, related since the stress pairs  $\sigma_1$ ,  $\sigma_2$  and (9) are each in equilibrium with the same  $N_{xx}$ . Therefore

$$\sigma_1 t_1 \phi_1 + \sigma_2 t_2 \phi_2 = 0$$

Consider a typical region between two adjacent cracks at distance  $2a$ , fig.1b. It is emphasized that the cracks do not have to be equidistant. For example,

the interdistance  $2a$  could be a random variable. For a typical intercrack region as shown in fig.1b the admissible stress field is constructed by integration of the two dimensional equations of equilibrium in the  $xz$  plane with the stresses (9). The integration produces residual unknown functions which are determined by satisfaction of traction continuity conditions at layer interfaces and zero traction conditions on the external laminate surface. The remaining admissible stresses are then

$$\begin{aligned}\sigma_{xz}^{(1)} &= \sigma_1 \phi'(x)z \\ \sigma_{zz}^{(1)} &= \sigma_1 \phi''(x)(ht_1 - z^2)/2 \\ \sigma_{xz}^{(2)} &= (\sigma_1/\lambda) \phi'(x)(h - z) \\ \sigma_{zz}^{(2)} &= (\sigma_1/\lambda) \phi''(x)(h - z)^2/2\end{aligned}\quad (10)$$

where  $\phi = \phi_1$ ,  $\lambda = t_2/t_1$  and prime superscript denotes  $x$  differentiation. These stresses have already been given in Hashin (1985). On the crack surfaces  $\sigma_{xz}^{(1)}$  and  $\sigma_{zz}^{(1)}$  must vanish and therefore

$$\phi(\pm a) = 1 \quad \phi'(\pm a) = 0 \quad (11)$$

The aggregate of the stress fields (9-11) for all intercrack regions are the admissible stress field. The stress energy densities for the layers 1 and 2 are:

$$\begin{aligned}2W_1 &= \sigma_{xx}^{(1)2}/E_T - 2\sigma_{xx}^{(1)}\sigma_{zz}^{(1)}\nu_T/E_T + \sigma_{zz}^{(1)2}/E_T + \sigma_{xz}^{(1)2}/G_T \\ 2W_2 &= \sigma_{xx}^{(2)2}/E_A - 2\sigma_{xx}^{(2)}\sigma_{zz}^{(2)}\nu_A/E_A + \sigma_{zz}^{(2)2}/E_T + \sigma_{xz}^{(2)2}/G_A\end{aligned}\quad (12)$$

where the elastic ply properties in (12) are:  $E_A$ ,  $\nu_A$  - axial Young's modulus and associated Poisson's ratio;  $E_T$ ,  $\nu_T$  - transverse Young's modulus and associated Poisson's ratio;  $G_A$ ,  $G_T$  - axial and transverse shear moduli.

For reasons of symmetry it is sufficient to evaluate the complementary energy functional for the regions  $-a_m \leq x \leq a_m$ ;  $0 \leq y \leq 1$ ;  $0 \leq z \leq h$ . Then for such a region and for an isothermal state, the second of (5) assumes the form

$$\begin{aligned}\tilde{U}_{C_m} &= \int_{-a_m}^{a_m} \int_0^{t_1} W_1 dz dx + \int_{-a_m}^{a_m} \int_{t_1}^h W_2 dz dx + \\ &\quad \frac{1}{2} \int_{-a_m}^{a_m} (\sigma_{zz}^2(x, t_1)/D_n + \sigma_{xz}^2(x, t_1)/D_s) dx\end{aligned}\quad (13)$$

where  $D_n$  and  $D_s$  are normal and shear interface parameters, and for the entire laminate

$$\tilde{U}_C = \sum \tilde{U}_{C_m} \quad (14)$$

The actual complementary energy is given for the present case by

$$U_C = \sigma^{02} V / 2E_x^* \quad \sigma^0 = N_{xx} / 2h \quad (15)$$

where  $V$  is the volume of the entire cracked laminate of thickness 1 in  $y$  direction. Introduction of the admissible stress field with functions  $\phi_m$  for each region into (14) results, according to the principle of minimum complementary energy, in an upper bound on (15). The lowest upper bound is obtained by minimizing the resulting functional with respect to the functions  $\phi_m$ . This is a standard problem in the calculus of variations resulting in Euler equations and boundary conditions for the minimizing functions which have the form

$$\frac{d^4 \phi_m}{d\xi^4} + p \frac{d^2 \phi_m}{d\xi^2} + q \phi_m = 0, \quad \phi_m(\pm \rho_m) = 1, \quad \frac{d\phi_m}{d\xi} \Big|_{(\xi=\pm \rho_m)} = 0 \quad (16)$$

where

$$\begin{aligned} \xi &= x/t_1 \quad \rho_m = a_m/t_1 \quad p = (C_{02} - C_{11})/C_{22} \quad q = C_{00}/C_{22} \\ C_{00} &= 1/E_T + 1/\lambda E_A \quad C_{02} = \frac{\nu_T}{E_T}(\lambda + \frac{2}{3}) - \frac{\nu_A}{3E_A}\lambda \\ C_{22} &= (\lambda + 1)(3\lambda^2 + 12\lambda + 8)/60E_T + \lambda^2/4D_n t_1 \\ C_{11} &= \frac{1}{3}(1/G_T + 1/\lambda G_A) + 1/D_s t_1 \end{aligned} \quad (17)$$

Evaluation of the complementary energy functional in terms of the functions  $\phi_m$  as was done in Hashin(1985), introduction of the result into the complementary inequality (6) with (15) as the actual complementary energy gives the result

$$1/E_x^* \leq 1/E_x^0 + \left(\frac{\sigma_1}{\sigma_0}\right)^2 \frac{C_{22}}{\lambda + 1} \frac{\langle \chi(\rho) \rangle}{\langle \rho \rangle}, \quad \chi_m(\rho) = -\frac{d^3 \phi_m}{d\xi^3} \Big|_{(\xi=\rho_m)} \quad (18)$$

where the brackets denote average with respect to the random variable  $a_m$ , half of the intercrack spacing. The form of  $\chi$  depends on the nature of the roots of the characteristic equation of (16). When these roots are of the form  $\pm(\alpha + i\beta)$ , where  $i = \sqrt{-1}$ , then the solution of (16) is of the form

$$\phi_m = A_m \cosh(\alpha\xi) \cos(\beta\xi) + B_m \sinh(\alpha\xi) \sin(\beta\xi) \quad (19)$$

where the constants are determined by the boundary conditions in (16). Then the associated  $\chi_m$  is

$$\chi_m = 2\alpha\beta(\alpha^2 + \beta^2) \frac{\cosh(2\alpha\rho_m) - \cos(2\beta\rho_m)}{\alpha \sin(2\beta\rho_m) + \beta \sinh(2\alpha\rho_m)} \quad (20)$$



If the roots are real, thus of the form  $\pm\alpha, \pm\beta$ , then

$$\begin{aligned}\phi_m &= A_m \cosh(\alpha\xi) + B_m \cosh(\beta\xi) \\ \chi_m &= \frac{\beta^2 - \alpha^2}{\cosh(\alpha\rho)/\alpha - \cosh(\beta\rho)/\beta}\end{aligned}\quad (21)$$

### 3.2. IMPERFECT INTERFACE MODEL

A physical interpretation of the interface parameters  $D_n$  and  $D_s$  has been given in Hashin (1990). If there is a thin elastic isotropic interphase of thickness  $t_i$  between the phases, then

$$D_n = (K_i + \frac{4}{3}G_i)/t_i \quad D_s = D_t = G_i/t_i \quad (22)$$

where  $K_i$  and  $G_i$  are the bulk and shear moduli of the interphase. It is easily shown that if the interphase is orthotropic, with material axes  $n, s$  and  $t$ , (22) becomes

$$D_n = C_{nn}/t_i \quad D_s = G_{ns}/t_i \quad D_t = G_{nt}/t_i \quad (23)$$

where  $C_{nn}$  is the normal stiffness and  $G_{ns}$  and  $G_{nt}$  are shear moduli. The first of (22,23) is strictly valid only when the interphase elastic moduli are much smaller than those of the constituents, but there is no such restriction with respect to  $D_s$  and  $D_t$ . If the interphase moduli are of the order of constituent moduli then the thin interphase effect is negligible and is equivalent to a perfect interface with displacement continuity. Consider a thin interphase in-between the layers of a cross-ply, fig.2. A relevant example is an oxidation protection layer between the laminae of a ceramic composite. Such a layer may develop many transverse cracks due to thermal stresses produced by manufacturing cooldown, fig. 2. These cracks are roughly orthogonal in fiber directions of the layers. In a ceramic fiber composite laminate, for example a SiC matrix reinforced by graphite fibers, the stiffness of the interphase layer is of the order of the stiffness of the layer material. For large crack density in the layer the shear moduli decrease very significantly, but not  $C_{nn}$ . Therefore such a cracked layer can be considered as an interface which is perfect for normal contact,  $[u_n] = 0$ , but is imperfect for shear. In that event the term in  $C_{22}$ , equ.(17), containing  $D_n$ , is negligible.

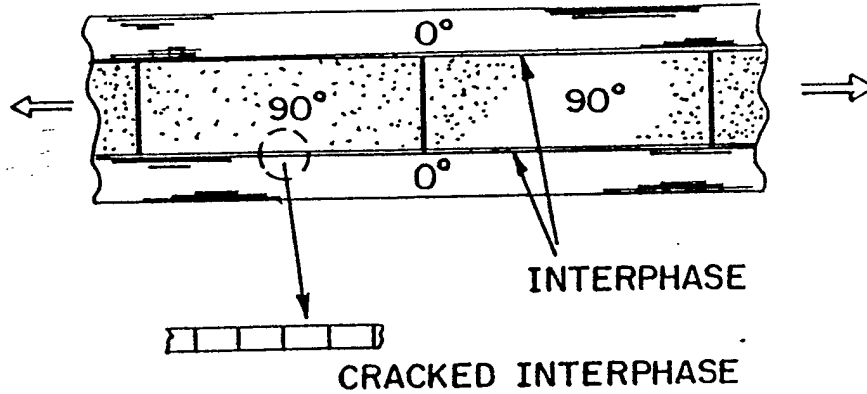


Figure 2. Laminate with damaged interphase

### 3.3. THERMAL EXPANSION

To evaluate the effective thermal expansion coefficient (TEC) of a cracked laminate it is very convenient to use the Levin relation as has been done for perfect interlaminar interface in Hashin (1988). For this purpose consider any elastic composite which is subjected to the homogeneous traction boundary conditions (7) and let the internal stresses due this loading be  $\sigma^M(x)$ . Denoting the local TEC  $\alpha(x)$  and the effective TEC  $\alpha^*$ , the Levin relation, Levin (1967), is expressed as

$$\int_V \alpha \cdot \sigma^M dV = \alpha^* \cdot \sigma^0 V \quad (24)$$

Levin's original derivation of (24) is based on displacement continuity, but it may be shown that it remains valid for interface displacement discontinuities which obey the relations (3) and therefore (24) may be employed in the present case with the stresses (9-10) and the functions  $\phi_m$  to give an approximate expression for the TEC. For the loading  $N_{xx}$  the only surviving component of  $\sigma_{ij}^0$  in (7) is  $\sigma_{xx}^0 = \sigma^0$  as defined by (15). Then from (24)

$$\alpha_{xx}^* \sigma^0 V = \int_0^L \left[ \int_0^{t_1} \alpha_T (\sigma_{xx}^{(1)} + \sigma_{zz}^{(1)}) dz + \int_{t_1}^h (\alpha_A \sigma_{xx}^{(2)} + \alpha_T \sigma_{zz}^{(2)}) dz \right] dx \quad (25)$$

where  $L$  is the length of the laminate of unit thickness in  $y$  direction. Insertion of the stresses into (25) with use of the boundary conditions of (16) yields

$$\alpha_{xx}^* = \alpha_{xx}^0 + \frac{\sigma_1}{\sigma_0} \frac{1}{1 + \lambda} (\alpha_A - \alpha_T) \langle \phi \rangle \quad (26)$$

where  $\alpha_{xx}^0$  is the TEC of the uncracked laminate,  $\alpha_A$  and  $\alpha_T$  are the axial and transverse TEC of the unidirectional fiber composite and  $\langle \phi \rangle$  is the average of the random variable  $\bar{\phi}_m$  which is defined as

$$\bar{\phi}_m(\rho_m) = \frac{1}{2\rho_m} \int_{-\rho_m}^{\rho_m} \phi_m(\xi) d\xi \quad (27)$$

Also

$$\alpha_{yy}^* \cong \alpha_{yy}^0 \quad (28)$$

### 3.4. EFFECTIVE SHEAR MODULUS

Let the cracked laminate shown in fig. 1 be subjected to constant shear membrane load  $N_{xy}$  which defines the average applied shear stress

$$\tau^0 = N_{xy}/2h \quad (29)$$

In this case the laminate is in a state of antiplane stress with respect to the y axis. Admissible stresses are defined as in Hashin (1985) by

$$\begin{aligned} \sigma_{xy}^{(1)} &= \tau^0[1 - \psi(x)] & \sigma_{yz}^{(1)} &= \tau^0\psi'(x)z \\ \sigma_{xy}^{(2)} &= \tau^0[1 + \frac{1}{\lambda}\psi(x)] & \sigma_{yz}^{(2)} &= \frac{\tau^0}{\lambda}\psi'(x)(h-z) \end{aligned} \quad (30)$$

Then a variational optimization as done above and in Hashin (1985) yields the results

$$\begin{aligned} \psi_m(\xi) &= \text{Cosh}(\mu\xi)/\text{Cosh}(\mu\rho_m) & \mu^2 &= \frac{3(1+1/\lambda)}{1+\lambda G_A/G_T+3G_A/t_1 D_s} \\ G_{xy}^* &\leq \frac{G_A}{1 + \langle \text{Tanh}(\mu\rho) \rangle / \lambda \mu \langle \rho \rangle} \end{aligned} \quad (31)$$

In the case of equidistant cracks  $a_m = a$ ,  $\rho_m = a/t_1$ , and all of the averages in all of the expressions above reduce to simple functions of  $\rho$  which are defined by removal of the brackets.

### 3.5. STRESS ANALYSIS AND CRACK OPENING DISPLACEMENTS

The optimal functions  $\phi_m$  and  $\psi_m$  define optimal admissible stresses by the relations (9,10,30). The effective properties  $E_x^*$  and  $G_{xy}^*$  based on these are strict lower bounds which also agree quite well with experimental data. The status of the stresses associated with the optimal functions is less clear which is a typical situation for any variational field approximation. It is, however, believed that these stresses are of qualitative importance, at least,

and the numerical results obtained, some of which are shown below, support this belief.

The results obtained in this work can be easily used to estimate the crack opening displacements (COD) when the cracks are equidistant. It is rigorously true that the stress energy  $U$  of a cracked elastic body, homogeneous or non-homogeneous, and the stress energy  $U_0$  of the same uncracked body, under same load, are related by

$$U = U_0 + \frac{1}{2} \sum \int_{S_m} T^0 \cdot [u] dS \quad (32)$$

where  $S_m$  is the surface of the  $m^{th}$  crack,  $T^0$  is the traction on same surface in the uncracked body and  $[u]$  is the COD. In the case of simple tension discussed above  $U$  is given by (15) and  $U_0 = (\sigma^0)^2 / (2E_x^0) V$  for the uncracked laminate. Also, the only surviving  $T_i^0$  is  $T_x^0 = \sigma_1$ . The COD is now estimated in the form of two equal and oppositely joined second order parabolas. Thus

$$[u_x] = 2\delta \left[ 1 - \left( \frac{z}{t_1} \right)^2 \right]$$

where  $2\delta$  is the maximum COD. It then follows easily that

$$\delta/t_1 = \frac{3}{2} \frac{\rho(1+\lambda)}{k_1} \sigma^0 (1/E_x^* - 1/E_x^0) \quad (33)$$

#### 4. Results

Illustrative results are presented for a  $[0^0, 90^0]$ , laminate in which the layers of equal thickness are T300/SiC ceramic unidirectional composites with fiber volume fraction 0.45. The relevant properties of the layer material are:

$$\begin{aligned} E_A &= 431.5 \text{ GPa} & E_T &= 113.6 \text{ GPa} \\ G_A &= 90.8 \text{ GPa} & G_T &= 39.3 \text{ GPa} \\ \nu_A &= 0.182 & \nu_T &= 0.446 \\ \alpha_A &= 2.39 \cdot 10^{-6} (C^0) & \alpha_T &= 5.49 \cdot 10^{-6} (C^0) \end{aligned}$$

It is assumed that in between the layers there is a thin oxidation protection interphase of isotropic  $B_4C$  material with thickness 0.02 of the layer thickness and with properties

$$E_i = 380 \text{ GPa} \quad G_i = 159.7 \text{ GPa} \quad \nu_i = 0.19$$

Due to thermal treatment the interphase may develop many through cracks. As has been explained above, this creates an orthotropic interphase which may be considered perfect in normal  $z$  direction but imperfect in

shear. Increase of crack density of the interphase may be considered as decrease of the effective shear stiffness of the interphase. All of the results given below are in the form of plot families where each plot is associated with a shear modulus value  $G_i/m$ ,  $m=1, 5, 10, 20, 50, 100, 200$ . Figs. 3-5 show plots of Young's modulus, TEC and shear modulus, all normalized with respect to their values for the uncracked laminate, as functions of crack density for the case of equidistant cracks, expressed by the parameter  $\rho$ . For large values of  $\rho$  the properties of the uncracked laminate are attained while for small values of  $\rho$  the properties reduce to those of a laminate in which the  $90^\circ$  layer has vanishing  $E_T$  and  $G_A$  but retains its  $E_A$  value. Such stiffness loss is associated with the concept of laminate netting analysis. The values of the properties decrease with decreasing interphase shear modulus. Thus for each property the uppermost plot is for undamaged interphase which may be regarded as a perfect interface while the lowest plot is for  $m=200$ . It is seen that the effect of interface imperfection, i.e. interphase damage, is not very significant for Young's modulus and TEC but is very significant for the shear modulus. It is also seen that the plots for normalized Young's modulus and TEC are very similar and indeed these normalized quantities are almost the same numerically. It should be realized that interphase damage has no effect on an uncracked laminate under in-plane loading since there are no interlaminar stresses in this case.

Figs. 6-7 show internal stresses as functions of  $x$ , for load  $N_{xx}$ , when the intercrack distance is  $2a = 5t_1$ . Fig. 6 shows the in-plane stresses  $\sigma_{xx}^{(1)}$  in the cracked layer and  $\sigma_{xx}^{(2)}$  in the uncracked layer functions of  $x$  for the case when the intercrack distance is  $2a = 5t_1$ , the family of plots being defined by the sequence  $G_i/m$ . It is seen that the tensile stress in the cracked  $90^\circ$  layer decreases with increasing interphase damage and therefore the stress in the uncracked  $0^\circ$  layer increases with damage. Fig. 7 shows similar plots for the interlaminar stresses  $\sigma_{xz}(x, t_1)$  and  $\sigma_{zx}(x, t_1)$ . These stresses decrease with increasing interphase damage and the effect is significant.

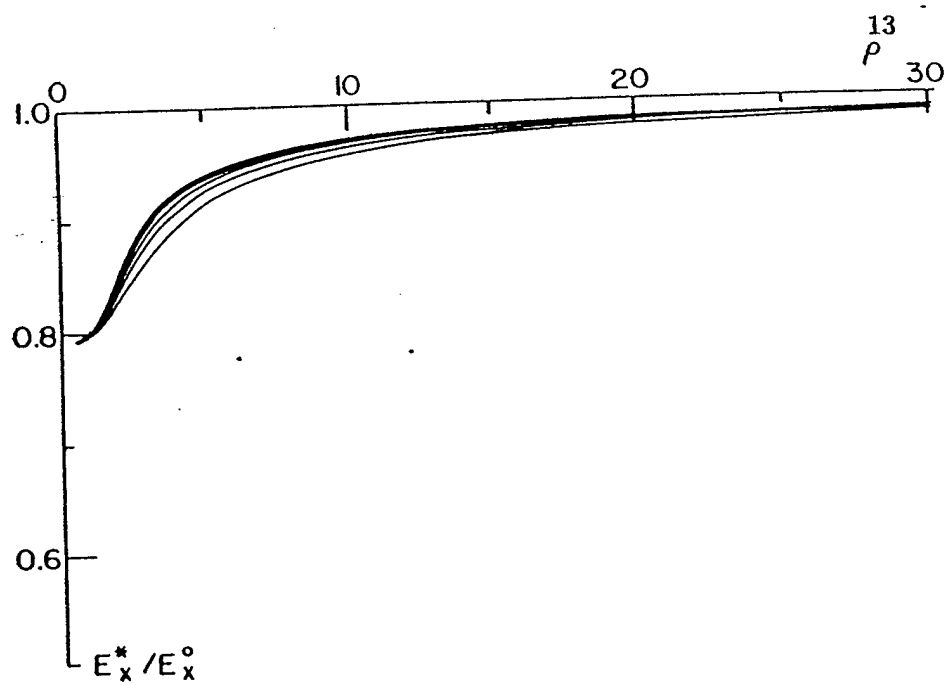


Figure 3. Effective Young's modulus versus crack spacing

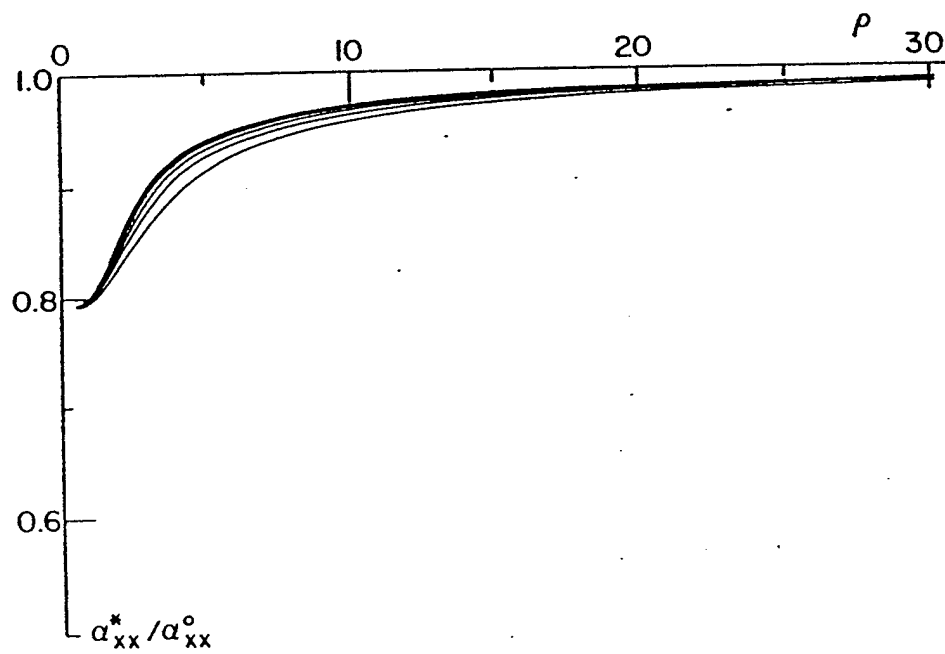


Figure 4. Effective thermal expansion coefficient versus crack spacing

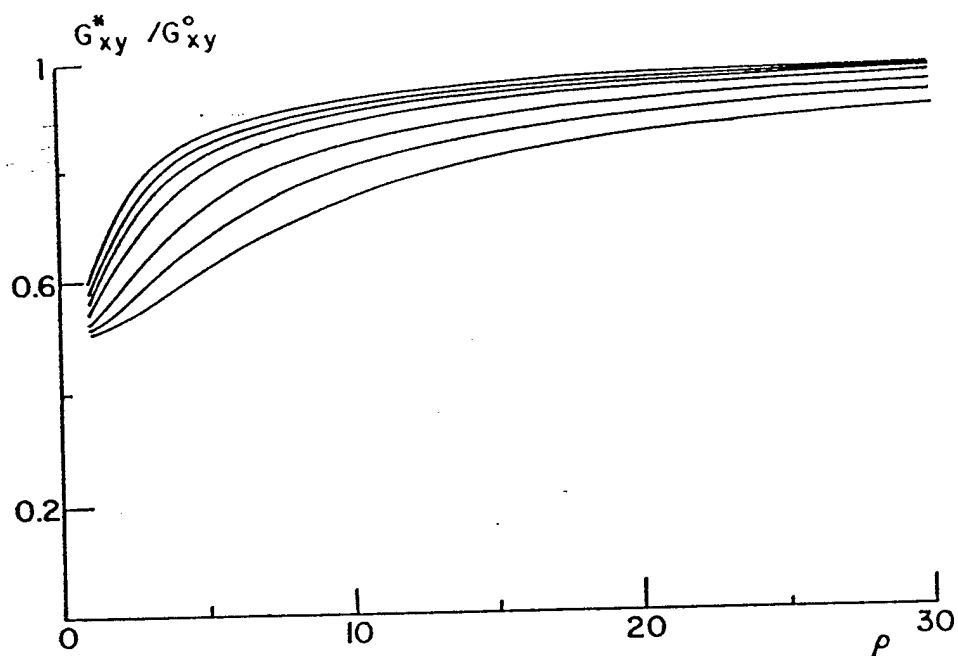


Figure 5. Effective shear modulus versus crack spacing

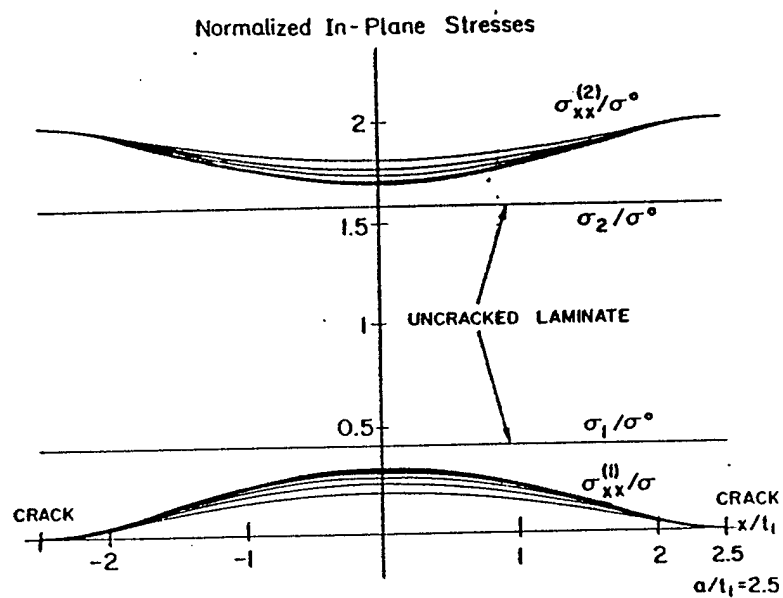


Figure 6. In-plane stresses in layers

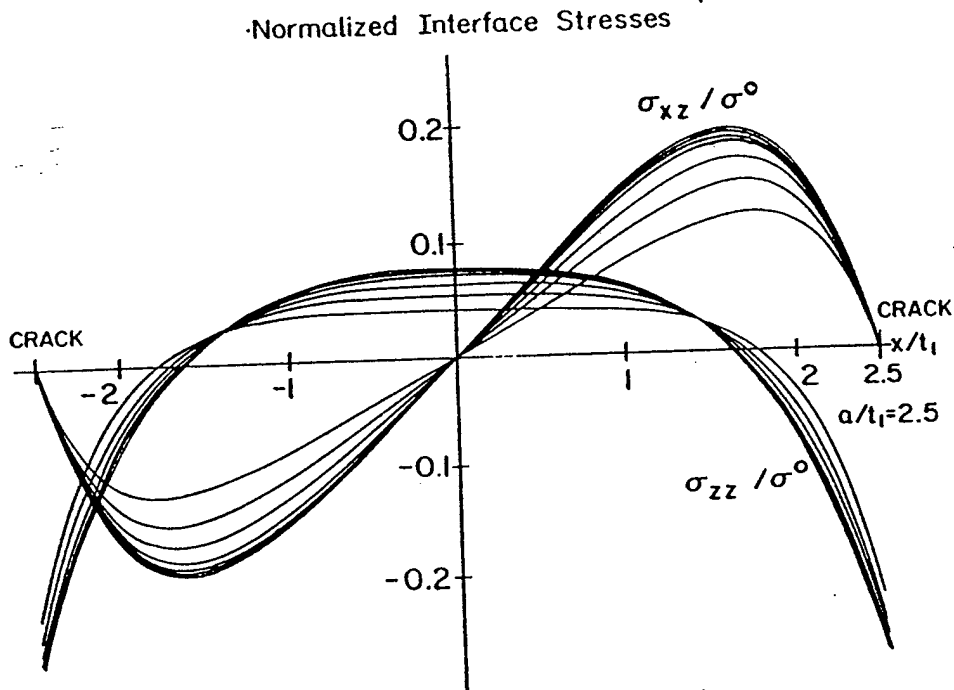


Figure 7. Interface stresses

## 5. Conclusion

Previously developed variational analysis of cracked laminates has been extended to the case of imperfect interlaminar interface by use of a generalized thermo-elastic variational principle for imperfect interface. In the present work detailed analysis has been confined to a cross-ply laminate in which only the  $90^\circ$  layer is cracked. But there is no difficulty to carry out similar analysis with imperfect interface for the case when all layers are cracked, on the basis of the admissible stress system which has been constructed in Hashin (1987) for orthogonally cracked laminates. It is also a straightforward matter to analyze mechanical and thermal stresses.

Present analysis has shown that for a cracked laminate with interlaminar interface which is imperfect in shear only, the quantitative effect of interface imperfection on effective Young's modulus and TEC is not drastic, but there is significant effect on the effective shear modulus and internal interlaminar stresses.



### Acknowledgement

Support of the Air Force Office of Scientific Research, Dr. Walter Jones contract monitor, through the Materials Sciences Corporation is gratefully acknowledged.

### References

- Hashin, Z.(1985) Analysis of cracked laminates: a variational approach, *Mechanics of Materials*, 4, 121-136
- Hashin, Z.(1987) Analysis of orthogonally cracked laminates under tension, *J.Appl.Mech.*, 54, 872-879
- Hashin, Z.(1988) Thermal expansion coefficients of cracked laminates, *Comp.Sci.Tech.*,31, 247-260
- Hashin, Z.(1990) Thermoelastic properties of fiber composites with imperfect interface, *Mechanics of Materials*,8, 333-348
- Hashin, Z.(1992) Extremum principles for elastic heterogeneous media with imperfect interfaces and their application to bounding of effective moduli, *J.Mech.Phys.Solids*,40, 767-781
- Laws, N. and Dvorak, G.J.(1988) Progressive transverse cracking in composite laminates, *J.Comp.Mat.*,22, 900-916
- Lee, J.W., Allen, D.H. and Harris, C.E.(1989) Internal state variable approach for predicting stiffness reductions in fibrous laminated composites with matrix cracks, *J.Comp.Mat.*,23, 1273-1291
- Levin, V.M. (1967) On the coefficients of thermal expansion in heterogeneous materials, *Mechanics of Solids* (translation of *Mekhanika Tverdogo Tela*), 2, 58-61.
- McCartney, L.N.(1992) Theory of stress transfer in a  $0^0 - 90^0 - 0^0$  cross-ply laminate containing a parallel array of transverse cracks, *J.Mech.Phys.Solids*,40, 27-68
- Nairn, J.A., Hu, S. and Jong, S.B., (1993) A critical evaluation of theories for predicting microcracking in composite laminates, *J.Mat.Sci.* 28, 5099-5111
- Reifsnider, K.L. and Jamison, R.(1982) Fracture of fatigue-loaded composite laminates, *Int.J.Fatigue*,6, 187-197
- Tsai, C.L., Daniel, I.M. and Lee, J.W.(1990) Progressive matrix cracking of crossply composite laminates under biaxial loading, in G.J.Dvorak and D.C.Lagoudas (eds.), *Microcracking-Induced Damage in Composites*, AMD-Vol.111, ASME, New York, pp.9-18
- Varna, J. and Berglund, L.A.(1994) Thermo-elastic properties of composite laminates with transverse cracks, *J.Comp.Tech.Res.*, 16, 77-87

DIFFERENTIAL SCHEME FOR EFFECTIVE THERMOELASTIC  
PROPERTIES OF CRACKED COMPOSITE MATERIALS

V. Vinogradov and Z. Hashin

# **Differential Scheme for Effective Thermoelastic Properties of Cracked Composite Materials**

## **Introduction**

Analytical determination of effective properties of composite materials containing randomly oriented microcracks becomes a much more difficult problem than the problem of small crack density discussed in the previous chapter. An undefined microgeometry and interaction between constituents make the simple analytical approach, like in the above-mentioned case, to be inapplicable. Thus, we must resort to an approximate scheme. In this chapter the differential scheme (DS) approximation will be applied to predict effective thermoelastic properties of composite materials containing microcracks.

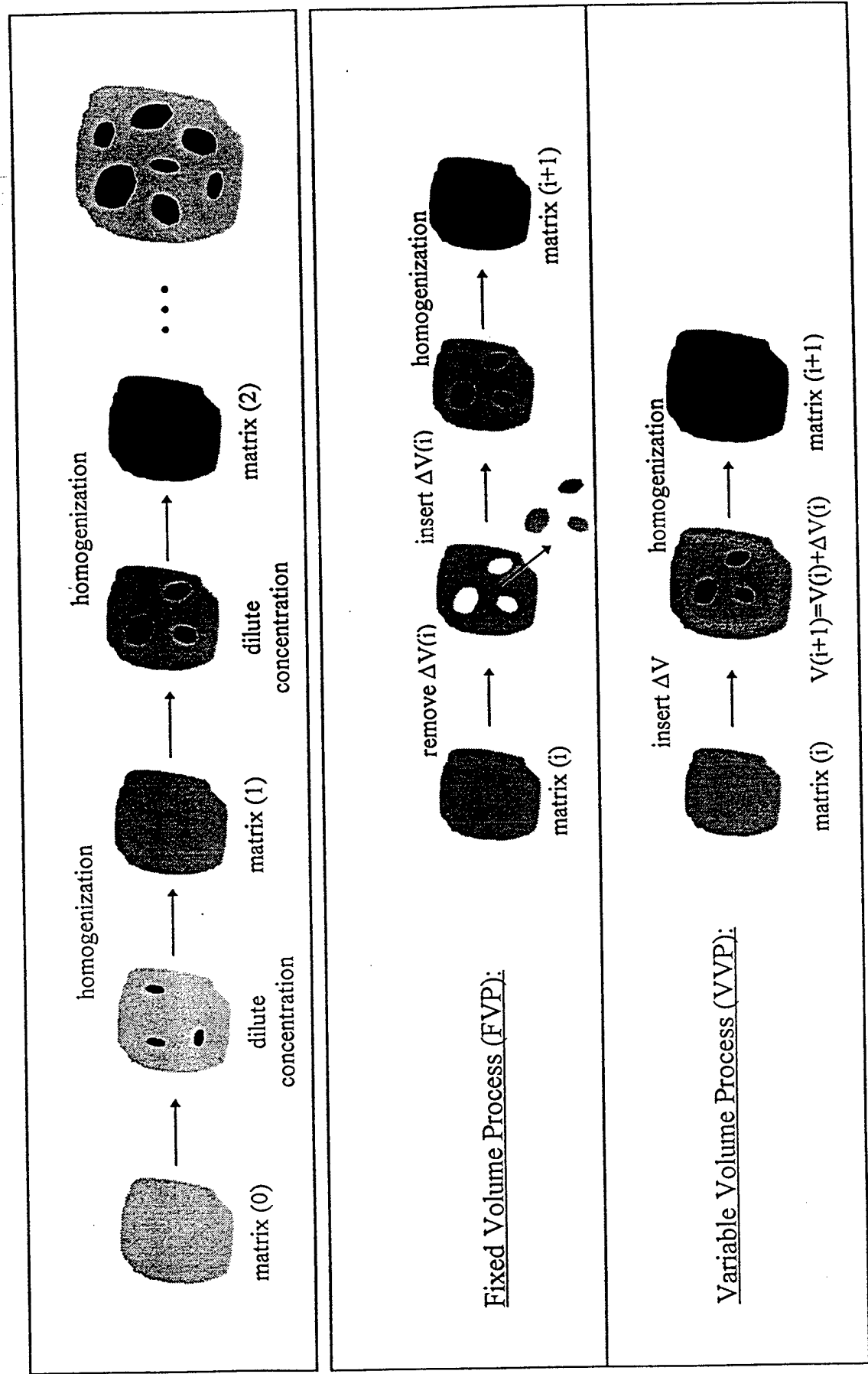
The DS is based on the notion of incremental construction of the composite material

by gradual addition of infinitesimal amounts of inclusions. According to this idea, for a two-phase composite of material 1 with moduli  $C^{(1)}$  and material 2 with moduli  $C^{(2)}$ , we start with homogeneous matrix material 1. Then, inclusions of phase 2 are embedded in the matrix in such a way that the inclusions are in dilute suspensions. This results in effective moduli  $C^*$  which may be obtained by the well-known solution for dilute concentration of inclusions. The next stage consists of imbedding grains of phase 2, that are in order of magnitude larger than the previous ones (so that the fundamental assumption that they "see" an effective medium with moduli  $C^*$  is quite accurate), and so on. The DS hierarchy of composites continues until phase 2 occupies its correct volume fraction.

We shall describe a procedure whereby a  $N$ -phase composite can be realized. The first of the two procedures considered here is characterized by keeping the volume of the composite fixed at during the entire process, called the Fixed Volume Process (FVP), and in the second, the volume of the composite is allowed to increase, the Variable Volume Process (VVP). A schematic representation of the processes is shown in Fig.3.1. It will be shown that both of the processes lead to the same canonical equations for the effective moduli.

Let us begin with volume  $V_0$  of material 0, an anisotropic, homogeneous, linear elastic solid with elastic moduli tensor  $C^{(0)}$ , which we refer to as the "backbone" material. Grains of materials  $1, 2, \dots, N$  are imbedded in material 0 in such a way that the volume remains fixed at  $V_0$ . This involves removing and replacing some of the original material (FVP). Materials  $1, 2, \dots, N$  are also anisotropic, homogeneous, linear elastic with moduli  $C^{(k)}$ ,  $k = 1, 2, \dots, N$ . The composite now has a new modulus tensor  $C^*$ , different from

Figure 3.1: The iterative construction process of the differential scheme.



$C^{(0)}$ . The construction process continues by removing the current material and replacing it with grains of the  $N$  materials until the phase volume fractions  $v_k$  reach their desired values  $v_k^f$ .

Let  $v_0, v_1, v_2, \dots, v_N$  be the current volume fractions of the materials  $0, 1, 2, \dots, N$  respectively, such that

$$v_0 + v_1 + v_2 + \dots + v_N = 1 \quad (3.1)$$

At each replacement the removed material must have the same volume fractions of the materials  $0, 1, 2, \dots, N$  as in the total volume. Thus, at each stage the material is assumed to be homogeneous. This can be realized if the replacement grains are an order of magnitude greater in size than those at the previous replacement. In addition, the grains must be dispersed at random and occupy an infinitesimal volume fraction.

Let the process be parameterized by an artificial parameter  $t$ , which is analogous to time. The origin of the time is conveniently chosen so that

$$v_k(t = 0) = 0, \quad (k = 1, 2, \dots, N). \quad (3.2)$$

For each  $t$  the material is homogeneous, i.e. any unit volume of the composite contains  $v_k(t)$  of material  $k$ .

The volume  $\Delta V(t)$  of the material removed at any time  $t$  is replaced with volumes  $\Delta V_k(t)$  such that

$$\Delta V_1(t) + \Delta V_2(t) + \dots + \Delta V_N(t) = \sum_{k=1}^N \Delta V_k(t) = \Delta V(t) \quad (3.3)$$

After the replacement the volume of material  $k$  is

$$V [v_k(t) + \Delta v_k(t)] = V v_k(t) - v_k(t) \sum_{i=1}^N \Delta V_i(t) + \Delta V_k(t) \quad (3.4)$$

where  $V = V_0$  is the volume of the composite, the first term in the right part of the equality is the volume of phase  $k$  before the replacement, the second term defines the removed volume and the third one represents the added volume of phase  $k$ . This relates the increments in volume fractions  $v_k(t)$  to the corresponding increments in  $V_k(t)$ . When  $\Delta V(t)$  is small, these equations assume the form

$$V \dot{v}_k(t) = \dot{V}_k(t) - v_k(t) \sum_{i=1}^N \dot{V}_i(t) \quad (3.5)$$

where  $\dot{f}(t) \equiv \frac{d}{dt}f(t)$ . This relation between  $\dot{V}_k(t)$ ,  $v_k(t)$  and  $\dot{v}_k(t)$  can be inverted to give  $\dot{V}_k(t)$  as:

$$\frac{\dot{V}_k(t)}{V} = \dot{v}_k(t) + v_k(t) \frac{\dot{v}(t)}{1 - v(t)} \quad (3.6)$$

where  $v(t) = \sum_{i=1}^N v_i(t)$ ,  $\dot{v}(t) = \sum_{i=1}^N \dot{v}_i(t)$ .

For the VVP process the same relation may be obtained taking into account that  $V$  is allowed to increase. Begin at  $t = 0$  with an initial volume  $V_0$ . At each step of the homogenization, incremental volumes  $\Delta V_k(t)$  of materials  $1, 2, \dots, N$  are added to the current total volume  $V(t) = V_0 + \sum_{k=1}^N V_k(t)$ . The volume fraction of material  $k$  is defined as

$$v_k(t) = \frac{V_k(t)}{V(t)} \quad (3.7)$$

Now we are retaining all the added material within the mixture. The derivative of (3.7)

with respect to time  $t$  has the same form as for the FVP:

$$\dot{v}_k(t) = \frac{\dot{V}_k(t) V(t) - V_k(t) \dot{V}(t)}{V(t)^2} = \frac{\dot{V}_k(t)}{V(t)} - \frac{v_k(t)}{V(t)} \sum_{i=1}^N \dot{V}_i(t)$$

Consequently the expressions for  $\dot{V}_k(t)/V(t)$  are the same as (3.6)

$$\frac{\dot{V}_k(t)}{V(t)} = \dot{v}_k(t) + v_k(t) \frac{\dot{v}(t)}{1 - v(t)}$$

with the only difference that the constant  $V$  in (3.6) is replaced here with  $V(t)$ , which is a function of  $t$ .

When the small amount of inclusions  $\Delta V(t)$  is added to the homogeneous material with stiffness  $\mathbf{C}^*(t)$  and compliance  $\mathbf{S}^*(t)$  the incremental change in the moduli is given by

$$\begin{aligned} \Delta \mathbf{C}^*(t) &= \sum_{k=1}^N (\mathbf{C}^{(k)} - \mathbf{C}^*(t)) \mathbf{A}^{(k)}(t) \frac{\Delta V_k}{V}(t) \\ \Delta \mathbf{S}^*(t) &= \sum_{k=1}^N (\mathbf{S}^{(k)} - \mathbf{S}^*(t)) \mathbf{B}^{(k)}(t) \frac{\Delta V_k}{V}(t) \end{aligned}$$

where  $\mathbf{A}^{(k)}(t)$  and  $\mathbf{B}^{(k)}(t)$  are fourth rank concentration tensors evaluated for dilute concentration of the inclusions in the matrix with moduli  $\mathbf{C}^*(t)$ , and defined by the linearity relations

$$\bar{\boldsymbol{\varepsilon}}^{(k)} = \mathbf{A}^{(k)}(t) \bar{\boldsymbol{\varepsilon}}$$

$$\bar{\boldsymbol{\sigma}}^{(k)} = \mathbf{B}^{(k)}(t) \bar{\boldsymbol{\sigma}}$$

Here  $\bar{\boldsymbol{\varepsilon}}^{(k)}$  and  $\bar{\boldsymbol{\sigma}}^{(k)}$  are average strain and average stress over phase  $k$ , the first when  $\bar{\boldsymbol{\varepsilon}}$  is



prescribed and the second when  $\bar{\sigma}$  is prescribed. In the limit as  $t \rightarrow 0$  we have

$$\begin{aligned}\dot{C}^*(t) &= \sum_{k=1}^N \left( C^{(k)} - C^*(t) \right) A^{(k)}(t) \frac{\dot{V}_k}{V}(t) \\ \dot{S}^*(t) &= \sum_{k=1}^N \left( S^{(k)} - S^*(t) \right) B^{(k)}(t) \frac{\dot{V}_k}{V}(t)\end{aligned}\tag{3.8}$$

where  $\frac{\dot{V}_k}{V}(t)$  are defined by (3.6). Because the relation  $\frac{\dot{V}_k}{V}(t)$  is common for both the FVP and the VVP, differential equations (3.8) are said to be canonical equations of the DS, independent of the specific material replacement process. Integration of (3.8) with use of initial conditions  $C^*(t=0) = C^{(0)}$  and  $S^*(t=0) = S^{(0)}$  gives the effective elastic moduli of multi-phase composite material.

It must be noted, that functions  $v_k(t)$  describe a path in the  $(v_1, v_2, \dots, v_N)$  space as  $t$  varies, and  $t$  may be considered as an arc length parameter. The path begins at the origin, it is restricted by the plane  $v_1 + v_2 + \dots + v_N = 1$  and terminates at the point  $(v_1^f, v_2^f, \dots, v_N^f)$ , which is associated with volume the fractions of the phases in the composite under consideration. An example of such a path for a three-phase composite is shown in Fig.3.2. It is apparent that any arbitrary functions  $v_k(t)$ , which lead to the same path in the  $(v_1, v_2, \dots, v_N)$  space, will give equal results for the effective moduli. Additional relations between the variables  $v_k(t)$  and  $V_k(t)$  for the construction procedures described above are given in NORRIS [20] and NORRIS et al. [21]. An explanation of the distinction between paths will be given in section 3.3.

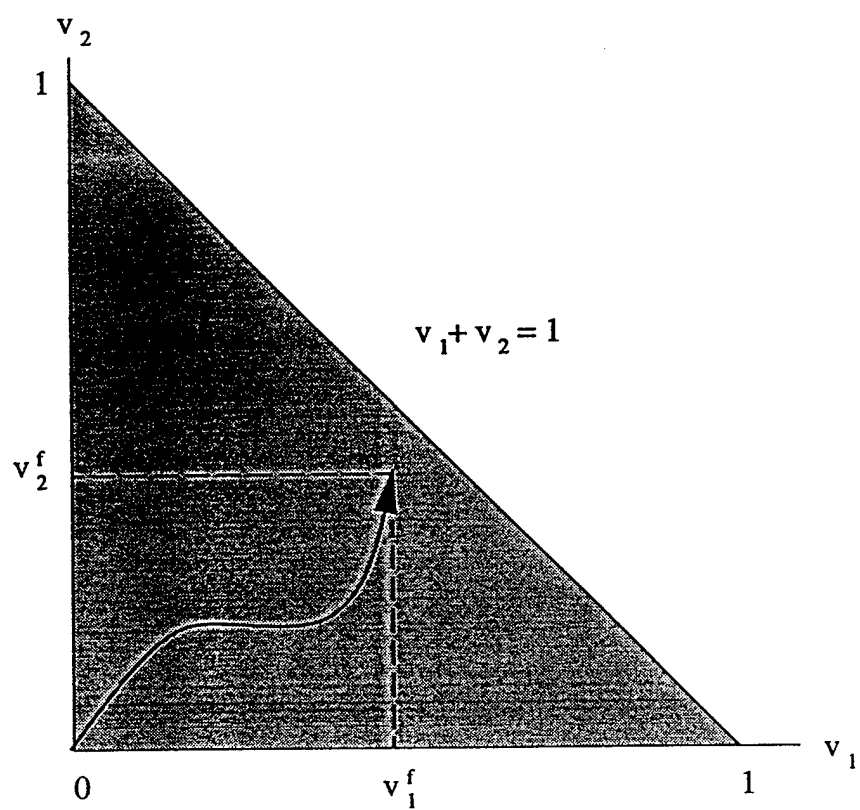


Figure 3.2: A homogenization path in the  $(v_1, v_2)$  plane.

## 3.2 Effective Thermal Expansion Coefficients

### 3.2.1 Development of Effective Thermal Properties

Consider a heterogeneous body of volume  $V$  subjected to temperature change  $\varphi$  (Fig.3.3). The body consists of an arbitrary anisotropic matrix 0 with moduli  $C^{(0)}$  and thermal expansion coefficients  $\alpha^{(0)}$ , and inclusions with moduli  $C^{(k)}$  ( $k = 1, 2, \dots, N$ ) and thermal expansion coefficients  $\alpha^{(k)}$ . At each point of the body the stresses and strains are related by

$$\begin{aligned}\epsilon(x) &= S(x)\sigma(x) + \alpha(x)\varphi \\ \sigma(x) &= C(x)\epsilon(x) + \Gamma(x)\varphi\end{aligned}\tag{3.9}$$

where  $\Gamma(x) = -C(x)\alpha(x)$  and  $S(x) = C^{-1}(x)$  is the compliance tensor. For given boundary conditions ( $T(S) = 0$ ;  $\varphi$ ) the average stresses and strains are defined by

$$\begin{aligned}\bar{\epsilon} &= \frac{1}{V} \int_V \epsilon(x) dV = \frac{1}{V} \int_{\Delta V} \epsilon(x) dV + \frac{1}{V} \int_{V-\Delta V} \epsilon(x) dV = \alpha^* \varphi \\ \bar{\sigma} &= \frac{1}{V} \int_V \sigma(x) dV = \frac{1}{V} \int_{\Delta V} \sigma(x) dV + \frac{1}{V} \int_{V-\Delta V} \sigma(x) dV = 0\end{aligned}\tag{3.10}$$

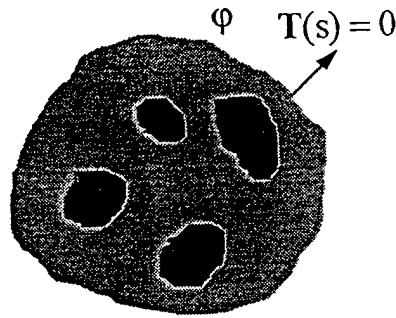


Figure 3.3: A composite body under temperature change  $\varphi$  ( $T(S) = 0$ ).

where  $\alpha^*$  are the effective thermal expansion coefficients of the composite,  $\Delta V$  defines the volume of inclusions and  $V - \Delta V$  defines the volume of the matrix. After substitution of (3.9a), the last equality in (3.10a) may be rewritten in the form

$$\begin{aligned}\alpha^* \varphi V &= \int_{\Delta V} \epsilon(\mathbf{x}) dV + \int_{V-\Delta V} \epsilon(\mathbf{x}) dV \\ &= \int_{\Delta V} [\mathbf{S}(\mathbf{x}) \sigma(\mathbf{x}) + \alpha(\mathbf{x}) \varphi] dV + \int_{V-\Delta V} [\mathbf{S}^{(0)} \sigma(\mathbf{x}) + \alpha^{(0)} \varphi] dV\end{aligned}$$

and by using the fact that the average stress is equal to zero (3.10b) we obtain the following result:

$$\alpha^* \varphi V = \alpha^{(0)} \varphi V + \int_{\Delta V} [\mathbf{S}(\mathbf{x}) - \mathbf{S}^{(0)}] \sigma(\mathbf{x}) dV + \int_{\Delta V} [\alpha(\mathbf{x}) - \alpha^{(0)}] \varphi dV \quad (3.11)$$

Because the compliance tensor  $\mathbf{S}(\mathbf{x})$  is a piecewise constant function, the integration in this equation may be replaced by the sum:

$$\alpha^* \varphi = \alpha^{(0)} \varphi + \sum_{k=1}^N [\mathbf{S}^{(k)} - \mathbf{S}^{(0)}] \frac{1}{V} \int_{\Delta V} \sigma(\mathbf{x}) dV + \sum_{k=1}^N [\alpha^{(k)} - \alpha^{(0)}] \varphi \frac{\Delta V_k}{V} \quad (3.12)$$

Now recalling the definition of average stress, this equation may be rewritten in the form

$$\alpha^* \varphi = \alpha^{(0)} \varphi + \sum_{k=1}^N [\mathbf{S}^{(k)} - \mathbf{S}^{(0)}] \bar{\sigma} \frac{\Delta V_k}{V} + \sum_{k=1}^N [\alpha^{(k)} - \alpha^{(0)}] \varphi \frac{\Delta V_k}{V} \quad (3.13)$$

or eliminating the temperature  $\varphi$  we obtain the exact result

$$\Delta \alpha = \sum_{k=1}^N [\mathbf{S}^{(k)} - \mathbf{S}^{(0)}] \mathbf{b}^{(k)} \frac{\Delta V_k}{V} + \sum_{k=1}^N [\alpha^{(k)} - \alpha^{(0)}] \frac{\Delta V_k}{V} \quad (3.14)$$

where  $\Delta\alpha = \alpha^* - \alpha^{(0)}$  and  $\mathbf{b}^{(k)}$  is a second rank tensor defined as the average stress in phase  $k$  due to an applied unit temperature change:

$$\bar{\sigma}^{(k)} = \mathbf{b}^{(k)}\varphi \quad (3.15)$$

Now return to the DS described in the previous section and consider the DS construction process at any instant of time  $t$ . An addition of inclusions of volume  $\Delta V$  to the homogeneous material with overall moduli  $\mathbf{C}^*$  and TEC  $\alpha^*$  will lead to the change of overall TEC  $\Delta\alpha^*$ , which according to (3.14) assumes the form

$$\Delta\alpha^*(t) = \sum_{k=1}^N [\mathbf{S}^{(k)} - \mathbf{S}^*(t)] \mathbf{b}^{(k)}(t) \frac{\Delta V_k}{V}(t) + \sum_{k=1}^N [\alpha^{(k)} - \alpha^*(t)] \frac{\Delta V_k}{V}(t) \quad (3.16)$$

In the framework of the DS, at each step of the construction process only infinitesimal amount of inclusions is embedded in the homogeneous material obtained at the previous step. Thus, equation (3.16) may be parameterized by the artificial time  $t$

$$\dot{\alpha}^*(t) = \sum_{k=1}^N [\mathbf{S}^{(k)} - \mathbf{S}^*(t)] \mathbf{b}^{(k)}(t) \frac{\dot{V}_k}{V}(t) + \sum_{k=1}^N [\alpha^{(k)} - \alpha^*(t)] \frac{\dot{V}_k}{V}(t) \quad (3.17)$$

and tensor  $\mathbf{b}^{(k)}(t)$  may be obtained by solving the problem where dilute concentration of inclusions of phase  $k$  is embedded into the matrix with effective properties  $\mathbf{C}^*(t)$  and  $\alpha^*(t)$ .

The differential equations (3.17) may be simplified by resorting to the so-called *decomposition scheme*, proposed by BENVENISTE & DVORAK [23]. According to their result, the concentration tensor  $\mathbf{b}^{(k)}$  can be uniquely determined in terms of the fourth rank

concentration tensor  $\mathbf{B}^{(k)}$  which relates the stresses in phase  $k$  to the external applied homogeneous traction  $T_i(S) = \sigma_{ij}^0 n_j$ , and is defined as

$$\bar{\sigma}^{(k)} = \mathbf{B}^{(k)} \sigma^0.$$

Their result can be rewritten for our case in the form

$$\mathbf{b}^{(k)}(t) = (\mathbf{B}^{(k)}(t) - \mathbf{I}) (\mathbf{S}^{(k)} - \mathbf{S}^*(t))^{-1} (\alpha^{(k)} - \alpha^*(t)) \quad (3.18)$$

where  $\mathbf{I}$  is the fourth-order unit tensor. Substitution of this relation into (3.17) leads us to following differential equations for components of the effective TEC tensor

$$\dot{\alpha}^*(t) = \sum_{k=1}^N (\mathbf{S}^{(k)} - \mathbf{S}^*(t)) \mathbf{B}^{(k)}(t) (\mathbf{S}^{(k)} - \mathbf{S}^*(t))^{-1} (\alpha^{(k)} - \alpha^*(t)) \frac{\dot{V}_k}{V}(t) \quad (3.19)$$

when  $\frac{\dot{V}_k}{V}(t)$  is defined by

$$\frac{\dot{V}_k}{V}(t) = \dot{v}_k(t) + v_k(t) \frac{\dot{v}(t)}{1 - v(t)}$$

Equations (3.19) and (3.8b) and the additional initial conditions  $\alpha^*(t=0) = \alpha^{(0)}$  give a set of coupled differential equations for estimation of the effective thermoelastic moduli of multi-phase composites.

Now assume alternative boundary conditions, when homogeneous displacements  $\mathbf{u}(S) = \varepsilon^0 \mathbf{x} = 0$  are applied to the external surface of the body (see Fig.3.4). In this case the expressions for  $\bar{\varepsilon}$  and  $\bar{\sigma}$  becomes

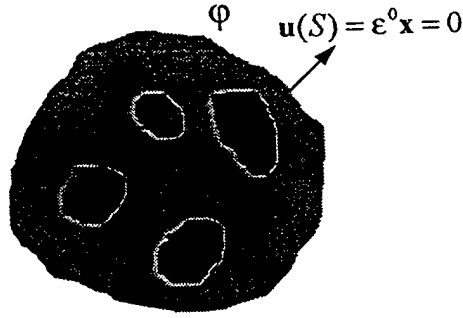


Figure 3.4: A composite body under temperature change  $\varphi$  ( $u(S) = 0$ ).

$$\begin{aligned}\bar{\varepsilon} &= \frac{1}{V} \int_V \varepsilon(\mathbf{x}) dV = 0 \\ \bar{\sigma} &= \frac{1}{V} \int_V \sigma(\mathbf{x}) dV = \Gamma^* \varphi,\end{aligned}\tag{3.20}$$

Analogous consideration of the problem results in the following set of coupled differential equations for components of tensor  $\Gamma^*$

$$\dot{\Gamma}^*(t) = \sum_{k=1}^N \left( C^{(k)} - C^*(t) \right) A^{(k)}(t) \left( C^{(k)} - C^*(t) \right)^{-1} \left( \Gamma^{(k)} - \Gamma^*(t) \right) \frac{\dot{V}_k}{V}(t) \tag{3.21}$$

which together with (3.8a) and the initial conditions  $\Gamma^*(t = 0) = \Gamma^{(0)}$  may be used to predict the overall thermal stress tensor  $\Gamma^*$ .

### 3.2.2 Proof of Consistency

It is required to prove that  $\alpha^*$  and  $\Gamma^*$  as predicted by (3.19) and (3.21) are mutually reciprocal in the sense that

$$\Gamma^* = -C^* \alpha^* \tag{3.22}$$

If the effective thermoelastic moduli obey this relation at the endpoint of the DS homogenization process, it must also be satisfied at each instant  $t$

$$\mathbf{\Gamma}^*(t) = -\mathbf{C}^*(t)\boldsymbol{\alpha}^*(t) \quad (3.23)$$

Let us take the derivative of  $\mathbf{\Gamma}^*(t)$  with respect to time  $t$

$$\frac{d}{dt}\mathbf{\Gamma}^*(t) = -\frac{d}{dt}(\mathbf{C}^*(t)\boldsymbol{\alpha}^*(t)) = -\frac{d}{dt}\mathbf{C}^*(t)\boldsymbol{\alpha}^*(t) - \mathbf{C}^*(t)\frac{d}{dt}\boldsymbol{\alpha}^*(t) \quad (3.24)$$

Substituting expressions (3.19) and (3.8a) for  $\dot{\boldsymbol{\alpha}}^*(t)$  and  $\dot{\mathbf{C}}^*(t)$  respectively into (3.24) we obtain

$$\begin{aligned} \dot{\mathbf{\Gamma}}^*(t) = & -\sum_{k=1}^N (\mathbf{C}^{(k)} - \mathbf{C}^*(t)) \mathbf{A}^{(k)}(t) \boldsymbol{\alpha}^*(t) \frac{\dot{V}_k}{V} \\ & - \sum_{k=1}^N \mathbf{C}^*(t) (\mathbf{S}^{(k)} - \mathbf{S}^*(t)) \mathbf{B}^{(k)}(t) (\mathbf{S}^{(k)} - \mathbf{S}^*(t))^{-1} (\boldsymbol{\alpha}^{(k)} - \boldsymbol{\alpha}^*(t)) \frac{\dot{V}_k}{V} \end{aligned} \quad (3.25)$$

which after simplification of the right side may be rewritten in the form

$$\begin{aligned} \dot{\mathbf{\Gamma}}^*(t) = & -\sum_{k=1}^N (\mathbf{C}^{(k)} - \mathbf{C}^*(t)) \mathbf{A}^{(k)}(t) \\ & \times \left[ \boldsymbol{\alpha}^*(t) - \mathbf{S}^*(t) (\mathbf{S}^{(k)} - \mathbf{S}^*(t))^{-1} (\boldsymbol{\alpha}^{(k)} - \boldsymbol{\alpha}^*(t)) \right] \frac{\dot{V}_k}{V} \end{aligned} \quad (3.26)$$

where the relation between concentration factor tensors  $\mathbf{B}^{(k)}(t)$  and  $\mathbf{A}^{(k)}(t)$ , given for dilute concentration of inclusions as

$$\mathbf{B}^{(k)}(t) = \mathbf{C}^{(k)} \mathbf{A}^{(k)}(t) \mathbf{S}^*(t), \quad (3.27)$$



was used. Recalling the equality  $C^*(t) S^*(t) = I$  proved for the DS by HASHIN [14] and the identity that results from it:

$$S^*(t) (S^{(k)} - S^*(t))^{-1} = - (C^{(k)} - C^*(t))^{-1} C^{(k)},$$

differential equations (3.26) reduce to

$$\dot{I}^*(t) = \sum_{k=1}^N (C^{(k)} - C^*(t)) A^{(k)}(t) (C^{(k)} - C^*(t))^{-1} (\Gamma^{(k)} - \Gamma^*(t)) \frac{\dot{V}_k}{V}(t),$$

which faithfully copies (3.21) obtained by direct treatment of (3.20).

This proves that (3.23) is satisfied and completes the self-consistency of the DS.

### 3.2.3 Levin's Formula

Consider a two-phase material which consists of the matrix with compliance  $S^{(0)}$  and thermal expansion coefficients  $\alpha^{(0)}$ , and inclusions with compliance  $S^{(1)}$  and TEC  $\alpha^{(1)}$ .

In this case equations (3.8b) and (3.19) reduce to

$$\begin{aligned} \dot{S}^*(t) &= (S^{(1)} - S^*(t)) B^{(1)}(t) \frac{\dot{v}_1(t)}{1 - v_1(t)} \\ \dot{\alpha}^*(t) &= (S^{(1)} - S^*(t)) B^{(1)}(t) (S^{(1)} - S^*(t))^{-1} (\alpha^{(1)} - \alpha^*(t)) \frac{\dot{v}_1(t)}{1 - v_1(t)} \end{aligned}$$

Eliminating the common multipliers from these equations we obtain

$$\dot{\alpha}^*(t) = \dot{S}^*(t) (S^{(1)} - S^*(t))^{-1} (\alpha^{(1)} - \alpha^*(t)) \quad (3.28)$$

Now define

$$\mathbf{x}(t) = \boldsymbol{\alpha}^{(1)} - \boldsymbol{\alpha}^*(t)$$

$$\mathbf{Y}(t) = \mathbf{S}^{(1)} - \mathbf{S}^*(t)$$

Accordingly, the derivatives of these tensors with respect to  $t$  are

$$\dot{\mathbf{x}}(t) = -\dot{\boldsymbol{\alpha}}^*(t)$$

$$\dot{\mathbf{Y}}(t) = -\dot{\mathbf{S}}^*(t)$$

and equations (3.28) assume the form

$$\dot{\mathbf{x}}(t) = \dot{\mathbf{Y}}(t) \mathbf{Y}(t)^{-1} \mathbf{x}(t) \quad (3.29)$$

The solution of these coupled differential equations may be written as

$$\mathbf{x}(t) = \mathbf{Y}(t) \mathbf{Y}(t)^{-1} \mathbf{x}(t) = \mathbf{Y}(t) \mathbf{z}(t)$$

where  $\mathbf{z}(t) = \mathbf{Y}(t)^{-1} \mathbf{x}(t)$ . Substitution of this into (3.29) leads to

$$\dot{\mathbf{Y}}(t) \mathbf{z}(t) + \mathbf{Y}(t) \dot{\mathbf{z}}(t) = \dot{\mathbf{Y}}(t) \mathbf{Y}(t)^{-1} \mathbf{Y}(t) \mathbf{z}(t)$$

Noting that the expression in the right side and the first term in the left one are equal, we obtain

$$\mathbf{Y}(t) \dot{\mathbf{z}}(t) = 0$$

which results in the following simple form for  $z(t)$

$$z_{ij}(t) = c_{ij} = \text{const.}$$

Therefore

$$\mathbf{x}(t) = \mathbf{Y}(t) \mathbf{c} \quad (3.30)$$

and recalling the definitions of  $\mathbf{x}(t)$  and  $\mathbf{Y}(t)$  we can rewrite (3.30) in the form

$$\boldsymbol{\alpha}^*(t) = \boldsymbol{\alpha}^{(1)} - (\mathbf{S}^{(1)} - \mathbf{S}^*(t)) \mathbf{c} \quad (3.31)$$

where  $c_{ij}$  may be found from the initial conditions at  $t = 0$ :

$$\boldsymbol{\alpha}^*(t = 0) = \boldsymbol{\alpha}^{(0)}$$

$$\mathbf{S}^*(t = 0) = \mathbf{S}^{(0)}$$

It follows that

$$\mathbf{c} = -(\mathbf{S}^{(2)} - \mathbf{S}^{(1)})^{-1} (\boldsymbol{\alpha}^{(1)} - \boldsymbol{\alpha}^{(2)})$$

which together with (3.31) yields the relation between  $\boldsymbol{\alpha}^*(t)$  and  $\mathbf{S}^*(t)$  at any instant  $t$

$$\boldsymbol{\alpha}^*(t) = \boldsymbol{\alpha}^{(1)} + (\mathbf{S}^{(1)} - \mathbf{S}^*(t)) (\mathbf{S}^{(2)} - \mathbf{S}^{(1)})^{-1} (\boldsymbol{\alpha}^{(1)} - \boldsymbol{\alpha}^{(2)})$$

and consequently at the endpoint of the homogenization process

$$\boldsymbol{\alpha}^* = \boldsymbol{\alpha}^{(1)} + (\mathbf{S}^{(1)} - \mathbf{S}^*) (\mathbf{S}^{(2)} - \mathbf{S}^{(1)})^{-1} (\boldsymbol{\alpha}^{(1)} - \boldsymbol{\alpha}^{(2)}) \quad (3.32)$$

This result is the well-known Levin's formula (see LEVIN [24]). It is interesting to note, that the result of the DS approximation satisfies Levin's formula, which is precise for any two-phase statistically homogeneous composite material with completely arbitrary phase geometry and elastic symmetry.

### 3.3 Path dependence of the homogenization process

The coupled systems of differential equations (3.8a),(3.8b),(3.19) and (3.21) depend upon the path we choose to consider in the  $(v_1, v_2, \dots, v_N)$  space. In fact, two different paths from the origin to the same endpoint  $(v_1^f, v_2^f, \dots, v_N^f)$  will, in general, not give the same result at the endpoint. In this section an effort will be made to explain the distinction between paths.

The key to the present consideration is the idea of realization, introduced by MILTON [25]. An approximate scheme is called realizable if we can describe a construction process to make a composite material with effective moduli predicted by the scheme. Thus, the Hashin-Shtrikman bounds for the bulk modulus of a two phase randomly disordered solid can be realized through the well known packed-spheres geometry (e.g. HASHIN [26]).

Let us list the features of the inner structure of composite materials, obtained by the DS construction processes described above.

- 1) The essential characteristic is the diversity of inclusion sizes.
- 2) Inclusions of each size are in dilute concentration,
- 3) They are dispersed at random and sufficiently separated.

The first feature suggested by ROSCOE [27] arises from the fact that at each construction step the composite has to look homogeneous to the inclusions being inserted, which is possible only if the inclusions are increasing in size at each succeeding step of the construction process. More specifically, the size of inserted inclusions must be comparable to the representative volume element (RVE) size.

From this point of view, different paths in the  $(v_1, v_2, \dots, v_N)$  space may be associated with different microstructures of a composite, or in other words, with different size distributions of inclusions.

Consider a composite, which satisfies the above-enumerated requirements for material microstructure. A composite of this kind contains inclusions of different sizes  $z_i$ , which may be ordered as the increasing sequence

$$z_1, z_2, z_3, \dots, z_r, \dots, z_M \quad (M \rightarrow \infty)$$

so that

$$z_1 \ll z_2 \ll z_3 \ll \dots \ll z_r \ll \dots \ll z_M$$

Each group of inclusions characterized by a common size  $z_r$  may contain a number of phases. The volume fraction of phase  $k$  in group  $r$  is denoted  $\Delta v_k^f(r)$ . In this case the following relations are satisfied

$$\begin{aligned} \sum_{r=1}^M \Delta v_k^f(r) &= v_k^f \\ \sum_{k=1}^N \Delta v_k^f(r) &= \Delta v^f(r) \end{aligned}$$

where  $\Delta v^f(r)$  is the volume fraction occupied by group  $r$ .

According to this, we can build the construction process starting with inclusions of size  $z_1$ , afterwards embedding inclusions of size  $z_2$  and so on, up to  $z_M$ , where the subscript index denotes now the step of the construction process.

First consider the VVP, according to which all the volume inserted to the composite remains till the end of the construction process and creates the final microstructure. Thus, using formula (3.7) we obtain the points  $v_k(r)$  on the homogenization path

$$v_k(r) = \frac{\sum_{i=1}^r \Delta v_k^f(i)}{v_0^f + \sum_{i=1}^r \Delta v^f(i)} \quad (3.33)$$

An example of a homogenization path built for a given 3-phase microstructure is shown in Fig.3.5. Size distribution of the inclusions' volume fractions of is shown in Fig.3.5a for phase 1 and in Fig.3.5b for phase 2. The homogenization path obtained by (3.33) is represented in Fig.3.5c.

The same equation (3.33) may be obtained from consideration of the FVP, when the volume of phase  $k$  added at step  $r$ ,  $\Delta v_k(r)$ , decreases repeatedly during the rest of the construction process. For any phase  $k$  the following relationships are satisfied.

1. The volume added at the last step  $M$  is not changed:

$$\Delta v_k(M) = \Delta v_k^f(M)$$

2. The volume added at step  $(M - 1)$  decreases because of the removing of  $\Delta v_k^f(M)$

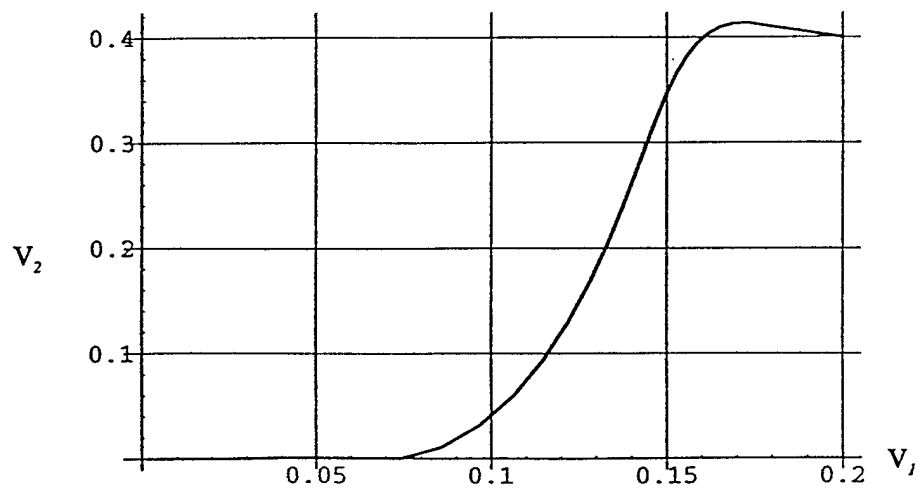
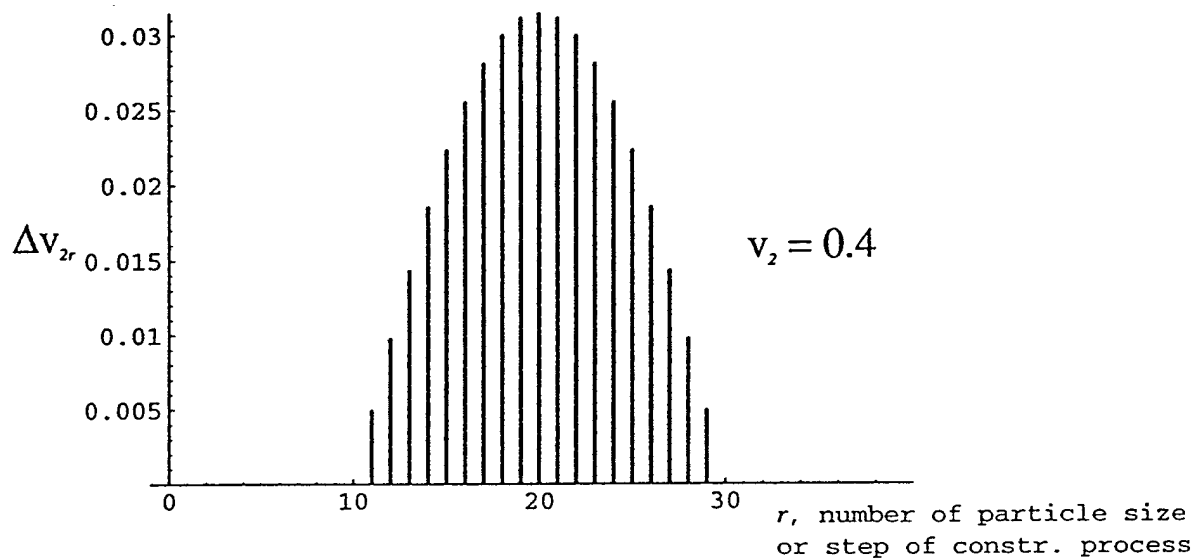
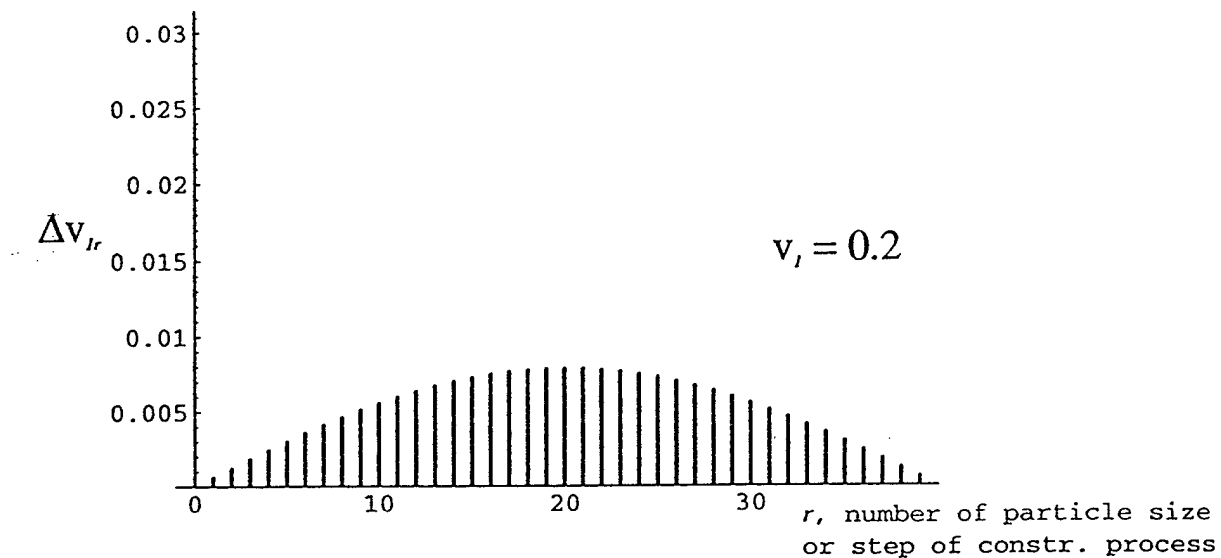


Figure 3.5: Example of particle-size distribution and corresponding

at step  $M$ :

$$\Delta v_k^f(M-1) = \Delta v_k(M-1) (1 - \Delta v(M))$$

3. The same as (2) for any step  $r$ :

$$\Delta v_k^f(r) = \Delta v_k(r) \prod_{i=r+1}^M (1 - \Delta v(i)) \quad (3.34)$$

On the other hand, the volume fraction  $\Delta v_k(m)$  of the inclusions characterized by size  $z_m$  that are added at any step  $m$  ( $m < r$ ) will decrease towards the step  $r$ , and will be equal to

$$\Delta v_k(m) \prod_{i=m+1}^r (1 - \Delta v(i))$$

Combining these expressions for  $m = 1$  to  $r$  we obtain the volume fraction of phase  $k$  at step  $r$  of the construction process

$$v_k(r) = \sum_{m=1}^r \left[ \Delta v_k(m) \prod_{i=m+1}^r (1 - \Delta v(i)) \right] \quad (3.35)$$

Substituting (3.34) into (3.35) we obtain

$$v_k(r) = \sum_{m=1}^r \left[ \Delta v_k^f(m) \frac{\prod_{i=m+1}^r (1 - \Delta v(i))}{\prod_{i=m+1}^M (1 - \Delta v(i))} \right] = \frac{\sum_{i=1}^r \Delta v_k^f(i)}{\prod_{i=r+1}^M (1 - \Delta v(i))} \quad (3.36)$$

Using again the recursion formula (3.34), the product in the denominator of this equation



can be obtained in terms of the group volume fractions at the endpoint

$$\prod_{i=r+1}^M (1 - \Delta v(i)) = 1 - \sum_{i=r+1}^M \Delta v^f(i) = v_0^f + \sum_{i=1}^r \Delta v^f(i)$$

and eventually

$$v_k(r) = \frac{\sum_{i=1}^r \Delta v_k^f(i)}{v_0^f + \sum_{i=1}^r \Delta v^f(i)}$$

which is precisely equivalent to formula (3.33) for the VVP.

This deduced relation proves that the homogenization path in the  $(v_1, v_2, \dots, v_N)$  space is uniquely determined by the *(size of inclusions)–(volume fraction of phase)* dependences, which describe the microstructure of the composite under consideration. The path is independent of choice between the construction processes discussed above, by means of which the DS is interpreted.

It must be noted, that in order that the DS equations give a reasonable approximation for effective moduli of a composite, its inner structure must comply with the above-listed requirements for the class of microgeometries obtained by the DS. If this is not the case, or if the microstructure is not defined and only volume fractions of phases are known, some assumptions of the path shape must be made to estimate the effective moduli of the composite material. For example, in the case when all inclusions have the same size, the straight line from the origin to the endpoint  $(v_1^f, v_2^f, \dots, v_N^f)$  may be chosen as a homogenization path.

In addition, we shall emphasize that details of the material microgeometry are impossible to obtain from a given path. If the unique *microstructure–path* correspondence exists, the *path–microstructure* dependence does not. As an example, the straight line

from the origin to the endpoint  $(v_1^f, v_2^f, \dots, v_N^f)$  corresponds to an infinite number of size-volume distributions, for which the phase volume fractions of inclusions of each size are in the same proportion as the volume fractions of phases in the entire composite.

### 3.4 DS for Cracked Composite Materials

The purpose of this section is to apply the DS approximation to estimate the effective thermoelastic properties of composite materials containing microcracks. It is possible to assign cracks to a special class of inclusions, and thus all the assumptions about the construction procedure can be extended to the present case. At each step of the process infinitesimal amounts of inclusions and cracks, larger in size than at the previous stages, are added to a homogeneous material. They are dispersed at random and well separated in such a way that the material remains statistically homogeneous at each instant  $t$ . Special features of a crack as an inclusion are that its stiffness vanishes  $C^c = 0$ , and it occupies an infinitesimal volume fraction  $v_c \rightarrow 0$ .

Let us rewrite equations (3.8a) and (3.19) in the form

$$\dot{C}^*(t) = \sum_{k=1}^{N+1} (C^{(k)} - C^*(t)) A^{(k)}(t) \left( \dot{v}_k(t) + v_k(t) \frac{\dot{v}(t)}{1 - v(t)} \right) \quad (3.37)$$

$$\begin{aligned} \dot{\alpha}^*(t) = & \sum_{k=1}^{N+1} (S^{(k)} - S^*(t)) C^{(k)} A^{(k)}(t) S^*(t) (S^{(k)} - S^*(t))^{-1} \\ & \times (\alpha^{(k)} - \alpha^*(t)) \left( \dot{v}_k(t) + v_k(t) \frac{\dot{v}(t)}{1 - v(t)} \right) \end{aligned} \quad (3.38)$$

where relation (3.27) was used and phase  $N + 1$  represents the cracks. Substituting  $C^c \equiv C^{(N+1)} = 0$  into these differential equations we obtain that the  $N + 1$  term in

(3.38) vanishes, and (3.37) reduces to

$$\begin{aligned}\dot{C}^*(t) = & \sum_{k=1}^N (C^{(k)} - C^*(t)) A^{(k)}(t) \left( \dot{v}_k(t) + v_k(t) \frac{\dot{v}(t)}{1 - v(t)} \right) \\ & - C^*(t) A^c(t) \left( \dot{v}_c(t) + v_c(t) \frac{\dot{v}(t)}{1 - v(t)} \right)\end{aligned}\quad (3.39)$$

with  $v = \sum_{k=1}^N v_k + v_c$ . Now multiply both side of (3.39) by  $v_c$  and perform the limit  $v_c(t) \rightarrow 0$  in such a way that the voids flatten out into cracks. Then

$$\begin{aligned}\lim_{v_c(t) \rightarrow 0} [v_c(t) \dot{C}^*(t)] = & \lim_{v_c(t) \rightarrow 0} \left[ v_c(t) \sum_{k=1}^N (C^{(k)} - C^*(t)) A^{(k)}(t) \left( \dot{v}_k(t) + v_k(t) \frac{\dot{v}(t)}{1 - v(t)} \right) \right] \\ & - C^*(t) P(t) \lim_{v_c(t) \rightarrow 0} \left( \dot{v}_c(t) + v_c(t) \frac{\dot{v}(t)}{1 - v(t)} \right)\end{aligned}\quad (3.40)$$

where  $v = \sum_{k=1}^N v_k + v_c \rightarrow \sum_{k=1}^N v_k$ , and the forth rank tensor  $P(t)$  is defined as

$$P(t) = \lim_{v_c(t) \rightarrow 0} (A^{(k)}(t) v_c(t))$$

and depends on moduli  $C^*(t)$  of the material around the cracks added at time  $t$  and the cracks' geometry.

As an example we specialize (3.40) to the important case when the cracked particulate composite material and its constituents are statistically isotropic, Fig.3.6. In this event all tensors appearing in (3.40) must be isotropic and we represent them in the convenient

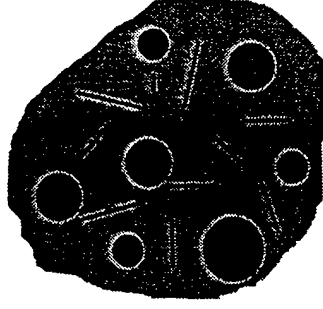


Figure 3.6: Schematic diagram for randomly distributed cracks and inclusions

form, HILL [28]

$$\begin{aligned}
 \mathbf{C} &= 3K \mathbf{I}' + 2G \mathbf{I}'' = (3K, 2G), \\
 \mathbf{A} &= (A_1, A_2), \\
 \mathbf{P} &= (P_1, P_2), \\
 I'_{ijkl} &= \frac{1}{3} \delta_{ij} \delta_{kl}, \quad I''_{ijkl} = \frac{1}{2} (\delta_{ik} \delta_{jl} + \delta_{il} \delta_{jk} - \frac{2}{3} \delta_{ij} \delta_{kl}), \\
 \mathbf{I}' \mathbf{I}' &= \mathbf{I}', \quad \mathbf{I}'' \mathbf{I}'' = \mathbf{I}'', \quad \mathbf{I}' \mathbf{I}'' = \mathbf{I}'' \mathbf{I}' = 0, \\
 \delta_{ij} I'_{ijkl} &= \delta_{kl}, \quad \delta_{ij} I''_{ijkl} = 0
 \end{aligned} \tag{3.41}$$

where  $K$  and  $G$  are the bulk and shear moduli respectively, and  $A_1, A_2, P_1, P_2$  are constants. Thus (3.40) assumes the form

$$\begin{aligned}
 \lim_{v_c \rightarrow 0} \left\{ v_c \left[ \dot{K}^* - \sum_{k=1}^N (K^{(k)} - K^*) A_1^{(k)} \left( \dot{v}_k + v_k \frac{\dot{v}}{1-v} \right) \right] \right\} &= -K^* P_1 \lim_{v_c \rightarrow 0} \left( \dot{v}_c + v_c \frac{\dot{v}}{1-v} \right) \\
 \lim_{v_c \rightarrow 0} \left\{ v_c \left[ \dot{G}^* - \sum_{k=1}^N (G^{(k)} - G^*) A_2^{(k)} \left( \dot{v}_k + v_k \frac{\dot{v}}{1-v} \right) \right] \right\} &= -G^* P_2 \lim_{v_c \rightarrow 0} \left( \dot{v}_c + v_c \frac{\dot{v}}{1-v} \right)
 \end{aligned} \tag{3.42}$$

where the dependence on  $t$  is omitted for convenience.

We restrict our consideration to the case of randomly distributed penny-shaped cracks when they are obtained by flattening ellipsoidal voids which have two equal semiaxes of length  $a$  and the third one  $pa$ , where  $p = \text{const}$  can be made indefinitely small. Then the volume fraction  $v_c$  is

$$v_c = \frac{\pi p \sum a^3}{V} = \pi p \alpha \quad (3.43)$$

where  $\alpha$  without indices is the crack density parameter (CDP) introduced in Chapter 2. Substituting this expression for  $v_c$  into (3.42) we obtain

$$\begin{aligned} \dot{K}^* &= \sum_{k=1}^N (K^{(k)} - K^*) A_1^{(k)} \left( \dot{v}_k + v_k \frac{\dot{v}}{1-v} \right) - K^* \frac{P_1}{\alpha} \left( \dot{\alpha} + \alpha \frac{\dot{v}}{1-v} \right) \\ \dot{G}^* &= \sum_{k=1}^N (G^{(k)} - G^*) A_2^{(k)} \left( \dot{v}_k + v_k \frac{\dot{v}}{1-v} \right) - G^* \frac{P_2}{\alpha} \left( \dot{\alpha} + \alpha \frac{\dot{v}}{1-v} \right) \end{aligned} \quad (3.44)$$

Now we refer to the results of Chapter 1 for the effective bulk and shear moduli for small density of open microcracks<sup>1</sup>(see Table 2.1). Assuming that  $\alpha$  is small, we can rewrite the result as

$$\begin{aligned} K^* - K &\cong -K \frac{16(1-\nu^2)}{9(1-2\nu)} \alpha \\ G^* - G &\cong -G \frac{32(5-\nu)(1-\nu)}{45(2-\nu)} \alpha \end{aligned}$$

which for any step of the DS procedure implies the form

$$dK^* = -K^* \frac{16(1-\nu^{*2})}{9(1-2\nu^*)} d\alpha$$

---

<sup>1</sup>The load-induced anisotropy discussed in the previous Chapter can not be considered in the framework of the DS. The reason for this is that if the applied loads change the material symmetry after the first step of cracks addition, the successive randomly oriented cracks are embedded into anisotropic material. In order to evaluate tensor  $\mathbf{P}$  we have to know the crack opening displacement  $[\mathbf{u}]$  (see Chapter 2) for a crack tilted to the material axes of symmetry, which is an extremely complicated problem.

$$dG^* = -G^* \frac{32(5-\nu^*)(1-\nu^*)}{45(2-\nu^*)} d\alpha$$

Recalling the definition of tensor  $\mathbf{P}$  it may be concluded that

$$\begin{aligned} P_1 &= \frac{16(1-\nu^{*2})}{9(1-2\nu^*)} \alpha = \kappa^* \alpha \\ P_2 &= \frac{32(5-\nu^*)(1-\nu^*)}{45(2-\nu^*)} \alpha = \eta^* \alpha \\ \text{with } \nu^* &= \frac{3K^* - 2G^*}{2(3K^* + G^*)} \end{aligned} \quad (3.45)$$

Therefore

$$\begin{aligned} \dot{K}^* &= \sum_{k=1}^N (K^{(k)} - K^*) A_1^{(k)} \left( \dot{v}_k + v_k \frac{\dot{v}}{1-v} \right) - K^* \kappa^* \left( \dot{\alpha} + \alpha \frac{\dot{v}}{1-v} \right) \\ \dot{G}^* &= \sum_{k=1}^N (G^{(k)} - G^*) A_2^{(k)} \left( \dot{v}_k + v_k \frac{\dot{v}}{1-v} \right) - G^* \eta^* \left( \dot{\alpha} + \alpha \frac{\dot{v}}{1-v} \right) \end{aligned} \quad (3.46)$$

where  $\kappa^*$  and  $\eta^*$  are defined by (3.45).

The differential equations (3.38) will reduce to

$$\dot{\alpha}^* = \sum_{k=1}^N \frac{K^{(k)}}{K^*} A_1^{(k)} (\alpha^{(k)} - \alpha^*) \left( \dot{v}_k + v_k \frac{\dot{v}}{1-v} \right) \quad (3.47)$$

where the influence of the cracks enters implicitly through  $K^*$ .

Again, the question about the correspondence between composite microstructure and an influence path is raised here. The relation (3.33) remains unchanged for inclusions, and for cracks it assumes the form

$$\alpha(r) = \frac{\sum_{i=1}^r \Delta \alpha^f(i)}{v_0^f + \sum_{i=1}^r \Delta v^f(i)}$$

where  $\Delta\alpha^f(i)$  is the CDP of the cracks of size  $i$  in the finite material.

As an example consider three different paths to the same endpoint  $(v_1^f, \alpha^f)$  for the DS construction process by which a three-phase material can be obtained (Fig.3.7). The first one is the straight line from the origin to the endpoint  $A(v_1^f, \alpha^f)$ . For each size  $i$ , the volume fraction of the particles and the density of the cracks are in the same proportion as in the composite.

According to the next path  $OCA$ , the smallest cracks are in order of magnitude larger than largest particles. Thus, the construction procedure is built in such a way that first the inclusions and then the cracks are added to the material. The first stage corresponds to the line  $OC$  along the axis  $v_1$ , and the line  $CA$  represents the insertion of the cracks. Note, that  $CA$  is a horizontal line because the embedding of the cracks does not change the volume of the composite, and hence the volume fraction of the inclusions.

The third path  $OBA$  is opposite to the previous one. We start with small cracks and increase the crack density to the value  $\frac{\alpha^f}{1-v_1^f}$  (point  $B$ ) in such a way that it will later decrease to the desired value  $\alpha^f$  (point  $A$ ) during removing of the cracks and their replacement by the larger particles (for the FVP), or during the material volume  $V$  increase with the insertion of the inclusions (for the VVP).

Elastic moduli  $K^*$  and  $G^*$  and thermal expansion coefficient  $\alpha^*$  of the cracked composite material, containing epoxy matrix and 40% of glass spheres as inclusions, are calculated for the described paths by (3.46)–(3.47) and shown in Fig.3.8–3.10. The phase properties are

	$E$	$\nu$	$\alpha$
matrix	3.45 GPa	0.35	$42 \cdot 10^{-6} \text{ }^{\circ}\text{C}^{-1}$
particles	72.40 GPa	0.2	$5 \cdot 10^{-6} \text{ }^{\circ}\text{C}^{-1}$

In all the cases of Fig.3.8–3.10 we show the effect of crack density on the effective properties. Both  $K^*$  and  $G^*$  vanish asymptotically with increasing crack density. Note, that the event when the size of the cracks is larger than the particle size corresponds to the upper curves, and the opposite case to the lower ones. If the difference in the results for  $K^*$  due to the influence path choice is insignificant, the shear modulus  $G^*$  depends more heavily on the path.

The dramatic effect of the path on the effective thermal expansion coefficient  $\alpha^*$  can be seen from Fig.3.10. If small cracks and cracks that are comparable to particles drastically decrease the value of  $\alpha^*$ , the cracks which are significantly larger than the particles have no influence on the effective thermal expansion (the upper curve in Fig3.10). This can be explained by that these cracks "see" an effective isotropic material which consists of the matrix and the inclusions added previously, and it is well-known that homogeneous heating of a homogeneous body containing cracks does not produce thermal stresses and does not change the thermal expansion of the body.



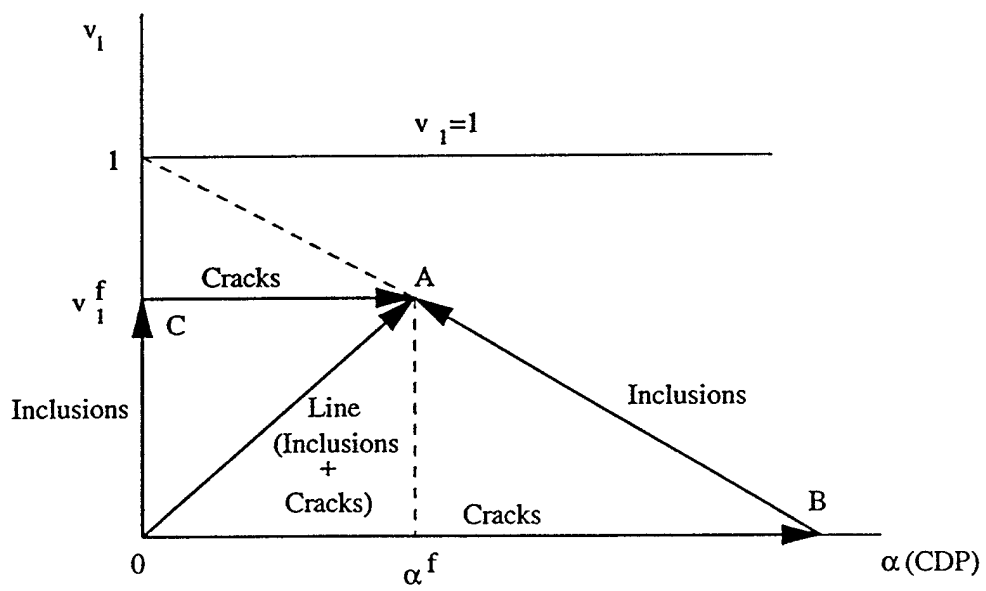


Figure 3.7: Three homogenisation paths in the  $(v, \text{CDP})$  plane to the same endpoint  $A$ .

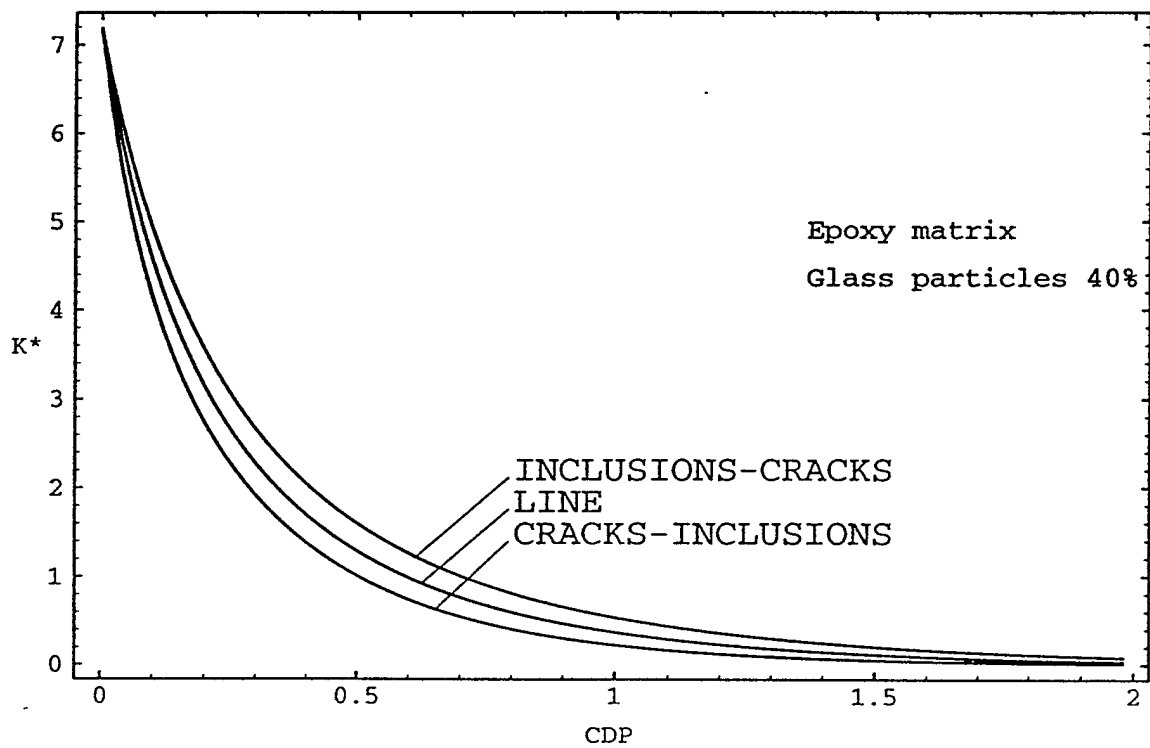


Figure 3.8: Variation of bulk modulus (GPa) with crack density.

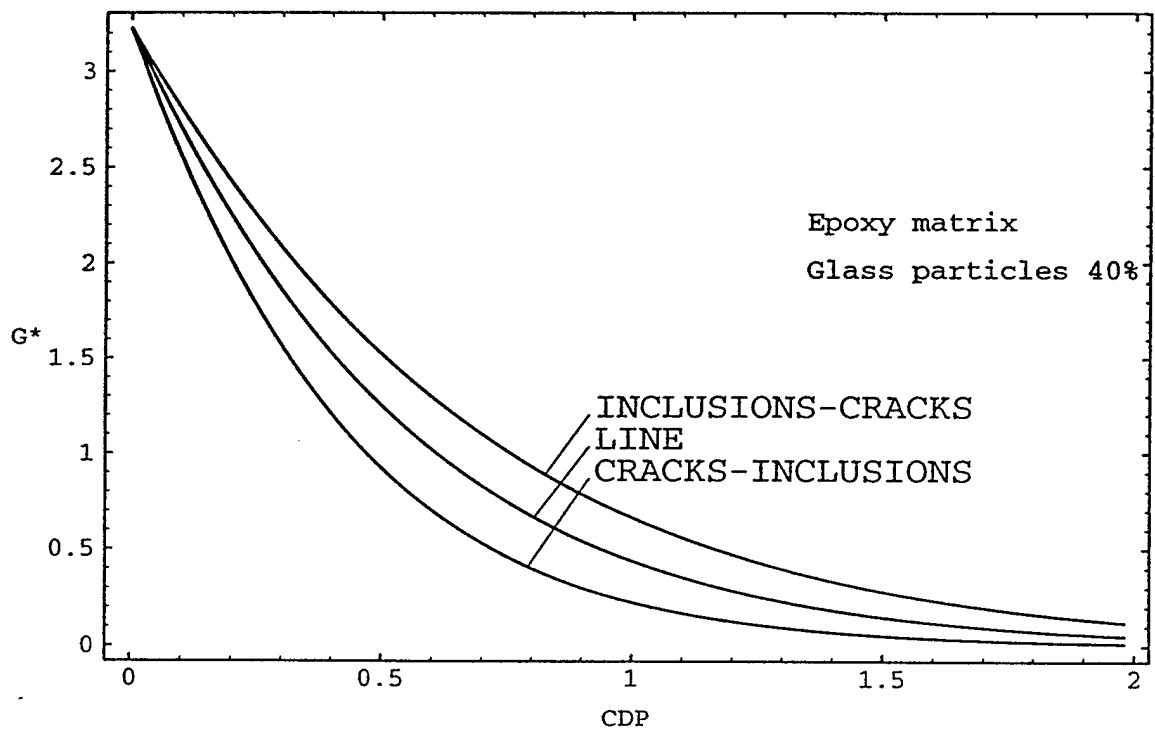


Figure 3.9: Variation of shear modulus (GPa) with crack density.

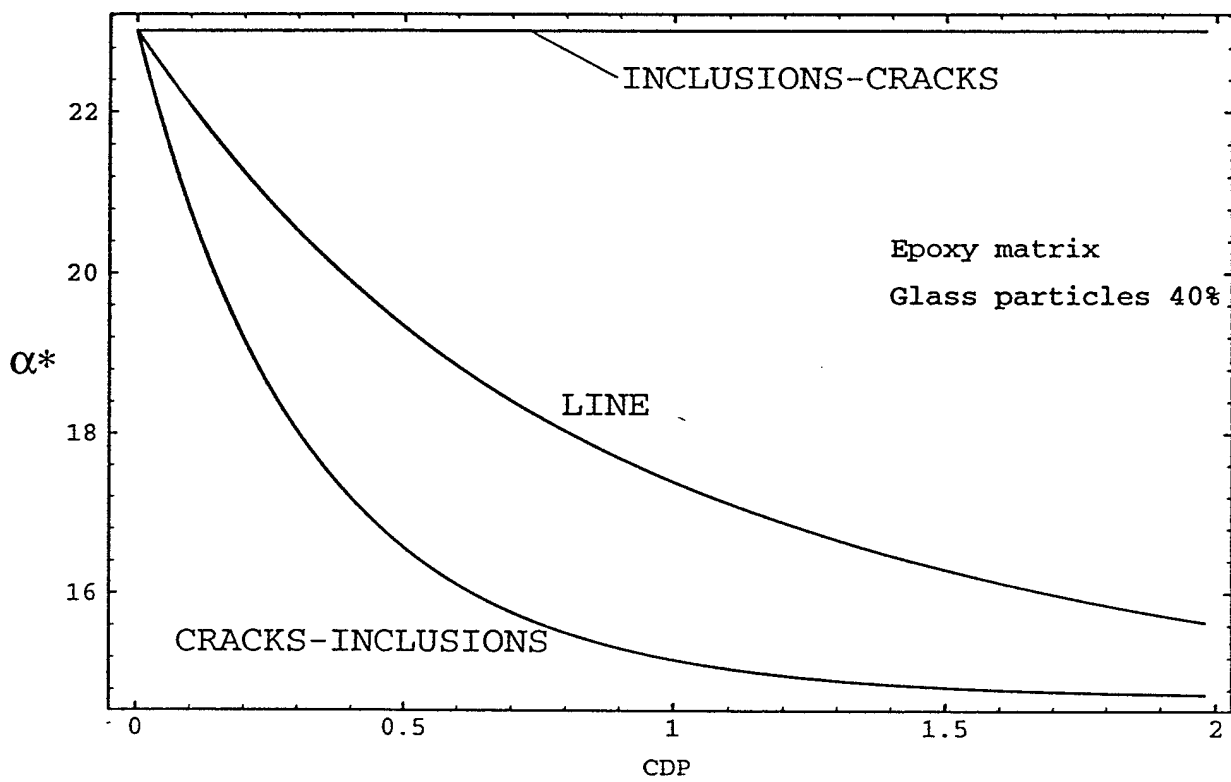


Figure 3.10: Variation of thermal expansion coefficient ( $10^{-6} \text{ } ^\circ\text{C}^{-1}$ ) with crack density.

MACRO-RESIDUAL STRAINS DUE TO CYCLIC LOADING OF  
COMPOSITES

Z. Hashin and B.W. Rosen

# **Macro-Residual Strains Due to Cyclic Loading of Composites**

## **INTRODUCTION**

It is well known that when a metal specimen is loaded into the plastic regime and then unloaded, permanent strain which is known as residual strain will remain. This phenomenon is explained by internal microscopic changes which take place within the slip systems of the crystals of which the metal is composed.

Similar phenomena are observed for ceramic matrix composites as is illustrated in fig.1 taken from ref [1]. Such composites consist of elastic-brittle constituents which by themselves do not exhibit any residual strains under load cycles. Yet when such composites are subjected to load cycles residual strains on the macroscale are observed. Characteristically, the residual strains grow with the number of cycles until they attain a limit value beyond which they do not increase, fig2,

[2].

In the present work the nature of this phenomenon is explained in terms of the residual thermal stresses produced by cooldown from the high formation temperature of over 1000 C° to room temperature and the damage in form of microcracking which develops during load cycling. It is shown analytically that the macro-residual strain can be expressed in terms of effective thermal expansion coefficients (TEC) of the composite as functions of the damage produced at the various stages of loading history. These TEC are defined in the secant sense for the temperature range under consideration. The theory is illustrated by evaluation of limit residual strains for uni-directional fiber composites and cross-ply laminates.

## THEORETICAL DEVELOPMENT

When a homogeneous stress-free body is in a state of uniform temperature  $\phi_0$  and the temperature is changed to another uniform state  $\phi$ , the body remains in a stress-free state. If, however, an initially stress-free composite body is subjected to such a temperature change, internal stresses develop due to the mismatch of elastic and thermal expansion properties of the phases. Such stresses are known as thermal or residual stresses. In the case of the elastic-brittle composites considered here sufficiently large thermal stresses will develop damage in the form of cracks, within the phase regions and/or on the interface. Such damage produced by a temperature change alone will be symbolically denoted as  $D^\phi$ , the strain and stress fields at this temperature will be written  $\epsilon^\phi(\mathbf{x}, D^\phi)$  and  $\sigma^\phi(\mathbf{x}, D^\phi)$ , respectively, and it is assumed that at temperature  $\phi_0$  there are no strains and stresses.

A thermoelastic stress-strain relation for temperature dependent properties within the temperature range  $[\phi_0, \phi]$  may be expressed in the alternate forms

$$\sigma = C(\phi) \epsilon + \Gamma(\phi) (\phi - \phi_0) \quad (a)$$

$$\epsilon = S(\phi) \sigma + \alpha(\phi) (\phi - \phi_0) \quad (b) \quad (1)$$

$$\Gamma = -C \alpha \quad (c)$$

where  $C, S$  and  $\alpha$  are temperature dependent stiffness, compliance and TEC tensors. It is implied that  $\alpha$  is a secant TET which is defined as the free thermal strain produced by the temperature change  $\phi - \phi_0$ , divided by the temperature change.

An effective secant TEC  $\alpha^*(\phi)$  of a composite material is defined in analogy with secant  $\alpha(\phi)$  in terms of the average strain produced by uniform temperature change of a composite which is not loaded. Spatially uniform temperature is a basic situation for composite materials for it is the steady state temperature of a composite which is placed in a uniform temperature environment. Since, by definition, there is no surface load the average stress vanishes and the average strain for temperature change  $\phi_0 \rightarrow \phi$ , which may be called the macro-free thermal strain, is written

$$\bar{\epsilon}\phi = \alpha^*(\phi, D\phi) (\phi - \phi_0) \quad (2)$$

where the TEC is also a function of the eventual damage produced by thermal stress. It is seen from (2) that the computation of effective TEC requires the evaluation of a strain field within a cracked composite material from which the average strain can then be determined. The form of (2) is based on the tacit assumption that it is only the final crack geometry which is of importance and not the history of crack formation. While this is obvious for temperature independent properties it may not be evident for the case of temperature dependence when it might be thought that the temperatures at which the various cracks appear are also of importance. It is shown in the appendix that indeed the temperature history of crack development is of no importance. One might visualize the situation as permission to translate cracks which were formed at various temperatures to formation at one same temperature. Thus we may formulate what may be called a temperature translation principle for crack formation : *the strain/stress fields within a cracked composite material with temperature dependent properties, produced by the temperature change  $\phi - \phi_0$ , is a function of the final crack configuration at temperature  $\phi$  and not of the temperature history of crack formation.*

Suppose now that the composite is subjected to load defined by the homogeneous traction boundary condition

$$T(S) = \sigma^0 n(S) \quad (3)$$

where  $S$  is the bounding surface,  $\sigma^0$  is a constant stress tensor, which is also the average stress in the composite, and  $n$  is the normal to  $S$ . The loading (3) produces additional damage  $D^T$  and additional strain and stress  $\epsilon^T(x, D\phi + D^T)$  and  $\sigma^T(x, D\phi + D^T)$ , respectively. Then average strain is added to (2) in consequence of the loading which is composed of two parts, one reversible and the other irreversible. The reversible part is of the form

$$\bar{\epsilon}^T = S^*(\phi, D\phi + D^T) \sigma^0 \quad (4)$$

where  $S^*$  is the effective compliance tensor of the damaged composite. When the composite is unloaded until  $\sigma^0 = 0$ , assuming that no additional damage is produced during the unloading,



the strain (4) will reduce to zero. The irreversible part of the strain added by the load is due to the fact that additional damage  $D^T$  has been produced by the load. Thus after unloading the composite material is in a new state of stress and strain associated with the damage state  $D^\phi + D^T$ . It follows from the temperature translation principle formulated above that this new state of strain is the same as in a specimen in which this damage state would have been produced after a temperature change  $\phi_0 \rightarrow \phi$  without the loading/unloading cycle. Therefore in analogy with (2) the average strain after unloading can be expressed in the form

$$\bar{\epsilon} = \alpha^*(\phi, D^\phi + D^T) (\phi - \phi_0) \quad (5)$$

Specimens which are tested at room temperature have been previously cooled down in manufacture and therefore the strain state (2) is considered as a zero strain state. Consequently, the load-unload cycle produces a macro-residual strain which is the difference between (5) and (2). Thus

$$\bar{\epsilon}^r = [\alpha^*(\phi, D^\phi + D^T) - \alpha^*(\phi, D^\phi)](\phi - \phi_0) \quad (6)$$

Thus the average residual strain is determined by the effective TEC at the damage states before and after the load cycle.

Similarly, if  $N$  load cycles of any amplitudes are applied and the cumulative damage due to these cycles is denoted  $D^N$  then on the basis of the arguments leading to the derivation of (6) the average residual strain will be

$$\bar{\epsilon}^r = [\alpha^*(\phi, D^\phi + D^N) - \alpha^*(\phi, D^\phi)](\phi - \phi_0) \quad (7)$$

It should be noted that from temperature translation the actual details of the loading history which produces a certain damage state are of no importance. If the same damage is produced by different loading histories - the residual strain will be the same, whether the loading is only one cycle or many cycles of different amplitudes.

It often happens that a brittle composite material becomes crack saturated. This implies that for increasing number of load cycles it becomes more and more difficult to produce additional cracks and the effective TEC approaches a limit asymptotically. An example of this for cracked laminates has been given in Hashin (1988) where it has been shown that the effective TEC of cross-ply laminates approaches asymptotic limits with increasing crack densities in the layers. It follows from (7) that in this situation the residual average strain approaches a limit  $\bar{\epsilon}^{rl}$ . This phenomenon is well known and examples based on actual experiments are shown in figs.1,2 [1,2].

Note that in accordance with the discussion above the value of  $\bar{\epsilon}^{rl}$  also depends solely on the end state of crack saturation and not on the history of formation.

## APPLICATIONS

It follows from the theory developed above that analytical evaluation of macro-residual strains requires : (a) Knowledge of the damage produced. (b) Analytical evaluation of the effective TEC as a function of the damage. Damage can be described on the basis of suitable observation of a specimen. It would of course be very desirable to be able to predict damage analytically. Work of this nature has been described in Nairn and Hu (1994) and Hashin (1996). Since ,however, this subject is still in its infancy it will not be considered here. The examples to be given here will be concerned with the relatively simple case when the the temperature change does not produce damage and the subsequent load cycling is continued until the specimen is crack saturated. Thus the purpose is to evaluate the limiting final value of macro-residual strain.

As a simple first example consider a one-dimensional model of a unidirectional fiber composite, fig. 3, where  $\alpha_m > \alpha_f$ . Here m,f denote matrix and fiber, respectively and the TEC are in fiber direction. Assume that cooldown from  $\phi_0$  to  $\phi$  produces no damage. Then the effective TEC  $\alpha_A^*$  in fiber direction is given with good approximation by

$$\alpha_A^*(\phi, D\phi) = \alpha_A^*(\phi, 0) = \frac{\alpha_m E_m v_m + \alpha_f E_f v_f}{E_m v_m + E_f v_f} \quad (8)$$

where  $v_m$  and  $v_f$  are the volume fractions and the Young's moduli are un fiber direction. More accurate expressions are available in the literature ; e.g. Rosen and Hashin (1970), Hashin (1979).

The composite is now loaded by tensile average stress  $\sigma^0$  in fiber direction. This produces tensile stress in the matrix which is superposed on the tensile matrix stress produced by cooldown (since by hypothesis  $\alpha_m > \alpha_f$ ). Assume that the specimen is loaded to the point of matrix crack saturation. This matrix crack accumulation is the damage  $D^T$ . The matrix then becomes ineffective and therefore the effective TEC reduces to  $\alpha_f$ . Thus

$$\alpha_A^*(\phi, D\phi + D^T) = \alpha_A^*(\phi, D^T) = \alpha_f \quad (9)$$

It follows from (7-9) that

$$\epsilon^{rl} = \frac{(\alpha_f - \alpha_m) E_m v_m}{E_m v_m + E_f v_f} (\phi - \phi_0) \quad (10)$$

Since  $\phi < \phi_0$  and  $\alpha_f < \alpha_m$  this is a positive residual strain.

The second example is concerned with a symmetric cross-ply laminate, fig.4, where the layers are made of unidirectional fiber composites. The laminate is cooled down from stress-free temperature  $\phi_0$  to temperature  $\phi$ . If no damage is produced by the cooldown, evaluation of the laminate TEC and internal stresses is elementary. For the case of equal layer thicknesses the TEC has the simple form

$$\alpha^{*0} = \alpha_A + (\alpha_T - \alpha_A) \frac{1 + \nu_A}{1 + 2\nu_A + E_A/E_T} \quad (11)$$

where  $\alpha_A$  and  $\alpha_T$  are axial (fiber direction) and transverse TEC of the unidirectional layer material,  $E_A$  and  $E_T$  are the Young's moduli for these directions and  $\nu_A$  is the axial Poisson's ratio.

Denoting the in-plane axial (in fiber direction) and transverse layer stresses  $\sigma_A$  and  $\sigma_T$ , respectively, we have

$$\sigma_A = \frac{E_A (\alpha_T - \alpha_A)}{1 + 2\nu_A + E_A/E_T} (\phi - \phi_0) \quad (12)$$

$$\sigma_T = -\sigma_A$$

All TEC in (11,12) are to be interpreted in the secant sense with respect to temperature change from stress-free temperature  $\phi_0$  to final temperature  $\phi$ .

In unidirectional fiber composites with polymeric or metallic matrix generally  $\alpha_T > \alpha_A$ . It follows from (12) that when laminates made of such materials are cooled down from  $\phi_0$ , transverse tensile stresses  $\sigma_T$  will develop. Such stresses may crack all layers along fiber directions producing so-called intralaminar cracks. In order to keep the analysis simple it will here be assumed that cooldown does not produce cracks. Next the laminate is subjected to tensile cyclic uniaxial stress  $\sigma^0$  in a direction transverse to the fibers in the inner layer, say, which is designated as the x direction. This load produces transverse tensile stresses in the inner layer which superpose on the tensile thermal stresses due to cooldown. It is assumed that cracks are produced by this cycling, fig. 4, and as is known from experiment, after a sufficient number of cycles crack

density in the inner layer becomes so large that no more cracks can be added by the load cycling which implies that a stage of crack saturation has been reached. The effective TEC in load direction for this limiting case has been given in Hashin (1988) in the form

$$\alpha^* = \alpha^{*0} + \frac{\alpha_A - \alpha_T}{1 + \lambda} (1 + B_0/C_0) k_x^1 \quad (13)$$

where

$$\begin{aligned} B_0 &= -(1 + 1/\lambda) \nu_A / E_A \\ C_0 &= 1/E_A + 1/\lambda E_T \\ \lambda &= t_2/t_1 \\ k_x^1 &= \sigma_{xx}^1 / \sigma^0 \end{aligned} \quad (14)$$

Here inner and outer layers have been labeled 1 and 2, respectively,  $t_1$  and  $t_2$  are layer thicknesses and  $\sigma_{xx}^1$  is the stress in the inner layer for an undamaged laminate. Expression (13) can be very much simplified to read

$$\begin{aligned} \alpha^* &= \alpha_A + \frac{\nu_A (\alpha_T - \alpha_A)}{\eta + \lambda} \\ \eta &= E_A / E_T \end{aligned} \quad (15)$$

Since  $\alpha^{*0}$  is an unwieldy expression for arbitrary  $\lambda$ , we shall restrict ourselves to the simple case of  $\lambda=1$ . Then, identifying (11) with  $\alpha^*(\phi, D\phi)$  and (14) with  $\lambda=1$  as  $\alpha^*(\phi, D\phi + D^T)$ , where in this case there is no thermal damage, we have from (6) after some algebra

$$\bar{\epsilon}_{xx}^r = - \frac{(\alpha_T - \alpha_A) (1 + \eta - 2\nu_A^2)}{(1 + \eta) (1 + \eta + 2\nu_A)} (\phi - \phi_0) \quad (16)$$

and it is seen that (16) is a positive strain increment, since  $\alpha_T > \alpha_A$  and  $\phi < \phi_0$ .

There is of course no difficulty to carry out all of the preceding calculations for the case of unequal thicknesses. This is best done numerically as the analytical results become unwieldy.

The situation  $\alpha_T < \alpha_A$  may arise in ceramic composites ; for example : the TEC of a material composed of Nicalon fibers and SiC matrix. In that case the stresses (12) reverse sign and  $\sigma_T$  is a compressive residual stress which can not produce cracking. If the laminate is now subjected to tensile cycling the compressive residual transverse stress subtracts from the tensile stress produced by external load. The applied tensile stress may be large enough to produce cracking but after unloading the inner layer will again be in compression and the cracks will be closed. Therefore there is no additional crack effect with respect to the state before loading and there will thus be no residual macro-strain.

Results of sample calculations of limit residual strain and layer properties for a ceramic matrix composite are shown in the table below. The material consists of T300 graphite fibers embedded in SiC matrix. The volume fraction of fibers is 0.4 ,the reference temperature is  $\phi_0 = 1025 \text{ C}^0$  and the laminate is cooled down to a temperature of  $\phi = 25 \text{ C}^0$ .

Table

Material	$E_A$	$E_T$	$\nu_A$	$\alpha_A$	$\alpha_T$	$\sigma_A$	$\sigma_T$	$\bar{\epsilon}_{xx}^{\ell}$
T300/SiC	434.5	166.1	0.179	4.45	7.34	-25.54	25.54	7.14
	GPa	GPa		$10^{-6}/\text{C}^0$	$10^{-6}/\text{C}^0$	MPa	MPa	$10^{-4}$

## CONCLUSION

It has been shown in general fashion that macro-residual strains produced in elastic-brittle composites under cyclic loading are tied to the internal thermal residual stresses and the damage produced by the cyclic load and that, furthermore, these residual strains can be analytically expressed in terms of effective TEC as functions of damage. The problem of evaluation of residual strains has thus been reduced to the well known problem of evaluation of effective TEC.

Some simple illustrative evaluation examples have been given and there is no difficulty to carry out more complicated calculations for cross-ply laminates in which all plies are cracked. The theory can also be readily applied numerically on the basis of numerical calculation of effective TEC for cases of interest.

## ACKNOWLEDGEMENT

Support by the Air Force Office of Scientific Research under contract with the Materials Sciences Corp, Dr. Walter Jones contract monitor, is gratefully acknowledged

## REFERENCES

1. Wang, M., "Damage and fracture in monotonic and cyclic loading of cross-woven C/SiC composites", Ph.D. dissertation, Materials Science and Engineering, University of Pennsylvania, (1994)
2. Wang, Z.G., Laird, C., Hashin, Z., Rosen, B.W. and Yen, C.F., "The mechanical behaviour of a cross-weave ceramic matrix composite. Part II Repeated loading", J.Mats.Sci., 26, 5335-5341, (1991)
3. Nairn, J.A., and Hu, S., "Matrix Microcracking" Chap.6 in Damage Mechanics of Composite Materials, Talreja, R., Ed., Elsevier Science, (1994)
4. Hashin, Z. "Finite thermoelastic fracture criterion with application to laminate cracking", J.Mech.Physics.Solids, (to appear)
5. Rosen, B.W. and Hashin, Z., "Effective thermal expansion coefficients and specific heats of composite materials", Int.J.Eng.Sci., 8, 157-173, (1970)
6. Hashin, Z., "Analysis of properties of fiber composites with anisotropic constituents", J.Appl.Mech., 46, 543-550, (1979)
7. Hashin, Z., "Thermal expansion coefficients of cracked laminates", Comp.Sci.Tech., 31, 247-260, (1988)

## APPENDIX

The governing differential equations of any homogeneous constituent phase of the temperature dependent thermoelastic composite body are obtained by introduction of (1a) into the

stress equilibrium equations. Thus

$$C(\phi)_{ijkl} u_{k,lj} = 0 \quad (A1)$$

where  $u(\mathbf{x})$  is the displacement and there is no contribution from the thermal term in (1a) since it is constant and thus its derivatives vanish.

From (1a) the traction vector associated with surface normal  $\mathbf{n}$  may be written

$$T_i = C_{ijkl} u_{k,l} n_j + \Gamma(\phi) (\phi - \phi_0) n_i \quad (A2)$$

The traction (A2) and the displacement  $\mathbf{u}$  must be continuous at the phase interfaces.

Let it be assumed that the composite is subjected to any temperature variation within the range  $[\phi_0, \phi]$  and a surface traction distribution  $T(S, \phi)$ . It follows from the mathematical nature of the composite boundary value problem (BVP) described above that : (a) The solution of the BVP for any temperature is a function of  $\phi$  and not of temperature history. (b) Since the BVP is linear in space its solution  $\mathbf{u}, \sigma$  at any temperature  $\phi$  can be constructed as the superposition

$$\mathbf{u} = \mathbf{u}^\phi + \mathbf{u}^T \quad (A3)$$

$$\sigma = \sigma^\phi + \sigma^T$$

where the  $\phi$  superscript indicates the solution of the BVP for the temperature input with  $T(S) = 0$  and the T superscript indicates solution for specified  $\phi$  with load input  $T(S, \phi)$ .

We now describe two different scenarios for the same composite body with bounding surface  $S$ . First, the temperature is changed from  $\phi_0$  to  $\phi_2$ , and a crack with surface  $S_c$  appears at temperature  $\phi_2$ . Second, the temperature is changed from  $\phi_0$  to  $\phi_1$ ; the same identical crack at same location appears at temperature  $\phi_1$  and then the temperature is changed to  $\phi_2$ . We wish to show that in the two cases the internal fields at temperature  $\phi_2$  are identical.

Consider first the case when the composite body undergoes a temperature change  $\phi_0 \rightarrow \phi_2$ , there is no load on  $S$ , i.e.  $T(S) = 0$ , and no crack appears. The stress field at any temperature  $\phi$  for this case is identified with  $\sigma^\phi(\phi)$  in (A3). The traction on the anticipated crack surface  $S_c$  which at this stage is a mathematical surface is denoted  $T(S_c, \phi)$ . Next we consider the same body with no load on  $S$  and no temperature change which is subjected to the traction  $-T(S_c, \phi)$  on  $S_c$ . The stress field produced by this load is identified with  $\sigma^T(\phi)$  in (A3). The stress field of the first scenario is

$$\sigma^1(\phi_2) = \sigma^\phi(\phi_2) + \sigma^T(\phi_2) \quad (\text{A4})$$

The stress field of the second scenario is

$$\sigma^2(\phi_2) = \sigma^\phi(\phi_2) + \sigma^T(\phi_1) + \sigma^T(\phi_2) - \sigma^T(\phi_1) \quad (\text{A5})$$

where the last two terms in (A5) are due to the temperature change  $\phi_1 \rightarrow \phi_2$ . In each case the tractions associated with the stress field vanish on the crack surface  $S_c$  and on the bounding surface  $S$ . It is seen that the two scenarios result in the same stress field and similarly in the same displacement and strain field.

Now the same reasoning can be applied again to two scenarios of an additional crack appearing at different temperatures to conclude finally by induction that temperature translation of cracks is valid for any number of cracks.



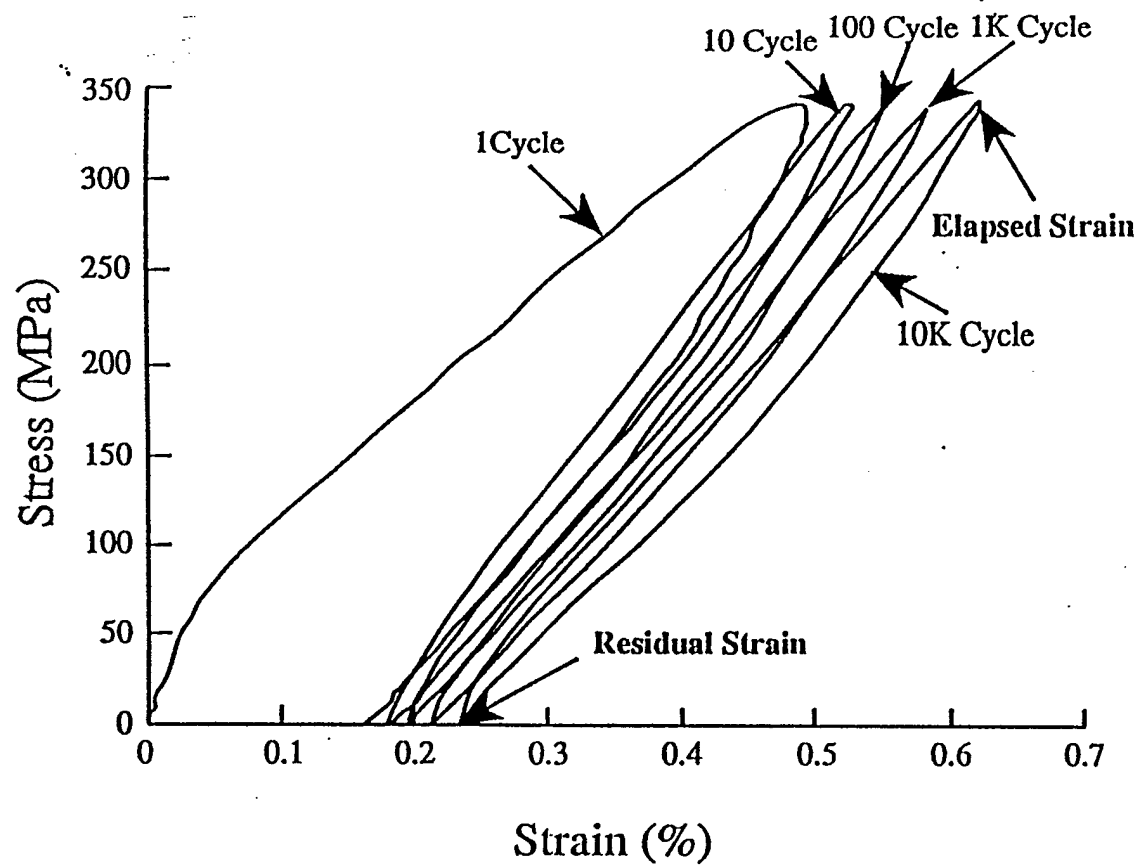


Fig.1 - Residual strain due to cyclic loading of ceramic matrix composite

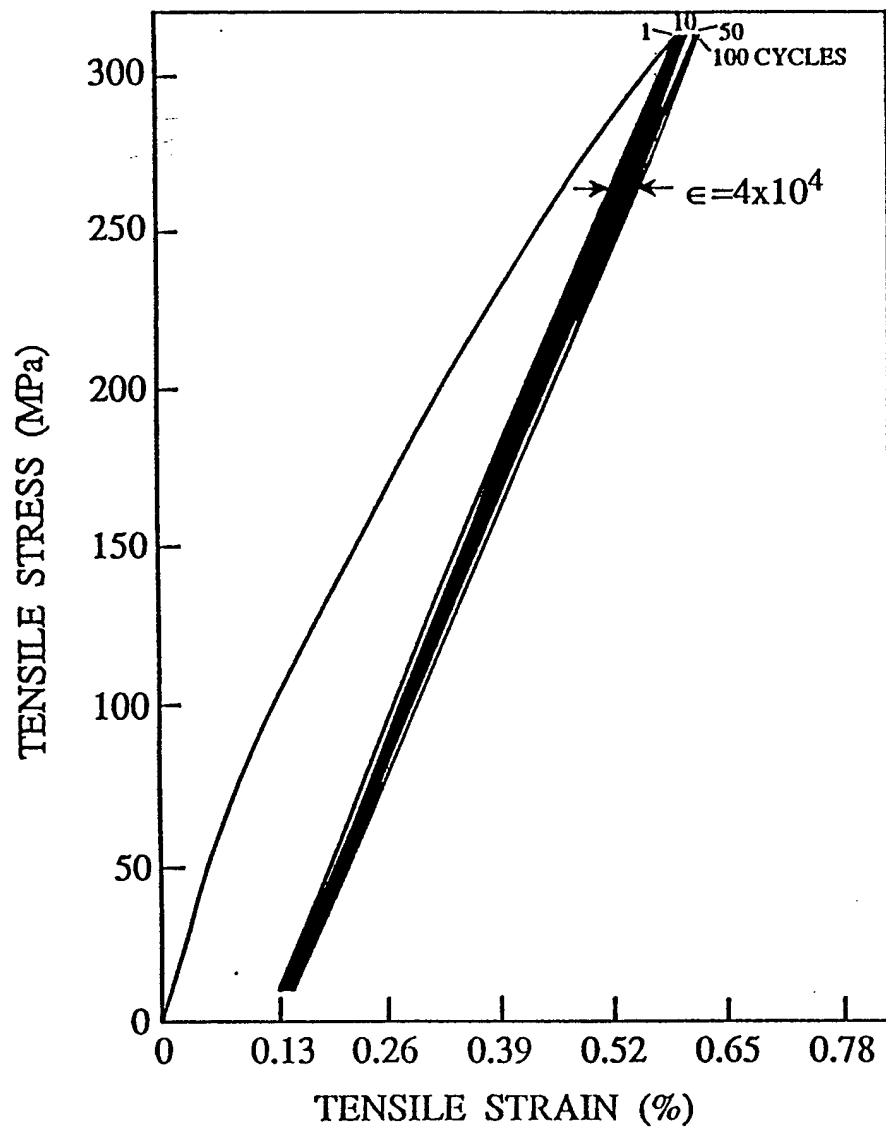


Fig.2 - Limit residual strain in cyclic loading of ceramic matrix composite

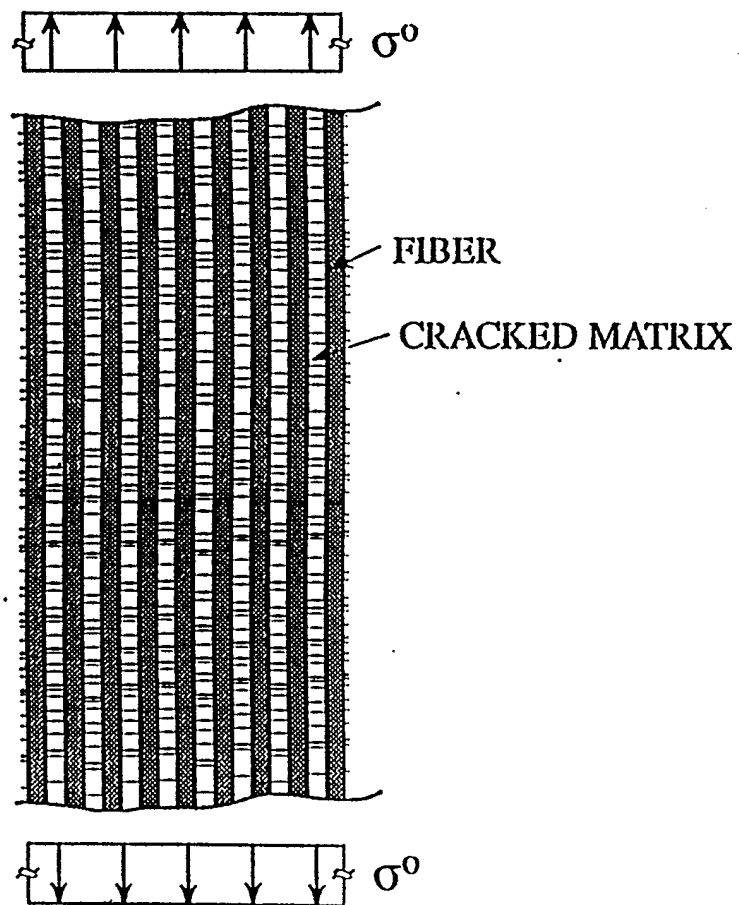


Fig.3 - Unidirectional fiber composite with cracked matrix

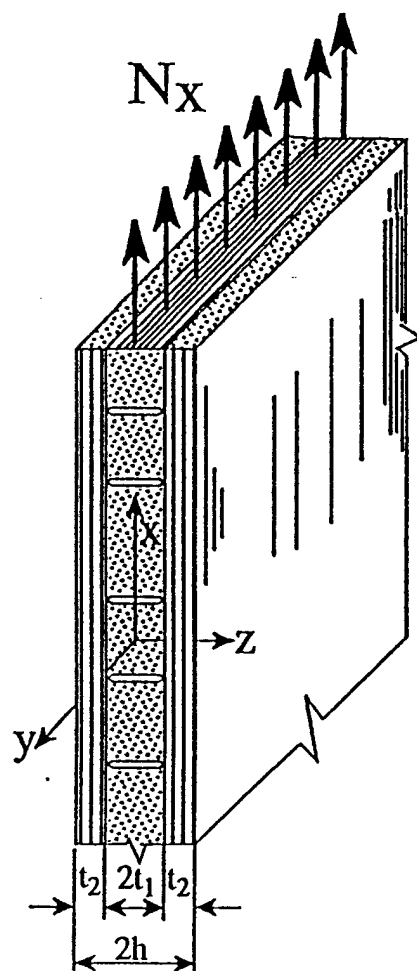


Fig.4 - Cracked cross-ply laminate

FINITE THERMOELASTIC FRACTURE CRITERION WITH  
APPLICATION TO LAMINATE CRACKING ANALYSIS

Z. Hashin

# Finite Thermoelastic Fracture Criterion with Application to Laminate Cracking Analysis

## Introduction

The dominant mode of damage development in composite materials with polymeric or ceramic matrix is the accumulation of cracks. In particulate composites and in unidirectional fiber composites such cracks occur as matrix cracks, interface disbonds and fiber breaks. In fiber composite laminates so-called intralaminar cracks accumulate within the layers, along the fibers. It is of primary importance to develop an analytical capability for prediction of such crack accumulations and it is with this goal that the present work is concerned.

The subject is within the realm of fracture mechanics but the approach is of necessity different from the one adopted in classical fracture mechanics. The latter is primarily concerned with differential extension of a single crack, or perhaps of several cracks with well defined locations. In composites the concern is with spontaneous appearance of many cracks of finite surface and ill defined locations. It may therefore be appropriate to refer to the subject as **finite fracture mechanics**. Spontaneous crack formation implies that new cracks appear in very short time and it is not possible or of interest to follow the history of their development. The formation of new cracks can thus be regarded as **fracture events**. No single crack produces failure and every crack is arrested by a boundary. The uncertainty of location of cracks introduces as important geometrical parameter the **crack density** and perhaps, as will be seen later, other global quantities such as standard deviation of crack spacings.

Furthermore, composites are manufactured at relatively high temperature and are subsequently cooled down to room temperature. This process introduces **residual stresses**, possibly of considerable magnitude, which cannot be ignored and must be incorporated into the formulation and analysis.

There are two major tasks in the analysis of the phenomena described above: (a) Establishment of a criterion for new crack formation. (b) Stress analysis of the cracked body for purpose of application of the fracture criterion. A current major research activity within the present subject involving these two tasks, is analysis of intralaminar cracking of fiber composite laminates which has grown into a voluminous literature. A recent review has been given by Nairn and Shu (1994).

Literally all of the work on cracked laminates has been concerned with so-called cross ply laminates which consist of layers with reinforcement directions of  $0^\circ$  or  $90^\circ$ . The most commonly used method of analysis has been shear lag, which appears to have been initiated for cracked laminates by Garrett and Bailey (1977). However, shear lag is a roughly approximate one dimensional method of analysis which brings in an artificial shear transfer zone in-between the laminate layers. The thickness of this zone is an unknown parameter which can only be obtained from some experimental information. Furthermore, the shear stresses as calculated by shear lag do not vanish on crack surfaces, as they should.

A two dimensional variational method of stress analysis has been established by Hashin (1985) based on the sole approximation that in-plane layer stresses are constant over layer thickness. This has been applied for laminates with one kind of layers cracked and has been generalized in Hashin (1987) to the case when all layers are cracked, which required a 3-D variational analysis. McCartney (1992) has constructed approximate elasticity solutions

which yield results similar to the ones obtained in Hashin (1985,1987). Varna and Berglund (1994) have generalized the variational method by permission of certain variations of in-plane stresses over layer thickness, at the price of considerable complexity; Nairn (1989) has generalized the Hashin (1985) analysis to thermoelasticity.

Regarding fracture analysis, there is here adopted the traditional point of view that a fracture criterion should be based on energy release. According to Nairn and Shu (1994) this approach was first applied to laminate cracking by Parvizi et al (1978) and has been subsequently used in many investigations which universally employed the shear lag approximation. Nairn (1989) was the first to use the much more accurate variational method in conjunction with energy release criteria to predict crack densities in cracked laminates, obtaining good agreement with experimental data; Nairn(1989), Liu and Nairn (1992).

In the present work it is first shown that the energy release required for formation of new finite crack surface, by load and/or temperature input, in a body which contains an initial field of residual stress can be expressed entirely by stress (or strain), thus providing a simple and convenient fracture criterion. Furthermore, on the basis of this result, it is shown that an upper bound on the energy release is obtained with admissible instead of actual stresses. Then a new simple method for thermoelastic analysis of cracked laminates is established which yields thermoelastic results by a simple replacement in corresponding isothermal results. On the basis of the above results crack formation criteria for cross-ply laminates are established in terms of statistical parameters of crack distribution. It is shown that these criteria assume simple forms for small and large crack densities.

## Thermoelastic Cracking Criterion

This section will be concerned with the development of a criterion for the spontaneous formation of new cracks due to surface load on a thermoelastic-brittle body in which there are residual stresses due to previous temperature history. Unlike classical fracture mechanics where infinitesimal increase of crack surface is considered the concern is here with finite increase.

Consider an elastic-brittle composite material body which is first subjected to temperature change  $T$  without load and is subsequently loaded by surface tractions  $T(S)$  on the bounding surface  $S$ . For composites the most common and important case is spatially constant temperature. Because of thermal expansion mismatch the temperature change will produce residual thermal stress  $\sigma^{r0}$  while the subsequent mechanical load will add mechanical stress  $\sigma^{m0}$ , resulting in an initial stress field  $\sigma^0 = \sigma^{r0} + \sigma^{m0}$ . Here and from now on boldface symbols denote tensors and vectors. Initial formation of internal cracks may have occurred due to temperature change and/or load and their surface is denoted  $S_{c0}$ . Now consider the possibility of spontaneous formation of additional cracks for same surface load  $T(S)$ . Then the thermal and mechanical stress fields change to  $\sigma^r$  and  $\sigma^m$ , the final total stress field is  $\sigma = \sigma^r + \sigma^m$  and the final crack surface is denoted  $S_c$ . Denoting by  $T$  the tractions associated with  $\sigma$  and all differences between final and initial quantities by the

symbol  $\Delta$ , (e.g.  $\Delta\sigma = \sigma - \sigma^0$ ;  $\Delta S_c = S_c - S_{c0}$ ), there are the following relations

$$\mathbf{T}^0(S_{c0}) = 0 ; \quad \mathbf{T}(S_c) = 0 ; \quad \Delta\mathbf{T}(S) = 0 \quad (1)$$

The stress-strain relations are

$$\begin{aligned} \epsilon^r &= \mathbf{S}\sigma^r + \alpha T ; & \epsilon^m &= \mathbf{S}\sigma^m \\ \Delta\epsilon^r &= \mathbf{S}\Delta\sigma^r ; & \Delta\epsilon^m &= \mathbf{S}\Delta\sigma^m \end{aligned} \quad (2)$$

where  $\mathbf{S}$  is the elastic compliance tensor and  $\alpha$  is the thermal expansion tensor. Frequent use will be made of the theorem of virtual work for a cracked body. This is written in the form

$$\int_V \sigma \epsilon dV = \int_S \mathbf{T} u dS + \int_{S_c} \mathbf{T} u dS \quad (3)$$

where  $S_c$  is the cracks' surface considered twice as if the cracks were very flat voids,  $\sigma$  and  $\epsilon$  are related or unrelated equilibrated stress and compatible strain, respectively, and  $\mathbf{u}$  is displacement. The contribution from the crack surface integral vanishes in the following instances:

$$\mathbf{T}(S_c) = 0 \quad (4)$$

$\mathbf{T}$  and  $\mathbf{u}$  are both continuous across  $S_c$

## Development of Fracture Criterion

When new crack surface  $\Delta S_c$  of area  $\Delta A_c$  forms without change of surface load the internal stress and strain fields change. There is a resulting change in internal mechanical energy which will here for reasons of subsequent development be expressed in terms of stress energy and will be denoted  $\Delta U^{i\sigma}$ . Since, by hypothesis, the surface load does not change during the process of new crack formation the external energy change is

$$\Delta U^e = \int_S \mathbf{T} \Delta \mathbf{u} dS \quad (5)$$

The internal mechanical energy change will be defined in terms of stress energy with density  $W$ , defined as

$$W(\sigma) = \frac{1}{2} \sigma \mathbf{S} \sigma \quad (6)$$

Then the internal energy change is

$$\Delta U^{i\sigma} = \int_V \Delta W dV = \int_V [W(\sigma) - W(\sigma^0)] dV \quad (7)$$

If in addition energy of amount  $\Delta\Gamma^c$  is required to open up the new crack surface, then the criterion for new crack formation is given by the energy balance

$$\Delta U^e = \Delta U^{i\sigma} + \Delta\Gamma^c \quad (8)$$



where,  $\Gamma^c$  is the critical energy release. It may be assumed that there exists a material surface energy per unit area of crack opening  $\gamma$ , in which case

$$\Delta\Gamma^c = \gamma\Delta A^c \quad (9)$$

It follows that  $\gamma$  is also the analogue of the critical energy release rate which is usually defined as the derivative of the energy release with respect to crack area.

From (1, 3, 4, 5)

$$\Delta U^e = \int_V \sigma \Delta \epsilon dV \quad (10)$$

and using (1) this can be expressed as

$$\Delta U^e = \int_V (\sigma^0 S \Delta \sigma + \Delta \sigma S \Delta \sigma) dV \quad (11)$$

The internal energy (7) can be expanded to read

$$\Delta U^{is} = \int_V (\sigma^0 S \Delta \sigma + \frac{1}{2} \Delta \sigma S \Delta \sigma) dV \quad (12)$$

It then follows from (8, 11, 12) that

$$\Delta\Gamma^c = \frac{1}{2} \int_V \Delta \sigma S \Delta \sigma dV \quad (13)$$

Thus, the critical energy release has been expressed entirely in terms of stress.

In view of (7, 12), eqn. (13) can be written

$$\Delta\Gamma^c = \int_V (\Delta W - \sigma^0 S \Delta \sigma) dV \quad (14)$$

The second integral in (13) can be transformed as follows

$$\int_V \sigma^0 S \Delta \sigma dV = \int_V \Delta \sigma S \sigma^0 dV = \int_V \Delta \sigma (\epsilon^0 - \alpha T) dV$$

Now from (1 - 4)

$$\int_V \Delta \sigma \epsilon^0 dV = \int_{S_c} \Delta T u^0 dS' = \int_{S_c} (T - T^0) u^0 dS' = - \int_{S_c} T^0 u^0 dS' = 0$$

Therefore

$$\int_V \sigma^0 S \Delta \sigma dV = - \int_V \Delta \sigma \alpha T dV \quad (15)$$

and an alternative form of  $\Delta\Gamma^c$  is

$$\Delta\Gamma^c = \int_V [W(\sigma) - W(\sigma^0) + (\sigma - \sigma^0) \alpha T] dV \quad (16)$$

There is an important consequence of the representation (16). If the surface load  $T(S)$  is achieved in a monotonic sequence of loads  $T^1, T^2, \dots, T^n, \dots, T$ , at the same temperature, and if (9) is valid with fixed  $\gamma$ , then for any load increase,  $T^{n-1}$  to  $T^n$ , say

$$\Delta\Gamma_n^c = \gamma \Delta A_n = \int_V [W(\sigma^n) - W(\sigma^{n-1}) + (\sigma^n - \sigma^{n-1}) \alpha T] dV \quad (17)$$

Summation of (17) over all sequential loading steps recovers the result (16) but with an important difference of interpretation. Previously the stress fields  $\sigma^0$  and  $\sigma$  were associated with same surface tractions while in the present case  $\sigma^0$  is associated with surface load  $T^i(S)$ , say, which for example may initiate cracking, while  $\sigma$  is associated with  $T(S)$  and a subsequent crack geometry produced during the sequential cracking process..

There is of course no difficulty to express (13, 16) in terms of strain by use of the relations (2).

In summary, if surface load  $T(S)$  admits increase of crack surface  $\Delta S_c$ , then the stress increments due to increase of crack surface must satisfy (13, 16) where  $\Delta \Gamma^c$  is the critical energy release required to produce the new crack surface. The criterion includes as special cases the situation when there are no residual stresses and on the other hand, the situation when cracking is due entirely to residual thermal stresses and there is no mechanical load. In the latter case (13, 16) becomes a criterion for crack formation due to temperature change alone. When energy required to open cracks is proportional to crack surface area, as expressed by (9), the criterion (13, 16) is also valid for the case when the total new crack area opens up sequentially during the loading process.

It should be further noted that: (a) Kinetic energy associated with the dynamics of spontaneous crack growth has been neglected. (b) The results obtained are valid for temperature dependent properties. Thus, if  $T$  is the temperature change relative to initial temperature  $T_0$ , then the compliance  $S$  should be taken at temperature  $T+T_0$  while the thermal expansion tensor  $\alpha$  should be defined in the secant sense over the interval  $(T_0, T_0 + T)$ . (c) Everything done here is valid for residual stresses which are not necessarily the result of temperature change, but it is necessary that their increments due to additional crack formation obey the relation  $\Delta \epsilon^r = S \Delta \sigma^r$ .

## Bounding of Energy Release

The complementary energy of an elastic body with internal stress field  $\sigma^0(x)$ , temperature change  $T(x)$  and tractions  $T$  prescribed on its entire external and internal surfaces is defined as

$$U_C(\sigma^0) = \int_V \left( \frac{1}{2} \sigma^0 S \sigma^0 + \alpha \sigma^0 T - \frac{1}{2} c_p \frac{T^2}{T_0} \right) dV \quad (18)$$

where  $T_0$  is a reference temperature and  $c_p$  is the specific heat at constant stress. Let it be assumed that due to internal changes, e.g. additional crack formation, the internal stress field changes to  $\sigma(x)$  while the temperature field remains unchanged. Then the new complementary energy is  $U_C(\sigma)$ . Now consider instead of the actual  $\sigma$  an admissible stress field  $\sigma^a$  which satisfies equilibrium, traction continuity and boundary conditions, but not compatibility, and define

$$\begin{aligned} U_C^a &= U_C(\sigma^a) & \Delta U_C^a &= U_C(\sigma^a) - U_C(\sigma^0) \\ \Delta \sigma^a &= \sigma^a - \sigma^0 & \Delta T^a &= T^a - T^0 \end{aligned} \quad (19)$$

It follows from (18, 19) that)

$$\Delta U_C^a = \int_V \Delta \sigma^a (S \sigma^0 + \alpha T) dV + \frac{1}{2} \int_V \Delta \sigma^a S \Delta \sigma^a dV \quad (20)$$

The parenthesis in the first integral is recognized as  $\epsilon^0$  and therefore this integral may be transformed by virtual work into

$$\int_V \Delta \sigma^a \epsilon^0 dV = \int_S \Delta T^a u^0 dS + \int_{S_c} \Delta T^a u^0 dS \quad (21)$$

The integral (21) vanishes, the proof being entirely analogous to the one given for the vanishing of the second integral in (11). Therefore

$$\Delta U_C^a = \frac{1}{2} \int_V \Delta \sigma^a S \Delta \sigma^a dV = \int_V W(\Delta \sigma^a) dV \quad (22)$$

This is a generalization of a similar result given in Hashin (1985) for the isothermal case.

Now define

$$\Delta U_C = U_C(\sigma) - U_C(\sigma^0) \quad (23)$$

where  $\sigma$  is the actual stress. Then as a special case of (22)

$$\Delta U_C = \frac{1}{2} \int_V \Delta \sigma S \Delta \sigma dV \quad (24)$$

By the thermoelastic principle of minimum complementary energy

$$U_C^a = U_C^0 + \Delta U_C^a \geq U_C = U_C^0 + \Delta U_C$$

and therefore

$$\Delta U_C^a \geq \Delta U_C \quad (25)$$

Recalling now the fracture process under fixed surface tractions described above, the stress field for fracture surface  $S_{c0}$  is identified as  $\sigma^0$  and the stress field for  $S_c = S_{c0} + \Delta S_c$  as  $\sigma$ . Then it follows from (13,24) that

$$\Delta U_C = \Delta \Gamma^c, \quad \Delta U_C^a \geq \Delta \Gamma^c \quad (26)$$

Thus (22) is an upper bound on the energy release  $\Delta \Gamma^c$ .

It should be noted that the proof given above is for the case when all cracks appear at same surface load. The proof is easily extended to the case when cracks form progressively, at different loads.

# Thermoelastic Analysis of Cracked Laminates

Application of the theory developed above to cracking of fiber composite laminates requires stress analysis of a cracked laminate. The laminates to be considered here consist of layers or plies which are unidirectional fiber composites. The present work is concerned with the simple case of  $[0_n^0/90_p^0]_s$  laminates, also known as cross-ply laminates. This implies that fiber directions are orthogonal,  $n$  and  $p$  are the number of plies in each layer and  $s$  stands for symmetric which means that the midplane is a plane of symmetry. The manufacturing temperature of the laminate may be identified as  $T_0$  and the room temperature is  $T_0 + T$ . Thus  $T$  is a negative cooldown temperature change. The case to be considered is initial cooldown of the laminate and subsequent loading by constant in-plane force  $N_x$ , fig.1.

Cooldown of such a laminate produces tensile stresses in transverse direction to the fibers which may produce cracks along the fibers, in the  $0^0$  and  $90^0$  layers. Such crack distributions have been considered in Hashin (1987) but for reasons of simplicity will not be considered here as it would complicate the analysis considerably. It will thus be assumed that cracks accumulate only with mechanical loading. Consequently such cracks, which are called **intralaminar** cracks, appear only in the  $90^0$  layer, for the transverse stress  $\sigma_{yy}$  in the  $0^0$  layer for  $N_x$  load is very small.

The usual assumption is made that the layers can be considered as anisotropic homogeneous with effective properties of the unidirectional fiber composite. Even with this simplification rigorous analysis of the stress fields in such a cracked laminate does not appear possible. Much of the work done has been based on the shear lag approximation. More accuracy has been achieved on the basis of variational analysis in terms of admissible stress. The first such analysis for the present kind of cracked laminate and for isothermal condition has been given in Hashin (1985). This analysis has been extended to loading after temperature change in Nairn (1989). In the present work the thermoelastic analysis is reconsidered and is presented in very simple form which is particularly convenient for evaluation of the energy release.

The average stress applied to the laminate is

$$\sigma = N_x/2h \quad (27)$$

When there are no cracks the stresses in each layer are constant, except for narrow edge boundary strips, and the only surviving stresses in the present case are  $\sigma_{xx}^0$  and  $\sigma_{yy}^0$ . For temperature change  $T$  and load (27) the stresses  $\sigma_{xx}^0$  in the different layers may be written

$$\sigma_{xx}^{01} = \sigma_1 = k_1\sigma + r_1T \quad \sigma_{xx}^{02} = \sigma_2 = k_2\sigma + r_2T \quad (28)$$

where the  $k$  and  $r$  coefficients depend on laminate geometry and material properties and the labels 1,2 from now on indicate the  $90^\circ$  and  $0^\circ$  layers, respectively. The admissible stress field is chosen as plane in the  $xz$  plane with  $\sigma_{xx}$  stresses constant over layer thickness. Thus

$$\begin{aligned}\sigma_{xx}^{a1} &= \sigma_1[1 - \phi_1(x)] \\ \sigma_{xx}^{a2} &= \sigma_2[1 - \phi_2(x)]\end{aligned}\quad (29)$$

where  $\phi_1$  and  $\phi_2$  are unknown functions. Insertion of (29) into the section force equilibrium condition in  $x$  direction yields the relation  $\phi_2 = -(t_1/t_2)\phi_1$ . Identifying  $\phi_1$  as  $\phi$  and using the equilibrium equations, interlaminar traction continuity and external boundary conditions [for details see Hashin (1985)] it follows that the admissible stress within a typical region between two cracks, fig.2, is given as

$$\begin{aligned}\Delta\sigma_{xx}^{a1} &= -\sigma_1\phi(x) & \Delta\sigma_{xx}^{a2} &= (\sigma_1/\lambda)\phi(x) \\ \Delta\sigma_{xz}^{a1} &= \sigma_1\phi'(x)z & \Delta\sigma_{xz}^{a2} &= (\sigma_1/\lambda)\phi'(x)(h-z) \\ \Delta\sigma_{zz}^{a1} &= \sigma_1\phi''(x)(ht_1 - z^2)/2 & \Delta\sigma_{zz}^{a2} &= (\sigma_1/\lambda)\phi''(x)(h-z)^2/2\end{aligned}\quad (30)$$

Here  $\lambda = t_2/t_1$ , primes denote  $x$  differentiation and conforming to previous notation the stresses (30) must be added to the stress field  $\sigma^0$  in the uncracked laminate to obtain the admissible stress  $\sigma^a$ . Note that the  $xz$  and  $zz$  stresses are zero in the uncracked laminate.

Since normal and shear stress must vanish on crack surfaces  $x = \pm a$  the function  $\phi$  must satisfy the boundary conditions

$$\phi(\pm a) = 1 ; \quad \phi'(\pm a) = 0 \quad (31)$$

As in Hashin (1985), an optimal function  $\phi$  is constructed by utilization of the principle of minimum complementary energy. It follows from (19) that instead of minimizing  $U_C^a$  it is sufficient to minimize (22). This requires the stress energy densities of the two layers with respect to the  $x, y, z$  coordinate system in terms of the plane stresses (30). Both layers are transversely isotropic with axis of symmetry  $y$  for layer 1 and  $x$  for layer 2. Therefore

$$\begin{aligned}2W^1(\sigma) &= \sigma_{xx}^2/E_T - 2\sigma_{xx}\sigma_{zz}\nu_T/E_T + \sigma_{zz}^2/E_T + \sigma_{xz}^2/G_T \\ 2W^2(\sigma) &= \sigma_{xx}^2/E_A - 2\sigma_{xx}\sigma_{zz}\nu_A/E_A + \sigma_{zz}^2/E_T + \sigma_{xz}^2/G_A\end{aligned}\quad (32)$$

where the elastic ply properties in (32) are:  $E_A$ ,  $\nu_A$  - axial Young's modulus and associated Poisson's ratio;  $E_T$ ,  $\nu_T$  - transverse Young's modulus and associated Poisson's ratio;

$G_A, G_T$  - axial and transverse shear moduli. Then for the region  $-a \leq x \leq a$ ;  $0 \leq y \leq 1$ ;  $0 \leq z \leq h$ ,

$$\Delta U_C^a = \int_{-a}^a \left[ \int_0^{t_1} W^1(\Delta \sigma^{a1}) dz + \int_{t_1}^h W^2(\Delta \sigma^{a2}) dz \right] dx \quad (33)$$

After the  $z$  integration is carried out minimization of the functional (33) becomes a classical problem of the calculus of variations which results in an Euler-Lagrange differential equation for the function  $\phi$ . Now it is evident from previous development that the variational solution for the thermoelastic and isothermal elastic cases are mathematically identical. Indeed the only difference between the two is the detailed form of (28) where in the first case  $T \neq 0$  and in the second  $T = 0$ . Thus the isothermal solution developed in Hashin (1985) can immediately be used to write down the thermoelastic solution simply by interpreting  $\sigma_1$  as (28). But before this is done it is necessary to take into account that intercrack distances are of different sizes. Let it be assumed that the  $90^\circ$  layer, of length  $L$  in  $x$  direction, is cracked into  $N$  pieces where any intercrack distance is denoted  $2a_n$ . Then the admissible  $\Delta \sigma^a$  for the region of such length and height  $h$  is defined by (30) with boundary conditions

$$\phi_n(\pm a) = 1, \quad \phi'_n(\pm a) = 0 \quad (34)$$

According to Hashin (1985) the Euler-Lagrange equation for  $\phi_n$  and associated boundary conditions are

$$\frac{d^4 \phi_n}{d\xi^4} + p \frac{d^2 \phi_n}{d\xi^2} + q \phi_n = 0, \quad \phi_n(\pm \rho_n) = 1, \quad \phi'_n(\pm \rho_n) = 0 \quad (35)$$

where

$$\xi = x/t_1, \quad \rho_n = a_n/t_1, \quad p = (C_{02} - C_{11})/C_{22}, \quad q = C_{00}/C_{22} \quad (36)$$

$$\begin{aligned} C_{00} &= 1/E_T + 1/\lambda E_A & C_{02} &= \frac{\nu_T}{E_T} \left( \lambda + \frac{2}{3} \right) - \frac{\nu_A}{3E_A} \lambda \\ C_{22} &= (\lambda + 1)(3\lambda^2 + 12\lambda + 8)/60E_T & C_{11} &= \frac{1}{3}(1/G_T + 1/\lambda G_A) \end{aligned} \quad (37)$$

This determines the functions  $\phi_n$  and thus the admissible stresses. For present purpose it is the quantity  $\Delta U_C^a$  which is of interest. As in Hashin (1985) this is given by

$$\Delta U_C^a = \sum_{n=1}^N \Delta U_{Cn}^a = \sigma_1^2 t_1^2 C_{22} \sum_{n=1}^N \chi(\rho_n) \quad (38)$$

where

$$\chi(\xi) = -\phi'''(\xi) \quad (39)$$

The characteristic equation of (35) is

$$r^4 + pr^2 + q = 0 \quad (40)$$

The form of  $\chi$  depends on the nature of the roots of (40). When these roots are complex, of the form  $\pm(\alpha + i\beta)$ , where  $i = \sqrt{-1}$ , then

$$\chi_n = \chi_n^c = 2\alpha\beta(\alpha^2 + \beta^2) \frac{\cosh(2\alpha\rho_n) - \cos(2\beta\rho_n)}{\alpha\sin(2\beta\rho_n) + \beta\sinh(2\alpha\rho_n)} \quad (41)$$

If the roots are real, thus of the form  $\pm\alpha, \pm\beta$ , then

$$\chi_n = \chi_n^r = \frac{\beta^2 - \alpha^2}{\coth(\alpha\rho_n)/\alpha - \coth(\beta\rho_n)/\beta} \quad (42)$$

Thus the form of the function  $\chi_n$  depends entirely on the material properties and stacking geometry of the layers.

## Analysis of Laminate Cracking

When the laminate described above develops cracks over length  $L$  in  $x$  direction, and all cracks appear simultaneously at external stress  $\sigma$ , then the energy release per unit length in  $y$  direction needed to open up these cracks is bounded from above by (38). In view of previous experience with cracked laminate energy calculation, Hashin (1985), it is expected that (38) is an accurate approximation for the energy release. It is now assumed that there is a surface energy  $\gamma$  per unit area along fibers, which is a material property of the unidirectional ply material. Since by hypothesis the layer is broken into  $N$  pieces there are  $N - 1$  cracks and therefore  $\Delta A_c = (N - 1)t_1$ , per unit length in  $y$  direction and  $0 \leq z \leq h$ . Then it follows from (9, 38)

$$\sigma_1^2 t_1 C_{22} \sum_{n=1}^N \chi(\rho_n) = (N - 1)\gamma \quad (43)$$

If, however, cracks initiate at some external average stress  $\sigma_i$  and develop progressively as the external stress increases to  $\sigma$  then it may be shown on the basis of the interpretation of 17 for progressive cracking that 43 is modified to

$$[(\sigma^2 - \sigma_i^2)/E_x^* + 2(\sigma - \sigma_i)\alpha_x^* T] h \sum_{n=1}^N \rho_n + \sigma_1^2 t_1 C_{22} \sum_{n=1}^N \chi(\rho_n) = (N - 1)\gamma \quad (44)$$

Since  $N$  is generally a large number,  $N - 1$  may be replaced by  $N$ . Then (44) can be written

$$[(\sigma^2 - \sigma_i^2)/E_x^* + 2(\sigma - \sigma_i)\alpha_x^* T] (1 + \lambda) t_1 \bar{\rho} + (k_1 \sigma + r_1 T)^2 t_1 C_{22} \bar{\chi} = \gamma \quad (45)$$

where an overbar denotes mean value and  $E_x^*$ ,  $\alpha_x^*$  are the effective Young's modulus and thermal expansion coefficient, respectively, of the uncracked laminate in  $x$  direction.

The numbers  $\rho_n$  can be regarded as the values of a random variable  $\rho$  with probability density function, (PDF),  $P(\rho)$ . Then  $\bar{\chi}$  can be expressed as

$$\bar{\chi} = \int_0^{\infty} P(\rho)\chi(\rho)d\rho \quad (46)$$

The specific form of the PDF is of course not known and it would appear that the choice should be based on experimental data. It may be assumed that the choice can be restricted to those PDF which are specified by the first two moments of  $\rho$ , namely the mean  $\bar{\rho}$  and the standard deviation  $\mu$  and in that case  $\bar{\chi} = \bar{\chi}(\bar{\rho}, \mu)$ . The most commonly used geometrical parameter for crack distribution is the crack density  $c$  which is the number of cracks per unit length, e.g. mm. Since the thickness of the cracked layer is  $2t_1$  it follows that

$$\bar{\rho} = 1/2ct_1 \quad (47)$$

Thus (45) is a relation between the input stress and temperature which produce the cracking, the geometrical parameters of the crack distribution and the surface energy.

It is instructive and helpful to consider the extreme cases of small and large crack density which are characterized by large and small  $\bar{\rho}$ , respectively. A typical plot of the function  $\chi(\rho)$  for a graphite/epoxy laminate, where the relevant form of  $\chi$  is (41), is shown in fig. 3. The unidirectional material is T300 graphite fibers in fiberite 934 epoxy with fiber volume fraction 0.55. The properties of the material are :  $E_A = 128GPa$ ,  $E_T = 8.44GPa$ ,  $G_A = 3.85GPa$ ,  $\nu_A = 0.3$ ,  $\nu_T = 0.35$ ,  $\alpha_A = -0.55 \cdot 10^{-6}/C^0$ ,  $\alpha_T = 35.9 \cdot 10^{-6}/C^0$ . It is seen that the plot consists of a linear portion for a range  $0 \leq \rho \leq \rho_1$ , a curved part and a horizontal asymptote for a range  $\rho_2 \leq \rho \leq \infty$ . Examination of such plots for a number of laminates made of fiber composites with typical fiber volume fractions 0.5 – 0.6 has shown that in all cases  $\rho_1 \sim 0.9$ ;  $\rho_2 \sim 2.2$ . This also seems to be the case when  $\chi$  is of the form (42). The nature of the plot is illuminated by series expansions of  $\chi$  near  $\rho = 0$  and asymptotic forms for large  $\rho$ . Thus for small  $\rho$

$$\begin{aligned} \chi_s^c &= (\alpha^2 + \beta^2)^2 \left[ \rho - \frac{(\alpha^2 + \beta^2)^2}{45} \rho^5 + O(\rho^7) \right] \\ \chi_s^r &= (\alpha\beta)^2 \left[ \rho - \frac{(\alpha\beta)^2}{45} \rho^5 + O(\rho^7) \right] \end{aligned} \quad (48)$$

And for large  $\rho$

$$\begin{aligned} \chi_i^c &\cong 2\alpha(\alpha^2 + \beta^2) \left\{ 1 - 2e^{-2\alpha\rho} [\cos(2\beta\rho) + \frac{\alpha}{\beta} \sin(2\beta\rho)] \right\} \\ \chi_i^r &\cong \alpha\beta(\alpha + \beta) \left[ 1 - \frac{2}{\alpha - \beta} (\beta e^{-2\alpha\rho} - \alpha e^{-2\beta\rho}) \right] \end{aligned} \quad (49)$$



The absence of a  $\rho^3$  term in (48) accounts for the substantial initial linear part of the plot and the rapid decrease of the exponentials in (49) accounts for the asymptote.

The asymptotic part of the  $\chi$  curve is associated with **crack initiation** at stress  $\sigma = \sigma_i$ . In that case the term multiplying  $\bar{\rho}$  in (45) vanishes and since the values of  $\rho$  are large the negative exponentials in (49) are neglected.

This leads to the small crack density or crack initiation relations

$$\begin{aligned} (k_1\sigma_i + r_1T)^2 2t_1 C_{22}\alpha(\alpha^2 + \beta^2) &= \gamma & \chi &= \chi^c \\ (k_1\sigma_i + r_1T)^2 t_1 C_{22}\alpha\beta(\alpha + \beta) &= \gamma & \chi &= \chi^r \end{aligned} \quad (50)$$

According to previous discussion these relations should be valid when all or most  $\rho_n$  are larger than 2.2. The actual magnitude of small crack density is independent of crack producing input  $\sigma_i, T$ . Equ. (50) may be used to determine in-situ  $\gamma$  when  $\sigma_i$  and  $T$  are known.

It should be noted that the value  $\rho \simeq 2.2$ , when  $\chi$  becomes flat, fig.3, does not imply small crack density for the in-plane stress  $\sigma_{xx}^1$ . When the cracks are far apart this stress builds up from zero on the crack surface to the value  $\sigma^1$ , (28), in the uncracked laminate. Stress variation for  $\rho = 2$  has been given in Hashin (1985) and it is seen that in this case there is strong crack interaction effect and  $\sigma_{xx}^1$  builds up only to about  $0.3\sigma^1$  midway between cracks. The explanation is that  $\sigma_{xx}^1$  depends on  $\phi$ , see (29), while  $\chi = -\phi'''$ . Therefore when  $\chi$  is constant  $\phi$  is cubic.

## Discussion and Conclusion

Previous approaches, Nairn (1989) in terms of the 2-D variational solution, Laws and Dvorak (1988) in terms of shear-lag solution, are different in the sense that it has been attempted to consider the details of progressive development of the crack patterns in order to evaluate at successive stages the energy releases needed to produce further cracking. This may thus be termed a local approach. The fundamental question which arises is: given the stress variation between two cracks which are distance  $2a_n$  apart. What is the probability of appearance of a new crack at any in-between location? But in reference to such a question it is necessary to consider the micro-mechanism of transverse failure of a ply. There is a distribution of flaws in the material which can take the form of small matrix cracks, pores and fiber/matrix interface disbonds. The weakness of a flaw may be defined by the magnitude of the stress which triggers it to develop an intralaminar crack. The weaker the flaw the less stress is required to initiate a running crack at the flaw site. Flaws of different weakness are randomly distributed along the layer ( $x$  direction) while, by comparison, the stress distribution between any two cracks may be assumed known and deterministic. Even with the assumption that only the stress  $\sigma_{xx}$  and not the other components are involved in the failure, the problem of local probability of failure seems intractable as nothing is

known about the statistics of flaw distribution. Wang (1984) has considered effect of flaw distributions by describing them as microcracks in the transverse  $yz$  plane, of size much smaller than layer thickness, assuming normal PDF for crack size and spacing. But those flaws were of necessity considered as classical cracks within the effective fiber composite, in spite of the fact that their size may be only that of a single fiber, which negates the effective property representation of their surroundings.

The most simplistic past approach has been semi-deterministic in that it has been assumed that a new crack will appear midway between cracks since this is the location of largest  $\sigma_{xx}^1$ . This approach is of course unacceptable as it completely ignores the presence of flaws. Nairn (1989) and Laws and Dvorak (1988) have adopted the more reasonable assumption that the probability of failure at any location  $x$  is proportional to the magnitude of  $\sigma_{xx}^1(x)$ . However, the latter analysis is based on the unrealistic stress field of the shear lag approximation and therefore the results obtained by Nairn should be much preferred since they are based on the much more realistic stress field as determined by the variational method.

The present approach is related to that of Nairn (1989) in that it is based on almost the same stress analysis of a cracked laminate but there are important differences. The approach may be termed global rather than local since no attempt has been made to follow the complex process of development of cracks. It is only in the intermediate range of curved  $\chi$  plot where crack geometry information beyond crack density  $c$  or equivalently  $\bar{\rho}$  is needed, and for this range it has been proposed to bring in the required additional information through the standard deviation of normalized intercrack distance  $\mu$ .

Another distinguishing feature of the method developed here is the expression of the fracture criterion (8) in terms of stress only, (13, 16). This establishes, as has been shown, that the expressions (45, 50) obtained for  $\gamma$  are rigorous upper bounds on this quantity. In all of the relevant previous literature (5), (8), (9) have been used as the fracture condition. This requires the evaluation of displacements from an approximate stress solution, thus from incompatible strains, and thus introduces additional approximation of uncertain magnitude.

The usually available information in the laminate cracking process is the input load  $\sigma$  and the crack density  $c$  which determines  $\bar{\rho}$ . There is of course no fundamental difficulty to determine  $\mu$  from section photographs. The input temperature change  $T$  is usually taken as the difference between room temperature and the manufacturing temperature  $T_0$  of the laminate. This is a problematic assumption for at  $T_0$  the laminate matrix is very soft and may be viscoelastic rather than elastic. In view of the elastic behavior requirement of the analysis it is better to define  $T_0$  as the temperature at which during the cooldown process the laminate becomes stiff enough to be considered elastic. This temperature is not easy to determine directly and it would seem that it should be backed out by comparison of the analytical results derived to experimental data of crack density versus applied load.

The most important physical property which must be determined is the surface energy per unit area or critical energy release rate  $\gamma$ . The simplest possibility is to regard  $\gamma$  as a material constant for any specific unidirectional fiber composite layer, independent of layer thickness. If so for a substantial range of crack density, about  $\bar{\rho} \geq 2.2$  the crack density is independent of input  $\sigma$ . Thus a plot of crack density (ordinate) versus  $\sigma$  (abscissa) should start with a vertical straight line for small to medium crack density. Extensive experiments of laminate crack accumulation for a series of different laminates, made of different materials have been

performed by Liu and Nairn (1992), and previously by Highsmith and Reifsnider (1982) and Wang (1984). There are cases when initial crack density growth is load independent as described above but in other cases initial crack density growth is accompanied by definite increase in  $\sigma$ . A possible explanation for the latter phenomenon is again the distribution of flaws in the material. As  $\sigma$  is applied the more severe flaws will be activated first but higher stress will be required to activate less severe flaws to result in cracks.

The theory developed should be compared to available experimental data. For this purpose it is necessary to have crack density versus applied stress data for several different laminates of different layup geometries (stacking sequence) made of the same layer unidirectional material. The values of  $\gamma$  and  $T$  must be backed out from such data with aid of (50) for small crack density. Then verification consists of ability to represent the other data which have not been used for  $\gamma, T$  determination with these values. Such verification has been given by Liu and Nairn (1992) with reasonably good results on the basis of their analysis. Fig. 4 shows crack densities versus load for 3 different laminates, as reported by Liu and Nairn (1992), where the unidirectional material is composed of T300 graphite fibers and Fiberite 934 epoxy matrix. The values of  $\bar{\rho}$ , for the different laminates corresponding to crack density  $c$ , (47), are shown near the experimental data of each laminate. It is seen that for the  $[0/90]_s$  and  $[0/90_2]_s$  laminates the experimental data are within the asymptotic flat range of the  $\chi$  curve when crack density is independent of the value of applied stress, (50), and the experimental data verify this, with some scatter. On the other hand the  $[0/90_4]_s$  data enter into the range of curved  $\chi$  when  $\bar{\rho} < 2.2$  and it is seen that these data deviate substantially from a vertical straight line. The calculations were performed with the values  $T = -160^\circ, \gamma = 1000$  Joule/m. Detailed verification of experimental results, in particular for progressive cracking, is deferred to the future.

## Acknowledgments

Support of AFOSR through the Materials Sciences Corp., Fort Washington, PA, Dr. Walter Jones contract monitor, and the Nathan Cummings Chair of Mechanics of Solids, Tel Aviv University, is gratefully acknowledged. Also acknowledged are helpful scientific interchanges with Professors J. A. Nairn and Y. Benveniste and constructive critical comments of Professor L. Slepyan and Mr. V. Vinogradov.

## REFERENCES

- Garrett, K.W. and Bailey, J.E. (1977) Multiple transverse fracture in  $90^\circ$  cross-ply laminates of glass-fibre reinforced polyester. *J. Mater. Sci.* **12**, 157-168.
- Hashin, Z. (1985) Analysis of cracked laminates: A variational approach. *Mech. Mater.* **4**, 121-136.
- Hashin, Z. (1987) Analysis of orthogonally cracked laminates under tension. *J. Appl. Mech.* **54**, 872-879.
- Highsmith, A.L. and Reifsnider, K.L. (1982) Stiffness reduction mechanisms in composite laminates. *Damage in Composite Materials*. (ed. Reifsnider, K.L.) pp. 103-117. ASTM STP 115, American Society for Testing Materials.
- Laws, N. and Dvorak, G.J. (1988) Progressive transverse cracking in composite laminates. *J. Comp. Mater.* **22**, 900-916.
- Liu, S. and Nairn, J.A. (1992) The formation and propagation of matrix microcracks in cross-ply laminates during static loading. *J. Reinforced Plast. Comp.* **11**, 158-178.
- McCartney, L.N. (1992) A theory of stress transfer in a  $0^\circ$ - $90^\circ$ - $0^\circ$  cross-ply laminate containing a parallel array of transverse cracks. *J. Mech. Phys. Solids* **40**, 27-68.
- Nairn, J.A. (1989) The strain energy release rate of composite microcracking : A variational approach. *J. Comp. Mater.* **23**, 1106-1129.
- Nairn, J.A. and Shu, S. (1994) Matrix microcracking. *Damage Mechanics of Composite Materials*, (ed Talreja, R.), pp. 187-243. Elsevier Science BN.
- Parvizi, A., Garrett, K.W. and Bailey, J.E. (1978) Constrained cracking in glass fibre reinforced epoxy cross-ply laminates. *J. Mater. Sci.* **13**, 195-201.
- Wang, A.S.D. (1984) Fracture mechanics of sublaminate cracks in composite materials. *Comp. Technol. Rev.* **6**, 45-62.
- Varna, J. and Berglund, L.A. (1994) Thermo-elastic properties of composite laminates with transverse cracks. *J. Comp. Tech. Res.* **16**, 77-87

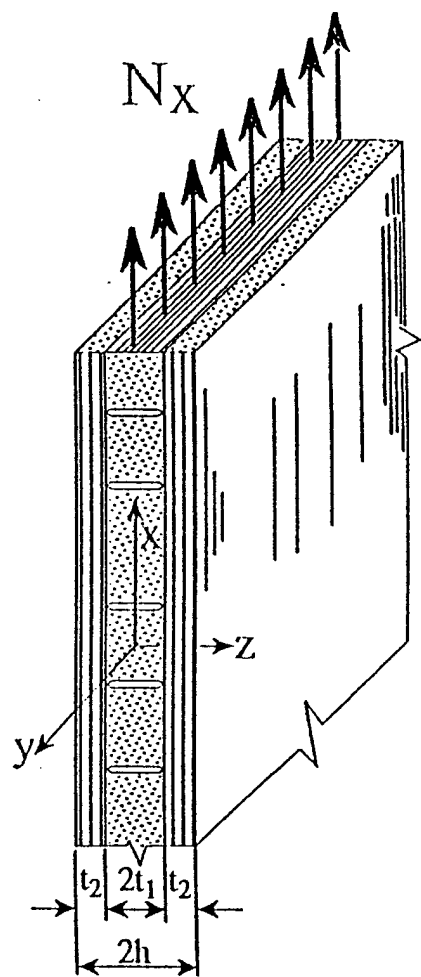


Fig. 1 - Laminate with  $90^\circ$  Layer cracked

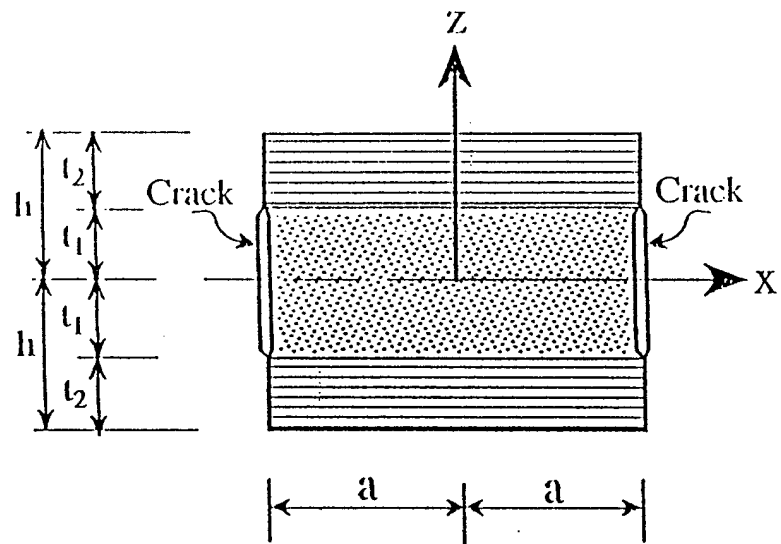


Fig. 2 - Region between Cracks

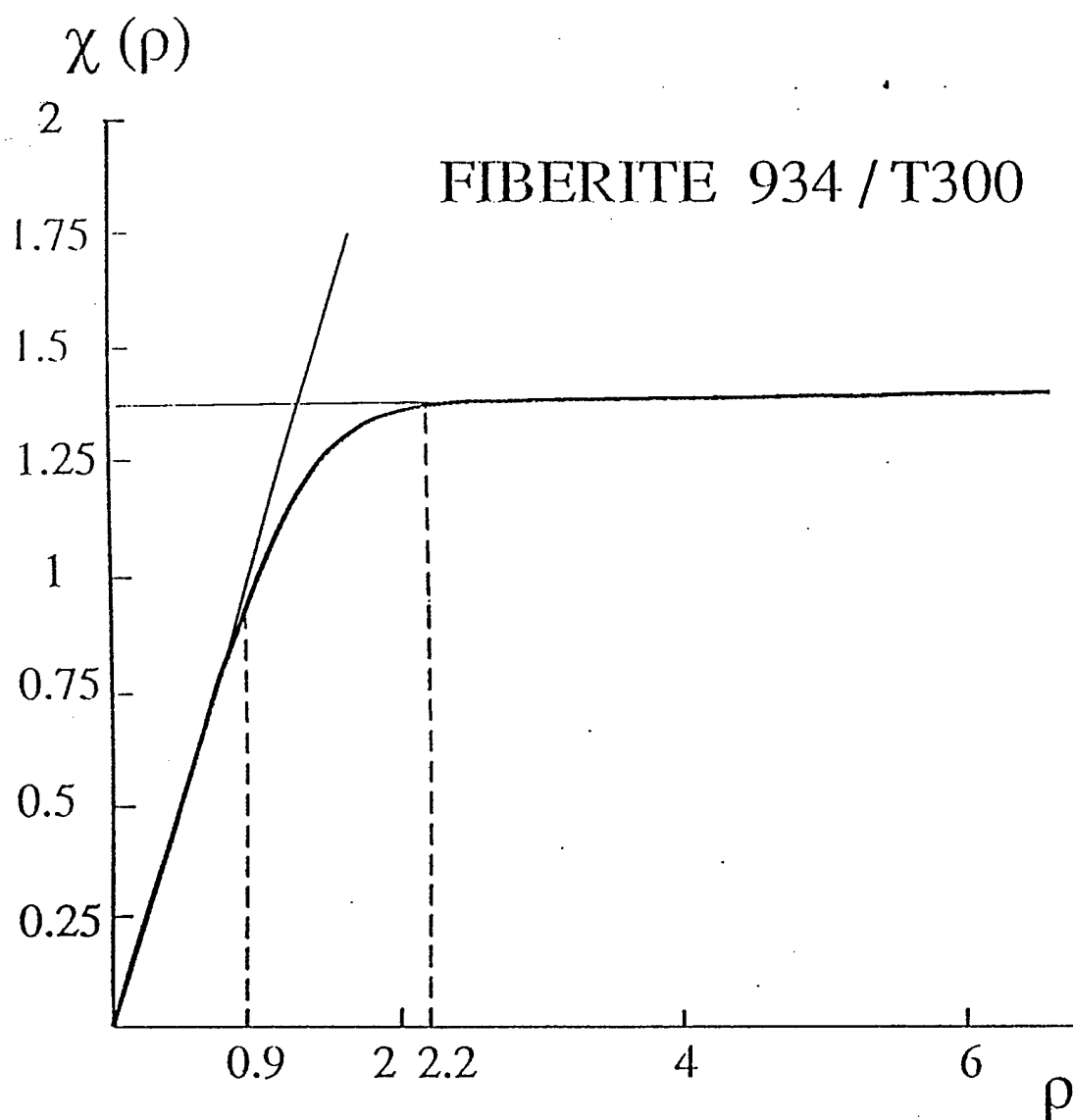


Fig. 3 - Plot of  $\chi$  Function

Fiberite 934/T300

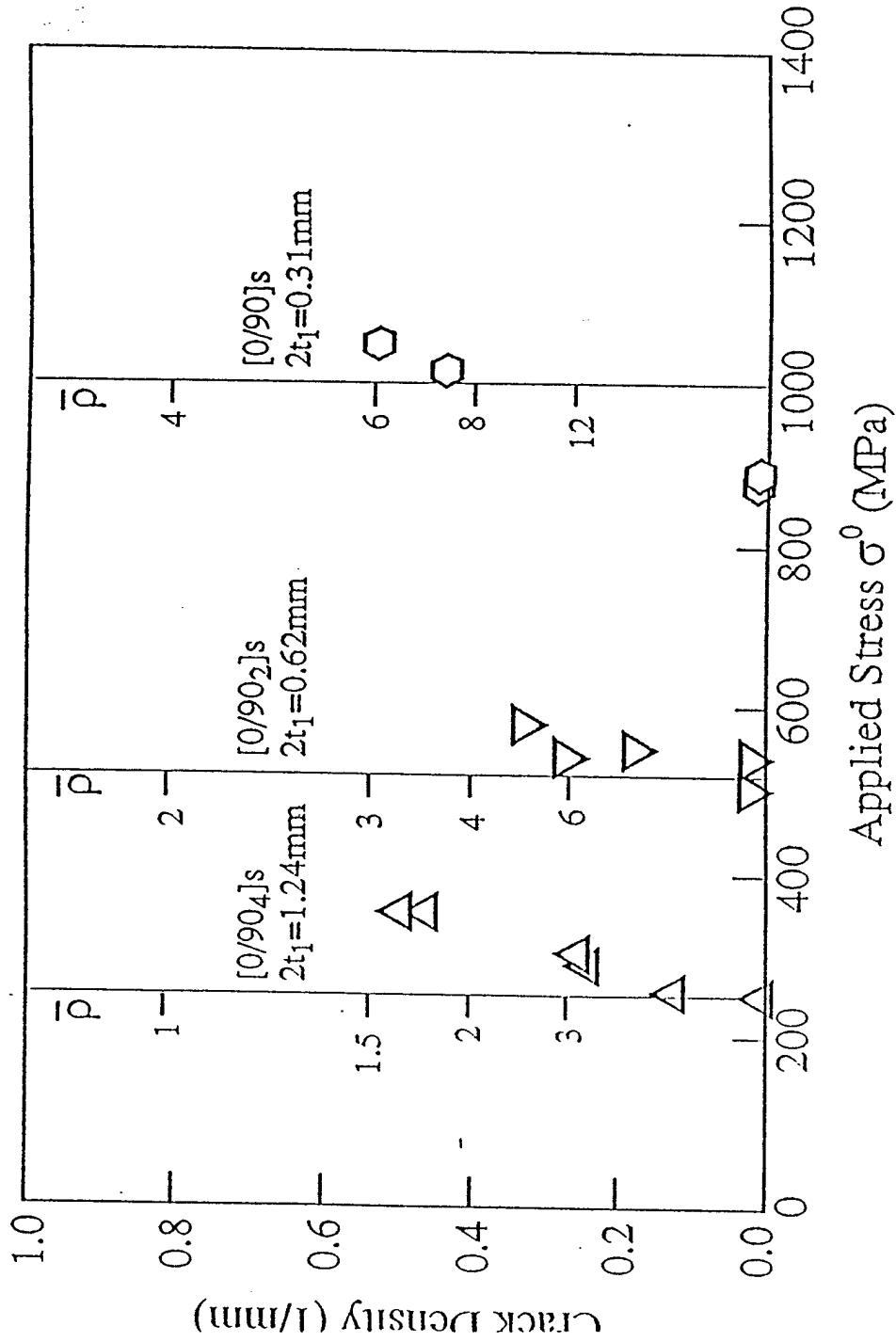


Fig. 4 - Crack Density versus Applied Stress.  
Experimental Data from Liu and Nairn (1992)



# INTERFACE DEBOND ANALYSIS

Z. Hashin and V. Vinogradov

# Interface Debond Analysis

## Introduction

Interface debonding in composite materials is a problem of great importance. Formation of interfacial cracks not only reduces the stiffness of composites, but also produces significant local stress concentrations which may result in appearance of microcracks and, in consequence, produce catastrophic failure.

In this connection two central questions are under discussion in the present chapter:

1. What applied mechanical and temperature loads produce interface debonding in composite materials ?
2. What parameters of a composite (such as volume fraction of inclusions, inclusion size and thermoelastic properties of phases) should be chosen to prevent interface debonding under given load input ?

As an answer to these questions we have to obtain a fracture criterion which will relate phases and interface properties and other details of the composite structure to critical

loads and temperature. A thermoelastic fracture criterion developed by HASHIN [22] is found to be successfully applicable for the above-mentioned purposes. In this section the method will be briefly outlined.

Consider a brittle elastic composite material body, subjected to an external mechanical load  $\mathbf{T}(S)$  and a homogeneous temperature change  $\varphi$ , which may be applied simultaneously or sequentially. Because of thermal expansion mismatch, the temperature change produces residual stresses in the composite and the mechanical load leads to mechanical stresses appearance resulting in stresses  $\sigma^0$ . Initial formation of internal cracks may have occurred due to temperature change and/or load, and their surface is denoted  $S_{c0}$ . Now consider the possibility of spontaneous formation of additional cracks for the same surface load  $\mathbf{T}(S)$ . Then the stress field changes to  $\sigma$  and the final crack surface is denoted  $S_c$ . When the new crack surface  $\Delta S_c = S_c - S_{c0}$  of area  $\Delta A_c$  forms without change of the surface load,  $\Delta \mathbf{T}(S) = 0$ , the external energy change is

$$\Delta U^e = \int_S \mathbf{T} \Delta \mathbf{u} dS \quad (4.1)$$

The internal mechanical energy change can be defined in terms of stress energy with density  $W$

$$W(\sigma) = \frac{1}{2} \sigma \mathbf{S} \sigma \quad (4.2)$$

The internal energy change can be written as

$$\Delta U^{i\sigma} = \int_V \Delta W dV = \int_V [W(\sigma) - W(\sigma^0)] dV. \quad (4.3)$$

If an additional energy of amount  $\Delta \Gamma^c$  is required to open up the new crack surface, then

the criterion for new crack formation is given by the energy balance

$$\Delta U^c = \Delta U^{i\sigma} + \Delta \Gamma^c \quad (4.4)$$

where  $\Delta \Gamma^c$  is the critical energy release. It may be assumed that there exists a material surface energy per unit area of crack opening  $\gamma$ , in which case

$$\Delta \Gamma^c = \gamma \Delta A^c \quad (4.5)$$

where  $\gamma$  is the analogue of the critical energy release rate which is usually defined as the derivative of the energy release with respect to crack area. It can be shown from (4.1)-(4.4) that the critical energy release can be expressed entirely in terms of internal stresses (see HASHIN [22]):

$$\Delta \Gamma^c = \frac{1}{2} \int_V \Delta \sigma S \Delta \sigma dV \quad (4.6)$$

For following applications this criterion can be transformed to integration over cracks surface. We can rewrite it as

$$\begin{aligned} \Delta \Gamma^c &= \frac{1}{2} \int_V \Delta \sigma S \Delta \sigma dV = \frac{1}{2} \int_V \Delta \sigma \Delta \epsilon dV \\ &= \frac{1}{2} \int_S \Delta T \Delta u dS \end{aligned} \quad (4.7)$$

Note, that according to the assumption that the traction on existing cracks remains zero,

the integration must be evaluated only over surfaces of newly developed cracks. Thus

$$\Delta\Gamma^c = \frac{1}{2} \int_{\Delta S_c} \Delta \mathbf{T} \Delta \mathbf{u} dS \quad (4.8)$$

or

$$\Delta\Gamma^c = \frac{1}{2} \int_{\Delta S_c} (\mathbf{T} - \mathbf{T}^0) (\mathbf{u} - \mathbf{u}^0) dS = -\frac{1}{2} \int_{\Delta S_c} \mathbf{T}^0 (\mathbf{u} - \mathbf{u}^0) dS \quad (4.9)$$

The surface integral for each crack is confined to the two congruent crack surfaces and thus each component of the normal appears twice, with opposite signs ( $\mathbf{n}^+ = -\mathbf{n}^-$ , see Figure 4.1).

Therefore

$$\begin{aligned} \Delta\Gamma^c &= -\frac{1}{2} \int_{\Delta S_c} \mathbf{T}^0 (\mathbf{u} - \mathbf{u}^0) dS = -\frac{1}{2} \int_{\Delta S_c^+} \mathbf{T}^{0+} (\mathbf{u}^+ - \mathbf{u}^0) dS \\ &\quad -\frac{1}{2} \int_{S_c^-} \mathbf{T}^{0-} (\mathbf{u}^- - \mathbf{u}^0) dS \\ &= \frac{1}{2} \int_{\Delta S_c^+} \mathbf{T}^0 (\mathbf{u}^- - \mathbf{u}^+) dS = \frac{1}{2} \int_{\Delta S_c^+} \mathbf{T}^0 [\mathbf{u}] dV \end{aligned} \quad (4.10)$$

where  $[\mathbf{u}]$  is the displacement jump across the crack surface, known as crack opening displacement (COD), and the integration must be evaluated once. By means of index

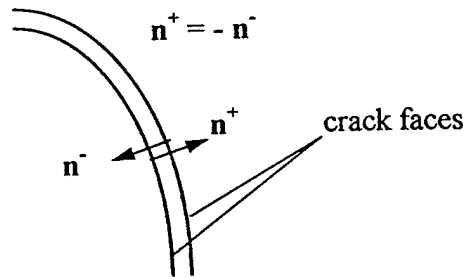


Figure 4.1: Crack faces.

notation (4.10) may be rewritten in the following form

$$\gamma \Delta A_c = \frac{1}{2} \int_{\Delta S_c} \sigma_{ij}^0 n_j [u_i] dS \quad (4.11)$$

By this is meant that the energy release can be expressed in terms of stresses in an undamaged material in the cracks' locations and displacements of the crack' faces (COD), of course, after development of the cracks. It should be noted here that kinetic energy associated with the dynamics of crack growth has been neglected.

## 4.2 Fiber Reinforced Materials under Transverse Load

Generally speaking, for a statistically homogeneous material body, location of new cracks and magnitude of applied forces or temperature which lead to crack appearance depend on loading conditions. For example, small concentrated forces or local heating may produce microcracks in bounded areas around them. In order to define the critical loading conditions as *composite material properties*, we assume here that the material remains statistically homogeneous after formation of the cracks .

Consider an infinite unidirectional fiber reinforced composite material body subjected to a homogeneous temperature change  $\varphi$  and an external applied homogeneous traction  $T_i(S) = \bar{\sigma}_{ij} n_j$  in the plane normal to the fibers. For effective transverse isotropy,  $\bar{\sigma}_{ij}$  may be chosen in the principal coordinate system  $\bar{\sigma}_{11} = \sigma_1$ ,  $\bar{\sigma}_{22} = \sigma_2$ ,  $\bar{\sigma}_{12} = 0$  which, if required, can be separated to hydrostatic part  $p = (\bar{\sigma}_1 + \bar{\sigma}_2)/2$  and deviatoric part  $\tau = (\bar{\sigma}_1 - \bar{\sigma}_2)/2$ . Then the tensile radial stresses in the interface between the matrix and the fibers may produce interfacial debonding around certain fibers. The further

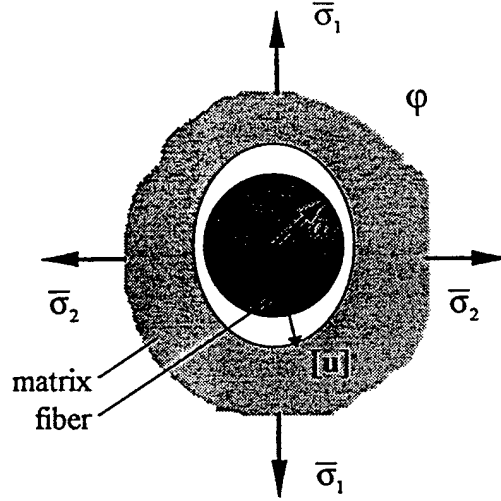


Figure 4.2: Fiber reinforced material under transverse load.

consideration will be restricted to the case of perfect debond, when there is no contact area between phases after development of the interfacial cracks, and the fiber surface is free from traction. For cylindrical surface of fibers it is convenient to consider the problem in polar coordinates. Then only the radial component of  $\mathbf{n}$  does not vanish on the interface (see Fig.4.2), and (4.11) can be rewritten in the form:

$$\gamma \Delta A_c = \frac{1}{2} \int_{\Delta S_c} \left\{ \sigma_{rr}^0 \left( u_r^{(m)} - u_r^{(f)} \right) + \sigma_{r\theta}^0 \left( u_\theta^{(m)} - u_\theta^{(f)} \right) \right\} dS \quad (4.12)$$

where  $m$  denotes the matrix and  $f$  denotes the fiber. Thus we need to solve two problems: first, we have to find the radial  $\sigma_{rr}^0$  and shear  $\sigma_{r\theta}^0$  stresses in the interface between the matrix and fibers before these fibers will separate from the matrix, and second, the displacements of the matrix  $u_\theta^{(m)}$  and the separated fibers  $u_\theta^{(f)}$  surfaces.

### 4.3 An Isolated Fiber in an Infinite Matrix

For one isolated fiber or dilute concentration of fibers when the interaction between fibers is negligible, the interfacial stress and strain fields may be described precisely. Consider first the case of perfect bond. The general two-dimensional plane strain solution in polar coordinates for transverse isotropic elastic phases assumes the following forms.

1. For isotropic load  $p$  and temperature input  $\varphi$ :

$$\begin{aligned} u_r &= (B + C/\rho^2) r; \\ \sigma_{rr} &= 2kB - 2GC/\rho^2 - 2k\alpha\varphi \end{aligned} \quad (4.13)$$

where  $k$  is the transverse bulk modulus,  $G$  is the transverse shear modulus,  $\alpha$  is the thermal expansion coefficient,  $r = r/a$  where  $a$  is the radius of the fiber and  $B$ ,  $C$  are constants which may be found from the following boundary conditions:

$$\begin{aligned} \text{The boundary condition on the external surface} \quad & \sigma_{rr}^{(m)}(r \rightarrow \infty) = p \\ \text{The displacement is continuous on the interface} \quad & u_r^{(m)}(a) = u_r^{(f)}(a) \\ \text{The traction is continuous on the interface} \quad & \sigma_{rr}^{(m)}(a) = \sigma_{rr}^{(f)}(a) \end{aligned} \quad (4.14)$$

The additional condition  $C_f = 0$  is needed to avoid singularity at  $r = 0$ .



2. For shear component  $\tau$ :

$$\begin{aligned}
u_r &= (A\rho^2 + B + C/\rho^2 + D/\rho^4) r \sin 2\theta; \\
u_\theta &= \left(\frac{2+\xi}{1-\xi}A\rho^2 + B + \frac{1}{1+\xi}C/\rho^2 - D/\rho^4\right) r \cos 2\theta; \\
\sigma_{rr} &= 2G\left(B - \frac{2}{1+\xi}C/\rho^2 - 3D/\rho^4\right) \sin 2\theta; \\
\sigma_{r\theta} &= 2G\left(\frac{3}{1-\xi}A\rho^2 + B + \frac{1}{1+\xi}C/\rho^2 + 3D/\rho^4\right) \cos 2\theta.
\end{aligned} \tag{4.15}$$

Here  $\xi = G/k$ ,  $A$ ,  $B$ ,  $C$  and  $D$  are constants, which again may be found from the boundary conditions at infinity and continuity at  $r = a$ :

$$\begin{aligned}
\sigma_{rr}^{(m)}(r \rightarrow \infty) &= \tau \sin 2\theta; \\
\sigma_{\theta\theta}^{(m)}(r \rightarrow \infty) &= \tau \cos 2\theta; \\
u_r^{(m)}(a, \theta) &= u_r^{(f)}(a, \theta); \\
u_\theta^{(m)}(a, \theta) &= u_\theta^{(f)}(a, \theta); \\
\sigma_{rr}^{(m)}(a, \theta) &= \sigma_{rr}^{(f)}(a, \theta); \\
\sigma_{r\theta}^{(m)}(a, \theta) &= \sigma_{r\theta}^{(f)}(a, \theta)
\end{aligned} \tag{4.16a}$$

and  $C_f = D_f = 0$  to avoid singularity at  $r = 0$ .

Note here that according to the well known result of Eshelby, the stress field in an isolated fiber embedded in an infinite body under homogeneous traction is also homogeneous, and thus we can obtain from (4.15d) that  $A_f = 0$ , and the six equations (4.16a) may be reduced to five. The same may be directly obtained from solution of (4.16a). The solution of three linear equations (4.14) for  $B_f$ ,  $A_m$ ,  $B_m$  and any five linear equations from (4.16a) for  $B_f$ ,  $A_m$ ,  $B_m$ ,  $C_m$  and  $D_m$  yields the following expressions for interfacial

stresses and displacements:

$$\begin{aligned}
\sigma_{rr}^0 &= q_{rr}^p p + q_{rr}^\tau \tau \sin 2\theta + q_{rr}^\varphi \varphi; \\
\sigma_{r\theta}^0 &= q_{r\theta}^\tau \tau \cos 2\theta; \\
u_r^0 &= (l_r^p p + l_r^\tau \tau \sin 2\theta + l_r^\varphi \varphi) a; \\
u_\theta^0 &= l_\theta^\tau \tau a \cos 2\theta;
\end{aligned} \tag{4.17}$$

where  $q_{rr}$ ,  $q_{r\theta}$ ,  $l_r$  and  $l_\theta$  are the interfacial stresses  $\sigma_{rr}$ ,  $\sigma_{r\theta}$  and the interface displacements  $u_r$ ,  $u_\theta$  respectively due to a unit loading input, the nature of which is noted by superscript index: the hydrostatic pressure  $p$ , the shear stress  $\tau$  and the temperature  $\varphi$ . These coefficients are functions of the matrix and fiber properties only:

$$\begin{aligned}
q_{rr}^p &= g \frac{1 + \xi_m}{g + \xi_f}; \quad q_{rr}^\tau = q_{r\theta}^\tau = 2g \frac{1 + \xi_m}{1 + g(1 + 2\xi_m)}; \\
q_{rr}^\varphi &= 2G_m g \frac{(\alpha_m - \alpha_f)}{g + \xi_f};
\end{aligned} \tag{4.18}$$

and

$$\begin{aligned}
l_r^p &= \frac{\xi_f}{2G_m} \frac{1 + \xi_m}{g + \xi_f}; \quad l_r^\tau = l_\theta^\tau = \frac{1}{G_m} \frac{1 + \xi_m}{1 + g(1 + 2\xi_m)}; \\
l_r^\varphi &= \alpha_f + \frac{\xi_f}{g + \xi_f} (\alpha_m - \alpha_f);
\end{aligned} \tag{4.19}$$

where  $g = G_f/G_m$ .

After the crack development  $\sigma_{rr}$  and  $\sigma_{r\theta}$  vanish on the interface and this situation may be simply obtained from (4.18) by substituting  $G_f = k_f = 0$ , thus assuming a void instead of a fiber. Analogously the displacements of the matrix surface may be obtained from (4.19) by putting  $G_f = k_f = 0$ . This leads to the following expressions for the

matrix surface displacements (4.19c,d):

$$u_r^0 = (l_r^p p + l_r^\tau \tau \sin 2\theta + l_r^\varphi \varphi) a;$$

$$u_\theta^0 = l_\theta^\tau \tau a \cos 2\theta;$$

with new coefficients:

$$l_r^p = \frac{1}{2G_m}(1 + \xi_m); \quad l_r^\tau = l_\theta^\tau = \frac{1}{G_m}(1 + \xi_m) \quad (4.20)$$

$$l_r^\varphi = \alpha_m$$

The fiber surface freely expands due to temperature change, so  $u_\theta^{(f)} = 0$  and  $u_r^{(f)} = \alpha_f a \varphi$ .

It results in the crack opening displacement<sup>1</sup>:

$$[u_r] = \{l_r^p p + l_r^\tau \tau \sin 2\theta + (\alpha_m - \alpha_f) \varphi\} a; \quad (4.21)$$

$$[u_\theta] = l_\theta^\tau \tau a \cos 2\theta.$$

Now replacing  $p$  and  $\tau$  by  $(\sigma_1 + \sigma_2)/2$  and  $(\sigma_1 - \sigma_2)/2$  respectively and substituting (4.17) and (4.21) into the debond criterion (4.12) with help of  $\Delta A_c = 2\pi a H$  and  $dS_c = a H d\theta$ , where  $H$  is the length of the fiber, one can obtain:

$$\begin{aligned} A(\sigma_{1cr}^2 + \sigma_{2cr}^2) + B(\alpha_m - \alpha_f)^2 \varphi_{cr}^2 + 2C\sigma_{1cr}\sigma_{2cr} \\ + 2D(\alpha_m - \alpha_f)(\sigma_{1cr} + \sigma_{2cr})\varphi_{cr} = \frac{2\gamma}{a} \end{aligned} \quad (4.22)$$

<sup>1</sup>Generally speaking, the separated fiber can move freely in the formed pseudovoid. But this has no influence on the inner elastic energy and hence may be omitted from consideration.

where  $A, B, C, D$  depend on the elastic properties of the matrix and fiber:

$$\begin{aligned} A &= \frac{g(1 + \xi_m)^2}{2G_m} \left[ \frac{1}{4(g + \xi_f)} + \frac{1}{1 + g(1 + 2\xi_m)} \right]; \\ B &= 2G_m \frac{g}{g + \xi_f}; \\ C &= \frac{g(1 + \xi_m)^2}{2G_m} \left[ \frac{1}{4(g + \xi_f)} - \frac{1}{1 + g(1 + 2\xi_m)} \right]; \\ D &= \frac{g}{2} \frac{(1 + \xi_m)}{(g + \xi_f)} \end{aligned} \quad (4.23)$$

The formula (4.22) relates the critical external forces and temperature change which produce interface debond, to phases properties, the critical energy release rate  $\gamma$  and fiber radius. The parameter  $\gamma$  is most probably controlled by chemical bond effectiveness, the fiber surface treatment and process of composite fabrication.

In spite of the fact that interfacial stresses do not depend on the fiber radius, the critical loads and associated critical stresses in the interface decrease with increasing of the fiber size, which means that fibers of larger radius are more sensitive to crack formation. Moreover, it follows that for a given external mechanical load and temperature there is a critical fiber size above which cracks will first appear and it can be calculated from (4.22). Note here that these conclusions are in conflict with the concept of ultimate stress which is a property of material, but not of geometry. According to the present approach, although the magnitudes of the stresses are independent of fiber size, the total stress energy depends on the volume of material under the influence of these stresses, which in turn, depends on the fiber size. That is, the larger the fiber radius, the larger the stressed volume both within and around the fiber, and thus, the larger the stress energy that is associated with the fiber (quadratic in the radius). The same may be said about the stress energy change due to debonding. On the other hand, the energy release

is linearly proportional to the crack area, and consequently to the fiber radius. It follows from here that for a larger fiber size, smaller stresses are required for the stress energy change to reach its critical value and for a crack to appear.

## 4.4 Arbitrary Concentration of Fibers

The above result leads us to conclude that in the case of arbitrary concentration of fibers, pseudovoids may form in a gradual manner according to the size distribution of fibers. After the first groups of fibers produce cracks in the interface around them under increasing load and temperature, the phase constitution of the composite changes: the third phase, pseudovoids, appears in the places of debonded fibers. Further increase of loads will cause new interfacial cracks to appear and hence the volume fraction of the fibers will decrease and the pseudovoids volume fraction will increase. This process of voids formation may continue until all fibers separate from the matrix, or in other words, the volume fraction of the voids is equal to the initial volume fraction of the fibers. Now the composite again contains two phases: the matrix and the pseudovoids instead of the fibers.

We restrict the following consideration to the particular case when all fibers have the same radius  $a$  and they separate from the matrix under the same external load and temperature. In order to use the criterion (4.12) the generalized self consistent scheme approximation (GSCS) will be applied to calculate the interfacial stresses and displacements for two extreme cases: a matrix with embedded fibers of volume fraction  $v_2$ , and a matrix containing voids of the same volume fraction  $v_2$ . In spite of the fact that the interface displacements and stresses obtained in framework of GSCS are approximate,

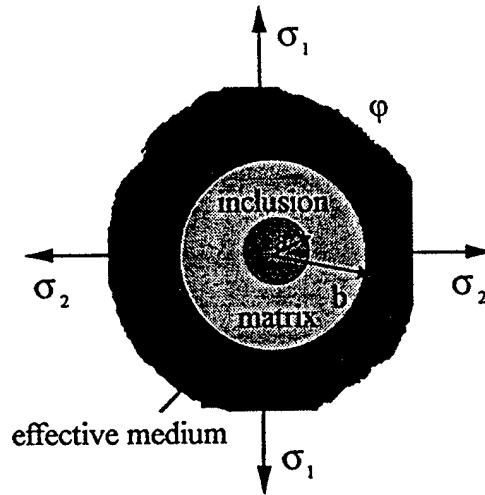


Figure 4.3: Generalized self consistent scheme (GSCS).

the energy change may be described in terms of changes of the effective thermoelastic moduli, which in turn agree very well with experimental data.

The essence of the GSCS is that in order to determine the stress and strain fields in the phases, the composite is represented as a composite cylinder, consisting of a fiber core and a matrix concentric shell, embedded in an infinite homogeneous material to which the effective properties are assigned. The radii of the fiber  $a$  and the matrix shell  $b$  are chosen in such a manner that  $(a/b)^2 = v_2$ , which is to say that the volume fraction of the fiber in the composite cylinder is equal to the volume fraction of fibers in the composite material (see Fig.4.3).

When this structure is subjected to a homogeneous temperature change  $\varphi$  and/or hydrostatic tension  $p$  is applied to the external surface, the stress field in material (0) and consequently on the composite cylinder surface is homogeneous ( $\sigma_{rr}^{(0)} = p$ ), and thus, the traction may be applied immediately to the cylinder surface ( $r = b$ ). This is consistent with the fact that the GSCS approximation gives precisely the same result for

the effective bulk modulus  $k^*$  as obtained by the composite cylinder assemblage (CCA), according to which the composite cylinder described above behaves just as a homogeneous transversal isotropic cylinder with the plane bulk modulus  $k^*$ . The foregoing is incorrect in the case of a transverse shear input  $\tau$ , because then the traction on the composite cylindric surface does not remain homogeneous under a homogeneous external traction. For more details about GSCS and CCA see CHRISTENSEN [30].

Thus, the CCA in the case of a hydrostatic tensile load and temperature, and the GSCS for the transverse shear will be used for the required interfacial stresses and displacements. Then the general elastic solutions (4.13) and (4.15) are valid with new boundary conditions:

1. Uncracked composite under hydrostatic load and temperature (CCA)

$$\begin{aligned}\sigma_{rr}^{(0)}(b) &= p \\ u_r^{(f)}(a) &= u_r^{(m)}(a) \\ \sigma_{rr}^{(f)}(a) &= \sigma_{rr}^{(m)}(a)\end{aligned}\tag{4.24}$$

and for pseudovoids

$$\begin{aligned}\sigma_{rr}^{(0)}(b) &= p \\ \sigma_{rr}^{(f)}(a) &= 0\end{aligned}\tag{4.25}$$

Inserting equations (4.13) into (4.24) we obtain three linear equations for unknown coefficients  $B_f$ ,  $B_m$  and  $C_m$  (again  $C_f = 0$  to avoid singularity at  $r = 0$ ). The solution results the following expression for interface stress

$$\sigma_{rr}^0 = \frac{k_f(G_m + k_m)}{v_1 k_m(G_m + k_f) + v_2 k_f(G_m + k_m)} p$$

$$+ \frac{2G_m k_m k_f v_1}{v_1 k_m (G_m + k_f) + v_2 k_f (G_m + k_m)} (\alpha_m - \alpha_f) \varphi \quad (4.26)$$

After crack formation, recalling that  $u_f = \alpha_f a \varphi$ , which means free expansion of fiber due to temperature change, equations (4.25) give us the desired COD

$$[u_r] = \left[ \frac{(G_m + k_m)}{2k_m G_m v_1} p + (\alpha_m - \alpha_f) \varphi \right] a \quad (4.27)$$

2. For the undamaged composite subjected to pure shear (GSCS) the boundary conditions are

$$\begin{aligned} \sigma_{rr}^{(0)}(r \rightarrow \infty) &= \tau \sin 2\theta, \\ \sigma_{r\theta}^{(0)}(r \rightarrow \infty) &= \tau \cos 2\theta, \\ u_r^{(f)}(a, \theta) &= u_r^{(m)}(a, \theta), \\ u_\theta^{(f)}(a, \theta) &= u_\theta^{(m)}(a, \theta), \\ u_r^{(m)}(b, \theta) &= u_r^{(0)}(b, \theta), \\ u_\theta^{(m)}(b, \theta) &= u_\theta^{(0)}(b, \theta), \\ \sigma_{rr}^{(f)}(a, \theta) &= \sigma_{rr}^{(m)}(a, \theta), \\ \sigma_{r\theta}^{(f)}(a, \theta) &= \sigma_{r\theta}^{(m)}(a, \theta), \\ \sigma_{rr}^{(m)}(b, \theta) &= \sigma_{rr}^{(0)}(b, \theta), \\ \sigma_{r\theta}^{(m)}(b, \theta) &= \sigma_{r\theta}^{(0)}(b, \theta) \end{aligned} \quad (4.28)$$

with the additional restriction  $C_f = D_f = 0$  to avoid singularity at  $r = 0$ . Comparing equations (4.28a,b) to (4.15c,d) it is seen that

$$A_0 = 0, \quad B_0 = \frac{\tau}{2G^*}$$



The insertion of (4.15) into (4.28) yields eight linear algebraic equations for the eight unknown coefficients:  $A_f$ ,  $B_f$ ,  $A_m$ ,  $B_m$ ,  $C_m$ ,  $D_m$ ,  $C_0$  and  $D_0$ . In addition, CHRISTENSEN & LO [29] have proved that

$$C_0 = 0$$

This precise condition has been found on the basis of the assumption that the average strain energy density of an embedded composite cylinder is equal to the average strain energy density of the composite material. Hence, the set of eight linear equations (4.28c)–(4.28j) gives  $G^*$  as well as the stress field in the interface between the fiber and the matrix, which can be written in the form

$$\begin{aligned}\sigma_{rr}^0 &= q_{rr}^r \tau \sin 2\theta \\ \sigma_{r\theta}^0 &= q_{r\theta}^r \tau \cos 2\theta\end{aligned}\tag{4.29}$$

In a similar manner, the COD may be obtained when a crack formed in the interface. In this case the continuity conditions at  $r = a$  (4.28c,d,g,h) must be replaced with

$$\begin{aligned}\sigma_{rr}^{(m)}(a, \theta) &= 0 \\ \sigma_{r\theta}^{(m)}(a, \theta) &= 0\end{aligned}$$

which means that the inner surface of the matrix shell is free from traction. Solution

of these six linear equations gives

$$\begin{aligned} [u_r] &= l_r^\tau a \sin 2\theta \\ [u_\theta] &= l_\theta^\tau a \cos 2\theta \end{aligned} \quad (4.30)$$

Superposition of (4.26), (4.27), (4.29) and (4.30) yields the following expressions for the required interfacial stresses and COD

$$\begin{aligned} \sigma_{rr}^0 &= q_{rr}^p p + q_{rr}^\tau \tau \sin 2\theta + q_{rr}^\varphi \varphi; \\ \sigma_{r\theta}^0 &= q_{r\theta}^\tau \tau \cos 2\theta; \\ [u_r] &= \{l_r^p p + l_r^\tau \tau \sin 2\theta + (\alpha_m - \alpha_f) \varphi\} a; \\ [u_\theta] &= l_\theta^\tau \tau a \cos 2\theta; \end{aligned} \quad (4.31)$$

where  $q_{rr}^p$ ,  $q_{rr}^\varphi$  and  $l_r^p$  are defined by (4.26) and (4.27), and  $q_{rr}^\tau$ ,  $q_{r\theta}^\tau$ ,  $l_r^\tau$ ,  $l_\theta^\tau$  are obtained from solution of GSCS equations as described above.

Substituting (4.31) into criterion (4.12) and evaluating the integration over all fibers' surfaces, one can obtain

$$\begin{aligned} A(\sigma_{1cr}^2 + \sigma_{2cr}^2) + B(\alpha_m - \alpha_f)^2 \varphi_{cr}^2 + 2C\sigma_{1cr}\sigma_{2cr} \\ + 2D(\alpha_m - \alpha_f)(\sigma_{1cr} + \sigma_{2cr})\varphi_{cr} = \frac{2\gamma}{a} \end{aligned} \quad (4.32)$$

where coefficients  $A$ ,  $B$ ,  $C$  and  $D$  are functions of the elastic properties of phases and the volume fraction of the fibers.

## 4.5 Numerical Results and Conclusions

The criterion (4.32) can be rewritten in the form

$$F(\sigma_{1cr}, \sigma_{2cr}, \varphi_{cr}) = 1 \quad (4.33)$$

where  $F(\sigma_{1cr}, \sigma_{2cr}, \varphi_{cr})$  is a quadratic polynomial function of critical applied stresses and temperature, which tend to perfect debond in the interfaces

$$\begin{aligned} F(\sigma_{1cr}, \sigma_{2cr}, \varphi_{cr}) \equiv & A \left( \left( \frac{\sigma_{1cr}}{c} \right)^2 + \left( \frac{\sigma_{2cr}}{c} \right)^2 \right) + B(\alpha_m - \alpha_f)^2 \left( \frac{\varphi_{cr}}{c} \right)^2 \\ & + 2C \left( \frac{\sigma_{1cr}}{c} \right) \left( \frac{\sigma_{2cr}}{c} \right) + 2D(\alpha_m - \alpha_f) \left( \frac{\sigma_{1cr}}{c} + \frac{\sigma_{2cr}}{c} \right) \left( \frac{\varphi_{cr}}{c} \right) \end{aligned} \quad (4.34)$$

and  $c = \sqrt{2\gamma/a}$ . In  $(\sigma_1, \sigma_2, \varphi)$  space (4.33) builds a second order surface which we will call the "DEBOND SURFACE".

In the  $(\sigma_1, \sigma_2)$  plane the curve  $F(\sigma_{1cr}, \sigma_{2cr}, 0) = 1$  is an ellipse (Fig.4.4b) with the semimajor axis tilted at an angle  $\pi/4$  to the axes  $\sigma_1$  and  $\sigma_2$ . The values of the ellipse semiaxes may be evaluated by substituting  $\sigma_{1cr} = \sigma_{2cr}$  for the semimajor axis (which corresponds to hydrostatic tension  $2p_{cr} = \sigma_{1cr} = \sigma_{2cr}$ ), and  $\sigma_{1cr} = -\sigma_{2cr}$  for the semiminor axis (for pure shear  $2\tau_{cr} = \sigma_{1cr} = -\sigma_{2cr}$ ).

Thus, if the point  $(\sigma_1, \sigma_2)$  which represents the current loading conditions is inside the ellipse, then there are no interfacial cracks in the material. Otherwise, if the loading path reach the ellipse surface, the energy release becomes enough to produce the interface debond.

For the most important case, when  $\alpha_f \ll \alpha_m$ ,  $k_f \gg k_m$  and  $G_f \gg G_m$ , the temper-

ature  $\varphi$  scarcely changes the values of the semiaxes, but it has influence on the ellipse center position. When the temperature increases  $\varphi > 0$ , the critical stresses decrease and the ellipse moves into the third quarter of the  $(\sigma_1, \sigma_2)$  plane along the line  $\sigma_1 = \sigma_2$ . Conversely, the ellipse center moves into the first quarter of the  $(\sigma_1, \sigma_2)$  plane along the line  $\sigma_1 = \sigma_2$  when  $\varphi < 0$ . In both these cases the ellipse remains symmetric around the lines  $\sigma_1 = \sigma_2$  and  $\sigma_1 = -\sigma_2 + 2h$ , where  $\sigma_1 = \sigma_2 = h$  is the center of the ellipse. The three-dimensional debond surface is shown schematically in Fig.4.4a. It is obviously seen that the surface presents an elliptic cylinder tilted to the  $(\sigma_1, \sigma_2)$  plane.

The debond surfaces  $(\sigma_{1cr}, \sigma_{2cr})$  for various volume fractions of fibers  $v_2$  and temperatures  $\varphi$  are shown in Fig.4.5 and Fig.4.6. The constituent properties used are:

Epoxy as matrix	Glass as fibers
$E_m = 0.4 \cdot 10^6 \text{psi}$	$E_f = 10.5 \cdot 10^6 \text{psi}$
$\nu_m = 0.35$	$\nu_f = 0.20$
$\alpha_m = 30 \cdot 10^{-6} \text{ } ^\circ\text{F}^{-1}$	$\alpha_f = 2.8 \cdot 10^{-6} \text{ } ^\circ\text{F}^{-1}$

It is interesting to note, that the ellipse moving along the line  $\sigma_1 = \sigma_2$  resembles the phenomenon of kinematic hardening, and the increasing of the ellipse semiaxes' values with fiber volume fraction decreasing is similar to isotropic hardening, which are both well known from the theory of plasticity. Of course, in the present problem this occurs for completely different reasons.

It should be noted here that not all points of the ellipses correspond to possible physical situations. For example, hydrostatic pressure and cooling can not produce interfacial cracks, because in this case the radial stresses in the interface are negative. In order to

exclude this type of problems, we have to require that

$$[u_r] \geq 0 \quad (4.35)$$

for all angles  $\theta$ , in such a way that there is no contact area between the matrix and the fibers (perfect debond), or in other words, the cracks' surfaces must be free of tractions. Substituting the expressions for COD (4.31c,d) into this inequality we obtain the ranges of critical stresses and temperatures that satisfy (4.35). The points of the debond surfaces which are inside these ranges are shown in Fig.4.5 and Fig.4.6 in black.

All the above leads us to the following most important conclusions:

1. The smaller the fiber radius that is chosen during fabrication of the composite, the larger the critical external applied loads and temperature which produce interface debond. For a given load and temperature input, the maximal allowable fiber radius can be estimated from the criterion (4.32).
2. As can be seen from Fig.4.5, composites with larger volume fraction of fibers are more susceptible to interface debond.
3. Decreasing the temperature does increase the critical mechanical loads, see Fig.4.6. This means that residual thermal stresses can prevent interface separation. On the other hand, in the case of overcooling, the appearance of positive tangential stresses in the matrix may produce matrix cracking, which is desirable to be avoided.
4. It may be assumed that the critical energy release rate  $\gamma$ , which can be found by experimental approach, is a property of the interface, but not of the volume fraction

of fibers or fiber radius. The higher the strength of interface between matrix and fibers, the larger the loads that must be applied to produce the interface failure.

These results may be used in design of fiber reinforced composite materials to prevent the interface separation and improve the composite's overall strength.

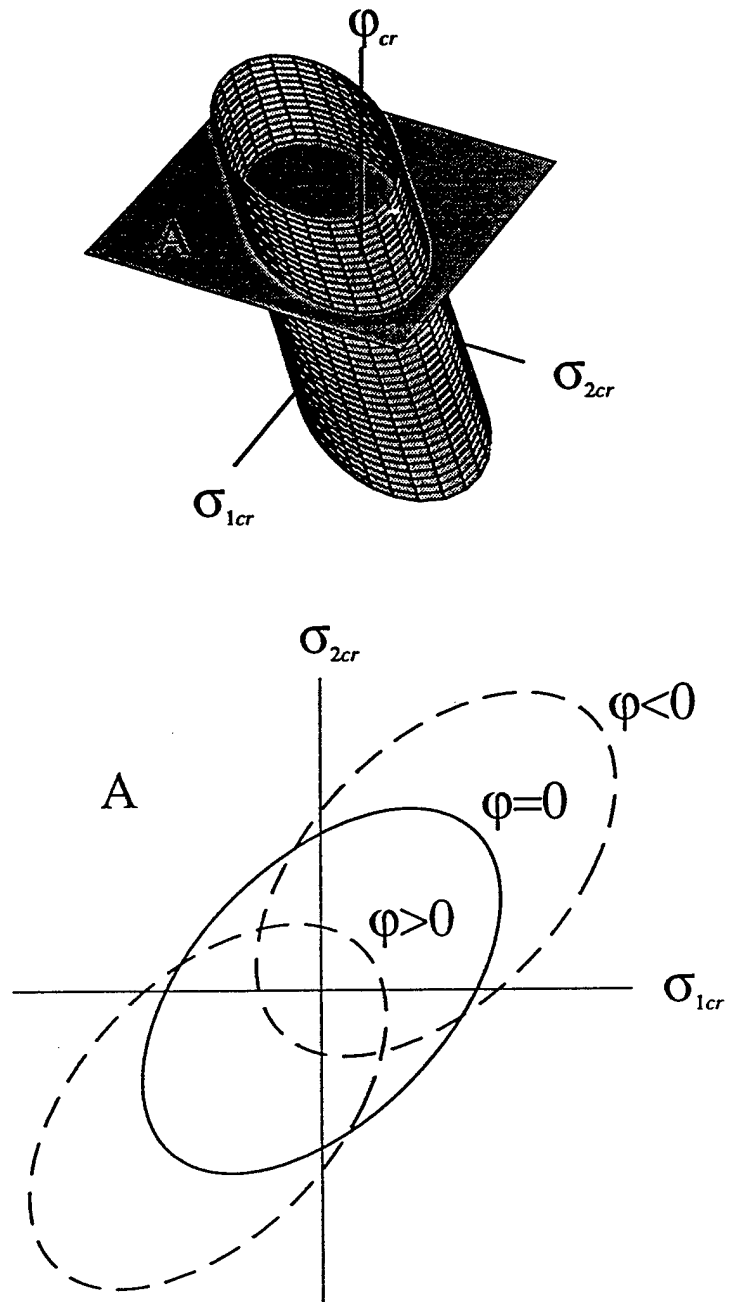


Figure 4.4: Debond surface.

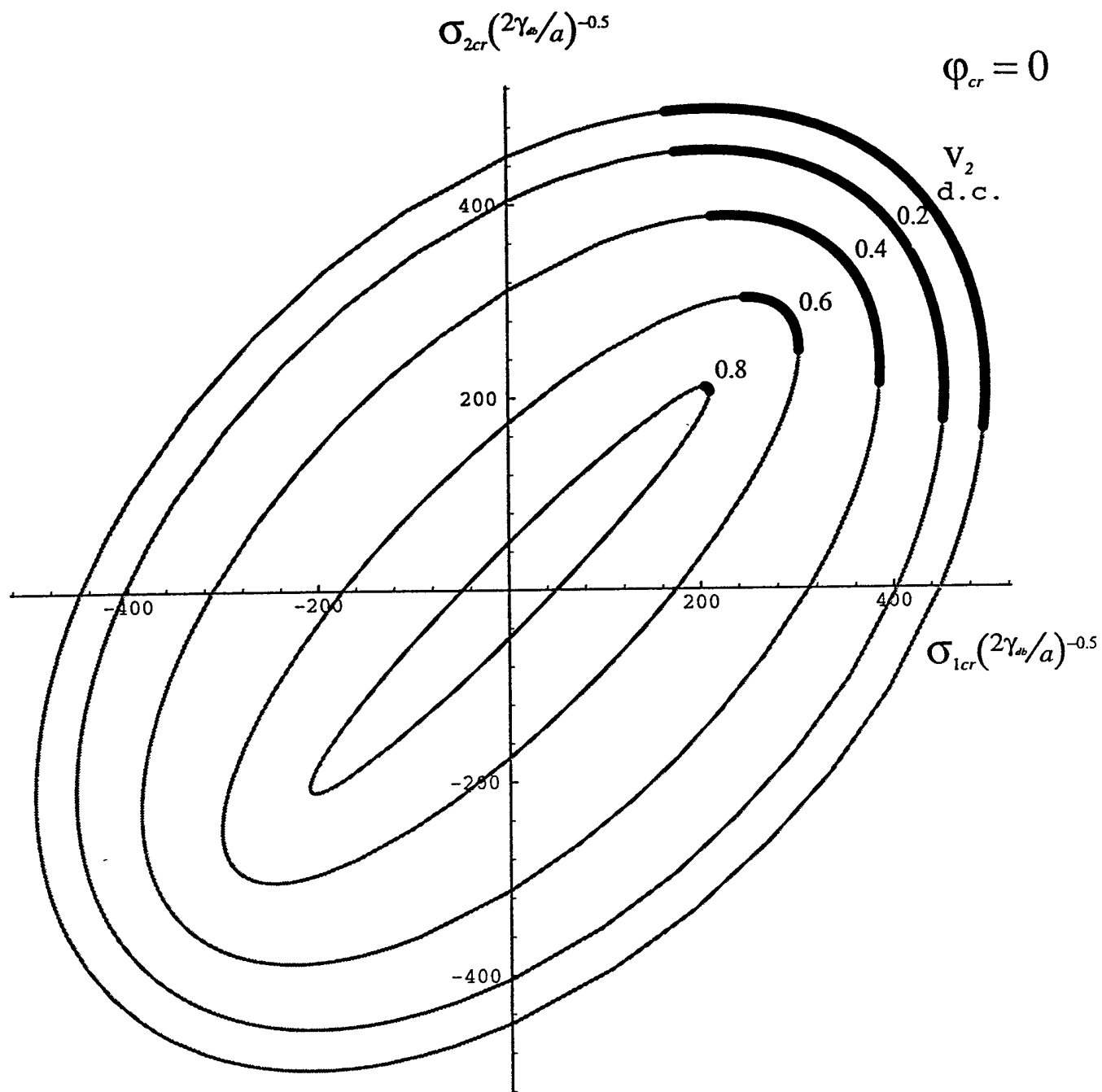


Figure 4.5: Debond surfaces for various volume fractions of fibers.



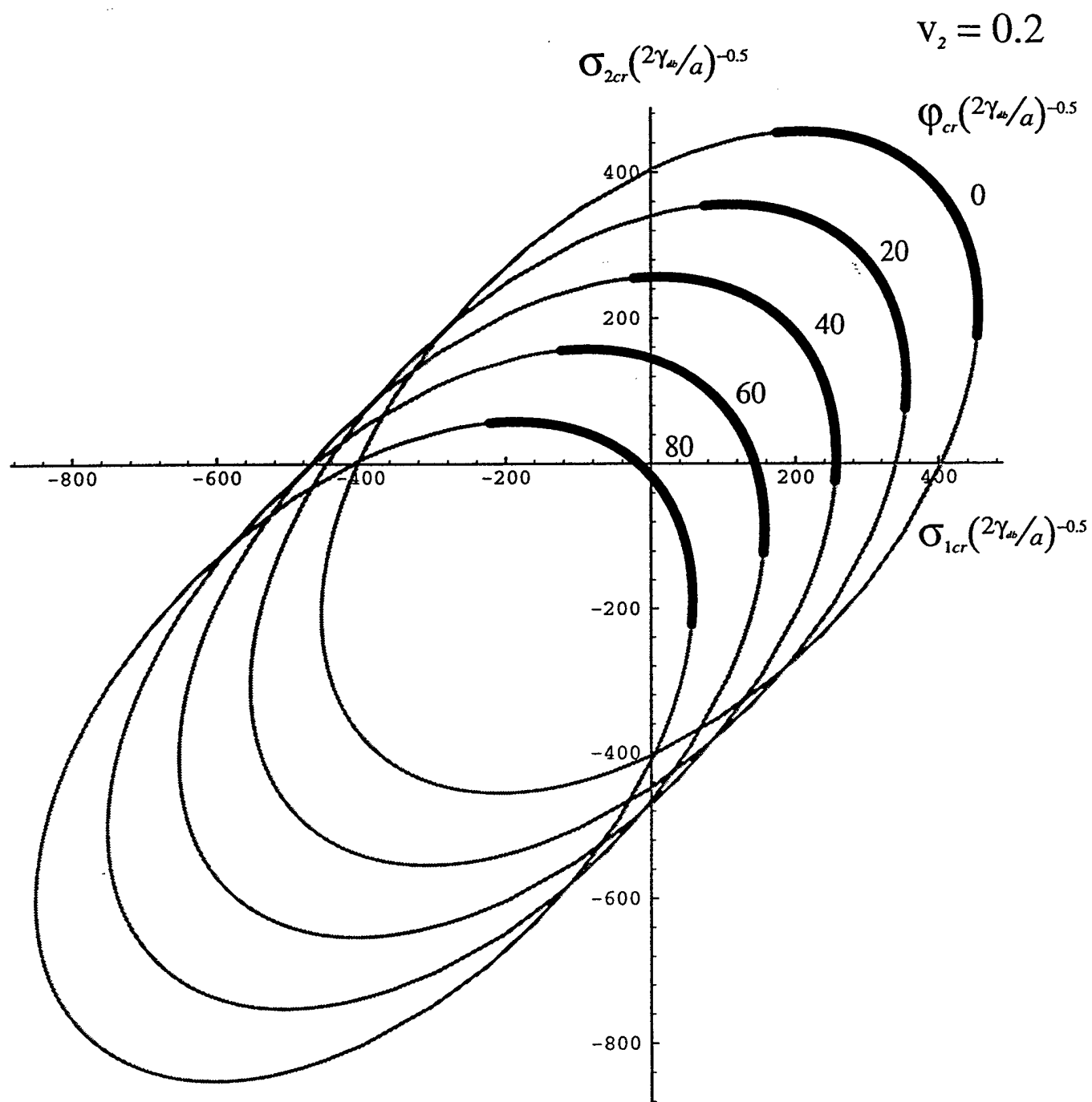


Figure 4.6: Debond surface for various temperature.

# Bibliography

- [1] BRISTOW, J.R. (1960), Microcracks, and the static and dynamic elastic constants at annealed and heavily cold-worked materials, *Br. J. Appl. Physics*, **11**, 81.
- [2] WALSH, J.B.(1969), New Analysis of attenuation in partially melted rock, *J. Geophys. Res.*, **74**, 4333.
- [3] SALGANIK, R.L. (1973), Mechanics of bodies with many cracks, *Izv. AN SSSR, Mekhanika Tverdogo Tela*, **8**, 149-158.
- [4] GRIGGS, D.T., JACKSON, D.D., KNOPOFF, L., and SHREVE, R.L. (1975), Earthquake prediction: Modelling the anomalous  $v_p/v_s$  source region, *Science*, **187**, 537-540.
- [5] GARBIN, H.D. and KNOPOFF, L. (1973), The compressional modulus of a material permeated by a random distribution of free circular cracks, *Quart. Appl. Mech.*, **33**, 301-303.
- [6] GARBIN, H.D. and KNOPOFF, L. (1975), The shear modulus of a material permeated by a random distribution of free circular cracks, *Quart. Appl. Mech.*, **33**, 296-300.

- [7] GARBIN, H.D. and KNOPOFF, L. (1975), Elastic moduli of a medium with liquid-filled cracks, *Quart. Appl. Mech.*, **33**, 301-303.
- [8] BUDIANSKY, B. and O'CONNELL, R.L. (1976), Elastic moduli of a cracked solid, *Int. J. Solids Struct.*, **12**, 81-97.
- [9] HORII, H. and NEMMAT-NASSER, S. (1983), Overall moduli of solids with microcracks: load-induced anisotropy, *J. Mech. Solids*, **31**, 155-171.
- [10] HOENIG, A. (1979), Elastic moduli of a non-randomly cracked body, *Int. J. Solids Struct.*, **15**, 137-154.
- [11] BENVENISTE, Y. and ABOUDI, J. (1987), The effective moduli of cracked bodies in plane deformations, *Engng Fracture Mech.*, **26**, 171-184.
- [12] HUANG, Y., HU, K.X. and CHANDRA, A. (1994), A generalized self-consistent mechanics method for microcracked solids, *J. Mech. Phys. Solids*, **42**, 1273-1291.
- [13] BENVENISTE, Y. (1986), On the Mori-Tanaka method in cracked solids, *Mech. Res. Comm.*, **13**, 193-201.
- [14] HASHIN, Z. (1988), The differential scheme and its application to cracked materials, *J. Mech. Phys. Solids*, **36**, 719-734.
- [15] KACHANOV, M. (1993), Elastic solids with many cracks and related problems, in *Advances in Applied Mechanics* (J. Hutchinson and T. Wu, eds.), **30**, 259-445.
- [16] HUANG, Y., HU, K.X. and CHANDRA, A. (1993), The effective elastic moduli of microcracked composite materials, *Int. J. Solids Struct.*, **30**, 1907-1918.

- [17] BASSANI, J.L. (1991), Linear densification and microcracking in sintering compacts, *Mech. Mater.*, **12**, 119-130.
- [18] BRUGGEMAN, D.A.G. (1935), Berechnung verschiedener physikalischer Konstanten von heterogenen Substanzen, *Annalen der Physik*, **24**, 636-679.
- [19] McLAUGHLIN, R. (1977), A study of the differential scheme for composite materials, *Int. J. Engng. Sci.*, **15**, 237-244.
- [20] NORRIS, A.N. (1985), A differential scheme for the effective moduli of composites, *Mech. Mater.*, **4**, 1-16.
- [21] NORRIS, A.N., CALLEGARY, A.J. and SHENG, P. (1985), A generalized differential effective medium theory, *J. Mech. Phys. Solids*, **33**, 525-543.
- [22] HASHIN, Z. (1996), Finite thermoelastic fracture criterion with application to laminate cracking analysis, *Mech. Mater.*, (to appear).
- [23] BENVENISTE, Y. and DVORAK, G.J. (1990), On a correspondence between mechanical and thermal effects in two-phase composites, in *Micromechanics and inhomogeneity - The T.Mura 65th anniversary volume*, (G.J. Weng, M. Taya, and H. Abé, eds.), Springer-Verlag, N.Y., 65-81.
- [24] LEVIN, V.M. (1967), Thermal expansion coefficients of heterogeneous materials, *Izv. AN SSSR, Mekhanika Tverdogo Tela*, **2**, 88-94.
- [25] MILTON, G.W. (1984), Microgeometries corresponding exactly with effective medium theories, in: D.L. Johnson and P.N. Sen, eds., *Physics and Chemistry of Porous Media*, AIP Conf. Proc., American Institute of Physics, New York, **107**, 66.

- [26] HASHIN, Z. (1983), Analysis of composite materials – a survey, *J. Appl. Mech.*, **50**, 481-505.
- [27] ROSCOE, R. (1952), The viscosity of suspensions of rigid spheres, *Brit. J. Appl. Phys.*, **3**, 267-269.
- [28] HILL, R. (1965), A self consistent mechanics of composite materials, *J. Mech. Phys. Solids*, **13**, 213-222.
- [29] CRISTENSEN, R.M. and LO, K.H. (1979), Solutions for effective shear properties of three-phase sphere and cylinder models, *J. Appl. Mech.*, **27**, 315-330.
- [30] CRISTENSEN, R.M. (1979), Mechanics of composite materials, Wiley-Interscience, N.Y.

## CONCLUSION

The research investigations presented in this report have been concerned with the effect of microcrack distributions on the thermoelastic response of composites and with prediction of the development of such microcracks. The underlying philosophy may be termed micromechanics of damage. This implies that defects such as cracks are explicitly recognized as internal surfaces on which the tractions vanish. This in contrast to continuum damage mechanics where damage is described as some mathematical entity (not uniquely defined ) which involves parameters to be determined by suitable experiments. Micromechanics of damage is mathematically more difficult but it's great advantage is in that it is clearly connected to the physics and geometry of the problems considered and it can yield results of universal validity as has been demonstrated in the studies presented here. The prediction of damage in the form of crack densities is a particularly important problem and it is believed that such efforts should be continued.